HEINRICH HEINE
UNIVERSITÄT
DÜSSELDORF

Plant growth dynamics in relation to soil moisture, oxygen concentration and pH-value

Inaugural-Dissertation

zur

Erlangung des Doktorgrades der

Mathematisch-Naturwissenschaftlichen Fakultät

der Heinrich-Heine-Universität Düsseldorf

vorgelegt von

Stephan Bloßfeld

aus Issum-Sevelen

September 2008

Aus dem Institut für ökologische Pflanzenphysiologie und Geobotanik
der Heinrich-Heine Universität Düsseldorf

Gedruckt mit der Genehmigung der
Mathematisch-Naturwissenschaftlichen Fakultät der
Heinrich-Heine-Universität Düsseldorf

Referent: Prof. Dr. R. Lösch
Korreferent: Prof. Dr. U. Schurr
Tag der mündlichen Prüfung: 29.10.2008

1. Introduction

For understanding bioprocesses in soils, especially carbon flow and allocation between roots, mycorrhizal fungi and microorganisms in the rhizosphere of terrestrial plants, knowledge of the spatial and temporal dynamics of the physical and chemical conditions of the root-rhizosphere-soil interface is essential. Herein the physico-chemical parameters pH, redox potential (E_h), and oxygen partial pressure (pO_2) hold key positions, because these parameters characterize the environmental conditions for the soil biota. Particularly in submerged soils these parameters govern the production and consumption of the greenhouse gases methane (CH_4) and dinitrous oxide (N_2O), by setting the necessary conditions for life and growth of either methanogenic and denitrifying or methanotrophic and nitrifying microbes, respectively (MISHRA *et al.* 1997; FRENZEL & KAROFELD 2000; LE MER & ROGER 2001; VALENTINE 2002; KIRK 2004). Furthermore, pH, E_h and pO_2 also affect the abundance of low-molecular-weight organic acids that are a major carbon and energy source for the soil biota, but also the key precursors for anaerobic CH_4 production, in the rhizosphere and in the bulk soil as well. Organic acids are commonly expected to be released by plant roots or mycorrhizal fungi (JONES 1998; CASARIN *et al.* 2003). But in submerged soils with oxygen-deficient, reducing conditions anaerobic bacterial and archaeal populations become the dominating metabolic source for organic acids like acetate and lactate (ROTHFUSS & CONRAD 1993; DANNENBERG & CONRAD 1999). In the course of anaerobic decomposition of organic matter several pathways like acidogenesis, acetogenesis or methanogenesis are operative, including either the production or the consumption of organic acids, depending on the availability of exogenous electron acceptors such as sulfate or ferric iron (DASSONVILLE & RENAULT 2002, HORI *et al.* 2007). However, these processes are neither stable over time, nor are they homogeneously distributed in the soil (JONES *et al.* 2003; LU *et al.* 2006; LU *et al.* 2007).

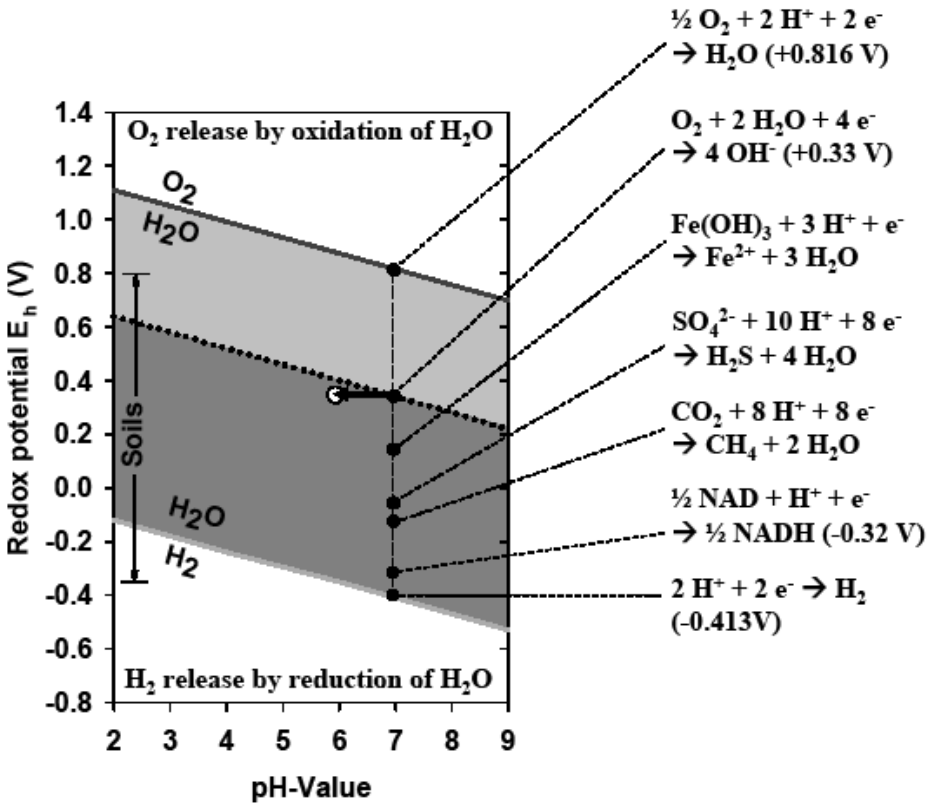

Figure 1. Scheme of the E_h-pH-stability of H_2O (redrawn from SCHEFFER & SCHACHTSCHABEL 2002) and selected reduction half-reactions of biological relevance at anoxic soil conditions (CHRISTEN 1988; SCHOPFER & BRENNICKE 2006). The light-grey area indicates the zone from O_2 saturation of the aqueous phase at atmospheric pressure (+0.82 V, pH 7) to anoxia (+0.35 V, pH 7). The dark-grey area indicates the anaerobic zone. The spots mark the redox potentials of the selected reduction half-reactions at pH 7. The arrow and the white dot indicate the acidification-induced shift towards increased anoxia at a given redox potential and saturation of dissolved O_2. The span of redox potential in soils is indicated at the left margin. (BLOSSFELD & GANSERT 2007)

Wetland plants are able to regulate the different key environmental physico-chemical parameters (pH; E_h; $p(O_2)$), and thus have a strong effect on the composition of the microbial populations in the soil. Therefore the production of organic acids and the emissions of greenhouse gases are influenced by the plants in different ways by (1) changing the rhizosphere pH by e.g. proton excretion or iron oxidation (NYE 1981; REVSBECH *et al.* 1999; KIRK 2004; HINSINGER *et al.* 2005), and (2) providing an aerobic, oxidative environment in the culms and the rhizosphere supporting the growth of aerobic bacteria via oxygen release from the roots into the oxygen-deficient soil (SORELL 1999; BRUNE *et al.* 2000; COLMER 2003a; WIEßNER *et al.* 2005). Depending on

the amount of oxygen released into the oxygen-deficient soil, anaerobic production of organic acids or CH_4 will be hampered or even ceases. On the other hand, root-induced oxygen supply favors oxidizing bacteria, e.g. those that oxidize Fe(II) to Fe(III) proximate to the root surface like *Acidithiobacillus ferroxidans*. Fe(III) in turn, is the substrate for Fe(III)-reducing bacteria (e.g. *Geobacter* spp., *Anaeromyxobacter* spp.), an important group of anaerobic bacteria in submerged soils that metabolize organic acids to CO_2 and CH_4 (KÜSEL *et al*. 2003, WEISS *et al*. 2003). Moreover, the plant-induced patchiness of oxic and anoxic conditions in the rooted soil by species-specific patterns of oxygen release from roots affects the redox potential (E_h) in the rhizosphere, and thus, the energy efficiency of the soil biota (CHABBI *et al.* 2000; WASSMANN & AULAKH 2000). Hence, wetland plants alter the prime environmental parameter oxygen in submerged soils, and as a consequence, alter the structure and abundance of the anaerobic microbial community along with essential biogeochemical processes (e.g. iron cycling).

The biogenic formation and consumption of organic acids, or CH_4 and N_2O in submerged soils additionally depends on the redox potential as a function of pH (Fig. 1; HOU *et al.* 2000; YU *et al.* 2001; YU & PATRICK 2003), as derived from the Nernst equation (GAMBRELL & PATRICK 1978; FISCHER *et al.* 1989). Under consideration of the dynamics of soil pH, the plant-induced oxygenation of the rhizosphere is even more crucial. Under strong acidic and anaerobic soil conditions most of the inorganic compounds and plants nutrients occur in their reduced form and are no longer available for further microbial reduction processes (SCHEFFER & SCHACHTSCHABEL 2002, KIRK 2004). Thus, microbial driven biogeochemical processes are slowed down under anoxic and acidic soil conditions (GOODWIN & ZEIKUS 1987). Conversely, the oxygenation of an acidic soil by plant roots will raise the redox potential to oxidative conditions, and thus, stimulate microbial activity and growth of the soil biota. Hence, any plant-induced alteration of pH and oxygen concentration in the root-soil interface inherently affects two of the three major physico-chemical parameters governing e.g. the greenhouse gas production and consumption in wetland soils (pH

and E_h). Therefore, quantitative high-resolution analyses of radial pH and oxygen gradients from the roots towards the submerged soil and axial gradients along growing roots are of primary importance for an advanced understanding of plant-mediated effects on microbial production of organic acids, or CH_4 and N_2O.

A very common and convenient method for mapping the pH and oxygen changes mediated by plant roots is the use of colored pH or oxygen indicators in transparent gels like agar (WEISENSEEL *et al.* 1979), or in agar-soil-contact methods (MARSCHNER & RÖMHELD 1983; PIJNENBORG *et al.* 1990; KOPITTKE & MENZIES 2004). However, the use of indicators is a rather qualitative method. A quantitative approach based on pH indicators was achieved by use of imaging methods like videodensitometry that provides a two-dimensional quantification of pH changes over a period of several hours within the root-soil interface (JAILLARD *et al.* 1996). Nevertheless, imaging of pH or oxygen patterns with indicator-based methods is restricted to homogeneous transparent, and thus, artificial substrates which do not reflect the biological, physical and chemical heterogeneity of natural soils (JAILLARD *et al*. 2003). Different types of pH and oxygen microelectrodes were broadly used for *in situ* analysis of radial and axial profiles of pH and oxygen changes along roots (TAYLOR & BLOOM 1998; BLOOM *et al.* 2003; ARMSTRONG *et al.* 2000). This method revealed detailed information about species-specific pH and oxygen dynamics at the root-soil interface. The major disadvantages of microelectrodes are that often the plant roots can be investigated only under artificial conditions, or movements of the sensors within the substrate disturb the natural conditions within the soils (ZHANG & PANG 1999; BEZBARUAH & ZHANG 2004). Additionally, two-dimensional mapping requires a grid of a considerable number of fixed microelectrodes that cannot be simply adjusted to the variable growth direction of the roots (FISCHER *et al.* 1989).

To avoid any disturbance of the natural conditions of the biogeochemical micro pattern in oxygen-deficient soils by the measuring technique itself, such as infiltration of oxygen or increased turbation of the submerged soil substrate by

moving the electrodes, new techniques for accurate high-resolution investigations of bioprocesses in natural conditions of submerged soils are required. However, as shown above and stated by others (GREGORY & HINSINGER 1999; JAILLARD *et al.* 2003), a quantitative non-invasive mapping of pH and oxygen in the rhizosphere and their spatial and temporal changes in soils under at least semi-natural experimental conditions is still missing.

For evaluation of the influence of wetland plant roots on the anaerobic microbial production and consumption of organic acids in the root-soil interface, minimal-invasive and high-resolution sampling of soil solution from the roots to the bulk soil is necessary. The state-of-the-art in sampling of soil solution is the use of microsuction cups, which are inserted into the soil either from the front (DESSUREAULT-ROMPRÉ *et al*. 2006) or from the back of a rhizotrone (GÖTTLEIN *et al.* 1996). The use of microsuction cups in combination with capillary electrophoresis (CE) provides a non-destructive *in situ* collection and detection of organic acids and inorganic ions (e.g. lactate, citrate, nitrate or ammonium) in the soil solution (WANG *et al*. 2004; GÖTTLEIN *et al.* 2005; THIELE *et al*. 2005). However, conventional microsuction cup techniques are disadvantageous for application in wetland soil conditions with respect to infiltration of atmospheric oxygen into the oxygen-deficient soil substrate, water leakage, and size.

To overcome these methodical limitations, a novel rhizotrone-based 2D imaging system was constructed, which allows high-resolution measurements of the spatial and temporal dynamics of pH and oxygen in the soil and in the root-soil interface without any disturbance of the biological and physico-chemical conditions caused by the method itself. Additionally, a novel rhizotrone for free-choice root in-growth in differentially treated soil compartments, equipped with microsuction raster access ports for minimal-invasive and high-resolution sterile sampling of soil solution across and along individual roots of wetland plants was developed. These novel techniques were used to investigate the effect of roots of selected wetland plants (i.e.

J. effusus, *J. inflexus* and *J. articulatus*) on the abundance of organic acids and on the dynamics of pH and oxygen patterns in the submerged soil. This study will provide evidence of the paramount significance of oxygen release and soil pH changes by the wetland plant roots on the heterogeneity and dynamics of the physico-chemical conditions in the rhizosphere, completely different from the bulk soil, along with contrasting biogeochemical processes that characterize the microenvironment of the rhizosphere.

2. Material and Methods

2.1. Investigated plant species

The selected plant species, *Juncus effusus* L., *Juncus inflexus* L., *Juncus articulatus* L. are very common wetland plant in Central Europe. One of the key anatomical differences between these species is the structure of the culm internal airspaces (aerenchyma). The aerenchyma of *Juncus effusus* is distinguished by a spongy type pith, whereas the aerenchyma of *Juncus inflexus and Juncus articulatus* are separated by several walls into caverns of different size (Fig 2). The volume of the caverns in the culms of *Juncus inflexus* reach up to 2.7 mm^3, whereas the volume of the caverns in the culms of *Juncus articulatus* reach up to 22.7 mm^3.

The plants were grown in pots under waterlogged conditions for at least two weeks before start of measurements. These waterlogged conditions were provided during the measurements as well. All investigations were conducted at the field research site or in the laboratory of the Institute of Geobotany of the Heinrich-Heine-University Düsseldorf. During the day-night cycles throughout the test series, temperature and relative humidity varied in the field between 11 °C – 39 °C and 25% – 98% respectively. In the laboratory air temperature ranged from 22.6 °C – 24.0 °C and relative air humidity ranged between 28.2% – 31.0% respectively.

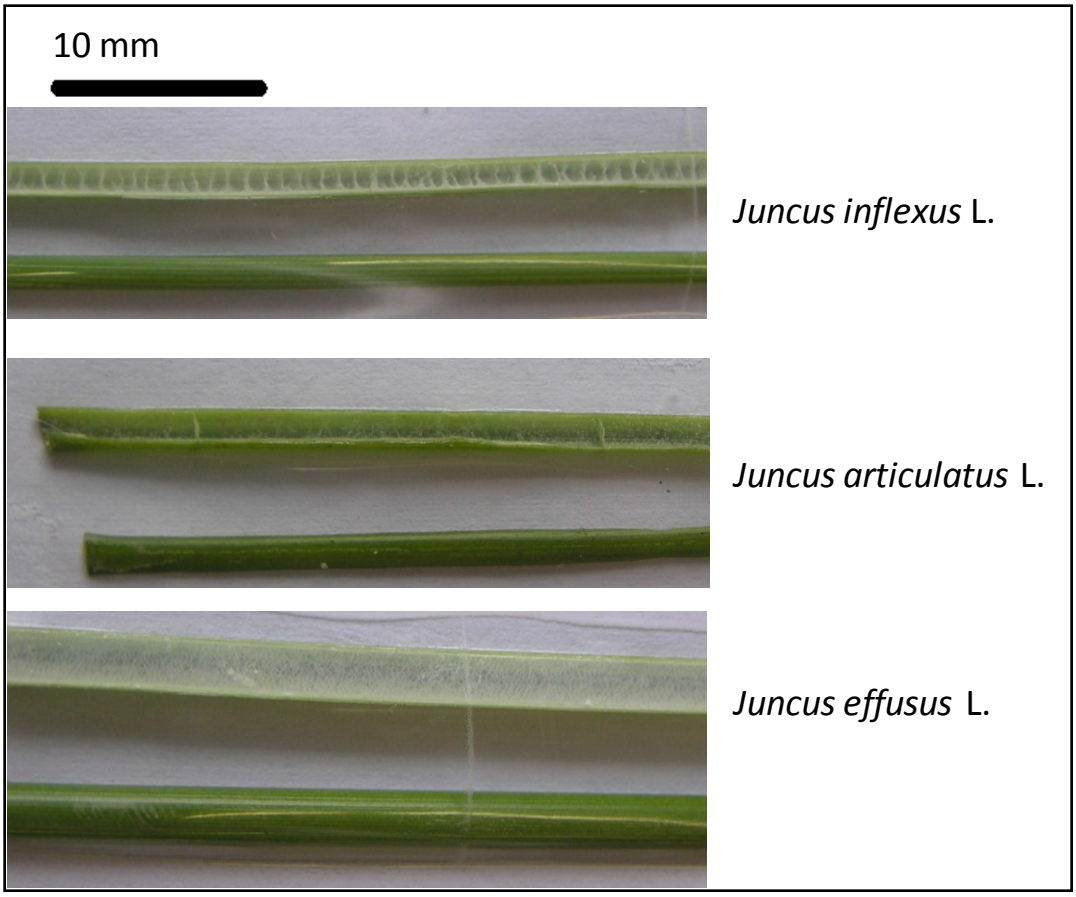

Figure 2. Longitudinal sections of the culms of the investigated plant species. The photographs illustrate the species-specific anatomical structure of the aerenchyma.

2.2. Soil moisture gradient experiment

For investigating the impact of varying soil moisture on plant growth and plant survival strategies, the three different species (*J. effusus, J. inflexus, J. articulatus*) were planted in controlled soil moisture gradient basins. The construction of these basins was based on the "Hohenheimer Modell", established by ELLENBERG (1953). The dimensions of the basins (length x width x height) were 120 cm x 100 cm x 60 cm (front side) / 120 cm (back side). The basins were filled with meager garden soil (Botanical Garden University of Düsseldorf) with an ascending slope of the surface of ca. 45° from the front to the back side of the basins. The lower part (front side) of the basins was permanently flooded, creating a soil moisture gradient from waterlogged (front side) to dry (back side). The soil moisture was continuously monitored by soil moisture sensors (ThetaProbe ML-2x, Delta-T Device Ltd., Cambridge, UK) at three

different soil moisture levels (dry, medium, wet). The data from the ThetaProbes were stored at 30 minutes intervals with data loggers (Squirrel 1000**,** Grant Instruments Ltd., Sheperth, UK). Due to the constant waterlogging, all soil moisture gradient basins generated similar moisture gradients from about 0.24 m^3 H_2O m^{-3} soil at dry levels to about 0.51 m^3 H_2O m^{-3} soil at wet levels (Tab. 1).

Table 1. Soil moisture conditions during the competition and monoculture experiments.

average soil moisture θ (m^3 H_2O m^{-3} soil)				
soil moisture	competition	*Juncus effusus* monoculture	*Juncus inflexus* monoculture	*Juncus articulatus* monoculture
dry	0.24 ± 0.03	0.27 ± 0.03	0.28 ± 0.02	0.26 ± 0.01
medium	0.42 ± 0.01	0.43 ± 0.03	0.41 ± 0.03	0.42 ± 0.02
wet	0.51 ± 0.02	0.48 ± 0.01	0.49 ± 0.01	0.50 ± 0.03

The experimental setup was designed with two different variations, monoculture and competition treatments:

(I) Monoculture treatment: for each species a separate basin was used where 30 individuals were planted in five transverse rows with six plant individuals each. These five rows corresponded to five different soil moisture levels (dry, low moisture, medium moisture, wet, waterlogged). The plant individuals originated from cuttings of different stock plants with similar fresh weight, leaf number and leaf length.

(II) Competition treatment: the same type of basins was used and within these competition basins all three plant species were treated in the same way as during monoculture, but planted alternately within each of the five rows. In all treatments the plants were grown during the vegetation period (May to September). At the end of the growing season the above-ground biomass of all plants was harvested. Key parameters of the leaves (leaf dry matter content, specific leaf length, leaf porosity, leaf length) were measured and used as indicators and measures of plant responses to soil moisture gradients and interspecific competition.

2.3. CO_2 and H_2O Gas exchange

Diurnal courses of photosynthesis and transpiration were measured with a LCA-4 porometer (ADC BioScientific Ltd., Hoddesdon, UK). For each species, five diurnal courses per plant species were conducted with different plant individuals. Each started between 0530 h and 0630 h (Central European Time, CET) by mounting 3-4 culms in the plant leaf chamber of the LCA-4, and ended between 1700 h and 1800 h (CET), according to the shading of the plants by a nearby building. The chamber was oriented parallel to the orientation of the upright culms. This assembly required an axial readjustment of the chamber during the course of day, following the course of the sun. Higher over-temperatures of the culms relative to the ambient could not be detected. Leaf area (A) was calculated by measuring the radius of both ends (r1, r2) and the length (l) of each clamped culm by a digital caliper and by using the formula of circumferential surface of a cone frustum:

$$A = \pi \, l \, (r1 + r2) \qquad (1)$$

To verify the results, the leaf area of five sample culms was additionally measured with slit and spread culms using a LI-3100 areameter (LI-COR inc., Lincoln, Nebraska, USA).

2.4. Aerenchyma internal oxygen measurements

Investigations of oxygen partial pressure in the aerenchyma of the culms were conducted by use of oxygen micro-optodes with a tip diameter of 150 µm, (PreSens Precision Sensing GmbH, Regensburg, Germany) in a field experiment as well as under laboratory conditions. The optode was mounted on a mini-manipulator (own construction, Fig. 3) equipped with a sliding carriage for reproducible positioning accurate to a tenth of a millimeter. By the use of this mini-manipulator the optode was horizontally inserted 0.5 mm into the culm at a height between 30 cm and 40 cm

above culm base. The penetrated part of the culm was sealed by malleable terostat mastic (Teroson Glas Tech Oy, Vaasa, Finland). The optode was operated by a Microx-TX device (PreSens GmbH). Microclimatic data (global radiation, PPFD, T_{air}) during the field and laboratory experiment were collected and logged by a Squirrel 1200 data logger (Grant Instruments Ltd., Sheperth, United Kingdom).

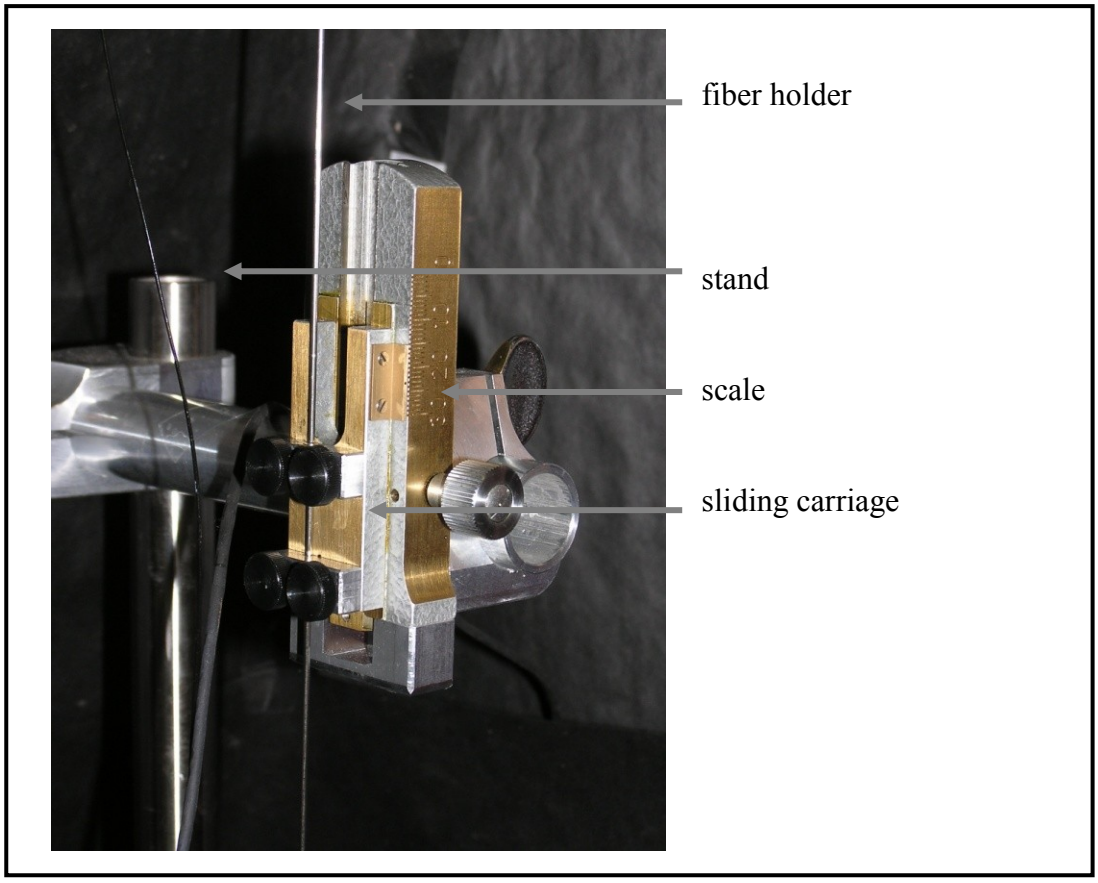

Figure 3. Mini-manipulator for accurate positioning of fiber-optic oxygen optodes.

2.5. Novel compartmented rhizotrone design for free-choice root ingrowth investigations

The rhizotrone was constructed by the workshop of the scientific unit Biology of the Heinrich-Heine-University for the specific requirements of the measurements as prescribed by the author. It was made of anodized aluminum (thickness = 8 mm, Jean Willems & Sohn, Düsseldorf, Germany), while the front plate was made of acrylic

glass of 3 mm thickness (Rhöm GmbH, Darmstadt, Germany). The inner dimensions of the box were 406 mm in width, 300 mm in height, and 30 mm in depth (Fig. 4). In contrast to common rhizotrones, two trapezoid metal bodies (Fig. 4 "A", surface area 115.5 cm^2, thickness 30 mm) and two metal bars (Fig. 4 "B", width = 30 mm, length = 150 mm, thickness = 8 mm) were attached to the back of the rhizotrone, connecting the back plate with the front plate. A groove (depth = 2.5 mm, width = 2.5 mm) was cut into the margin of the rhizotrone, the trapezoid bodies and into the metal bars to house a standard foam rubber cord (Fig. 4 "C", d = 3.0 mm) used as waterproof sealant between the acrylic glass and the metal body of the rhizotrone.

This design gave three compartments of equal volume (V = 550 cm^3) to be used for free-choice root in-growth investigations under differentially manipulated soil conditions in each test-compartment. A covering soil layer, the parent soil compartment (V = 450 cm^3), in equidistance from the test-compartments provided equal conditions for root growth in the beginning of the experiment, i.e. prior to the contact of roots with any substrate in the test-compartments. The trapezoid metal bodies increased the surface for thermal conductivity, and thus, considerably improved thermal homogeneity in the rhizotrone. In addition, by this construction the acrylic front plate proved to have excellent evenness, which is a prerequisite for accurate optical measurements from outside through the transparent window. Each test-compartment was equipped with a water inflow-outflow port in the ground plate, to be used for individual regulation of the water level (Fig. 4 "D"). For insertion of the raster access ports (see chapter 2.5.1.), a hole of 53 mm in diameter was drilled into the back plate of each test-compartment and the parent-compartment, respectively (Fig. 4 "E"). A ring-adapter (PVC, d_i = 53 mm, d_o = 65 mm, height = 10 mm) was attached from the back around each hole (Fig. 5 "F"). A groove in the inner wall of each adapter (width = 2 mm, depth = 1 mm) housed a conventional o-ring seal (d = 2 mm). Two fluid coolers with internal fin structure (FLKU 140, Fischer Elektronik GmbH, Lüdenscheid, Germany) were fixed from outside to the back of the rhizotrone, below and above the raster access ports,

covering 53.3% surface area of the back plate of the rhizotrone (Fig. 5 "G"). To increase thermal conductivity, a thermal compound (Conrad Electronic, Hirschau, Germany) was applied between the fluid coolers and the rhizotrone. The fluid coolers were connected in series to a water bath and flowed through with deionized water at 20 °C. For individual tilting the rhizotrone was mounted on a tiltable mount (Chapter 2.9.).

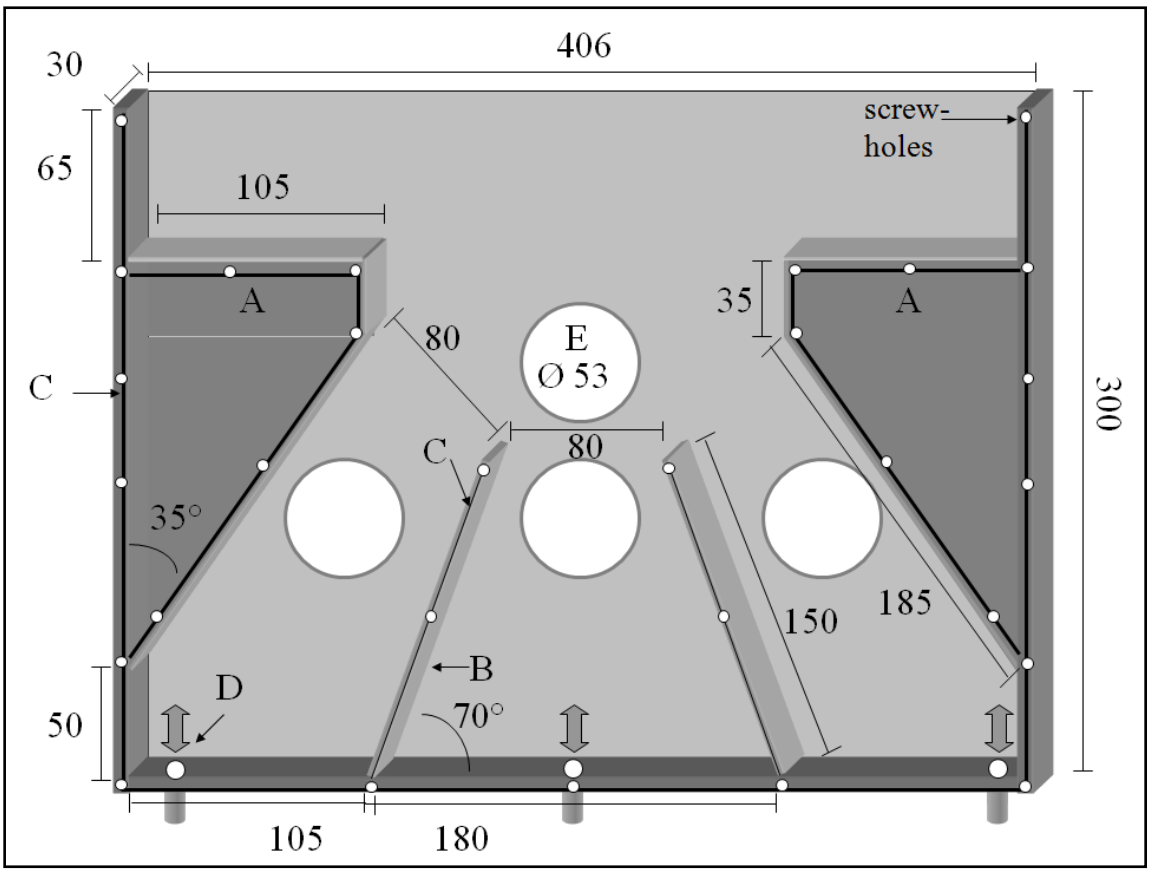

Figure 4. Front view of the rhizotrone (distances and dimensions in mm). Metal bodies (A, B) generated equal volumes of three test-compartments. The rhizotrone was sealed by conventional rubber cord (C) and each test-compartment was equipped with a water inflow/outflow port (D). Four holes (E) in the backside of the rhizotrone granted access to the soil. The drawing is not to scale.

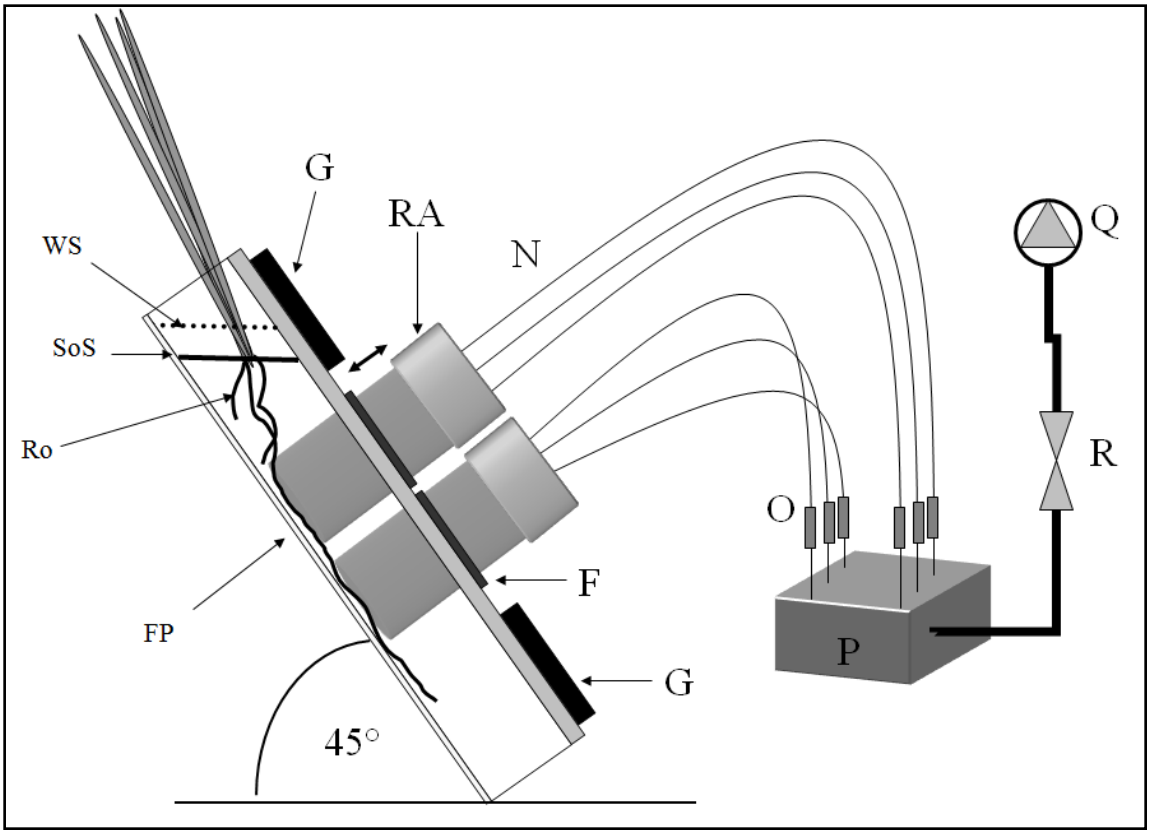

Figure 5. Raster access ports (RA) were placed through circular ring adaptors (F) close to the roots (Ro) that grew across the transparent front plate (FP). The water surface (WS) was always 2-3 cm above the soil surface (SoS). Steel capillaries (N) were inserted through the raster access ports (RA) for sampling soil solution. Sampling was done by connecting the capillaries via tubing connectors (O) to a vacuum sampling chamber (P). Vacuum was generated by a vacuum pump (Q). The vacuum was regulated by a manual valve (R). The temperature in the rhizotrone was controlled by two cooling devices (G) that were connected to a water bath. The drawing is not to scale.

2.5.1. Raster access ports

To get access to the solution of the bulk soil and of the rhizosphere in the test and parental compartments, four raster access ports were constructed. Each raster access port was made of two anodized aluminum cylinders that could be screwed into each other. Therefore, both the inner diameter of the outer cylinder "H" and the outer diameter of the inner cylinder "I" was 50 mm, respectively (Fig. 6). An aluminum adapter with an inside screw thread (d = 52 mm) was fixed on the top of the outer cylinder, whereas the inner cylinder had an outside screw thread (d = 52 mm). At one end of the outer cylinder the inside wall had a circular stop of 2.5 mm thickness to hold two circular acrylic glass raster plates (Fig. 6 "J1, J2", d = 50 mm, thickness =

3 mm). These raster plates were designed for insertion of micro capillaries or other devices suitable for measurements, e.g. pH microelectrodes or oxygen optodes, and experimental treatment in the rhizosphere. In this study, the raster plate in the rear ("J1") was equipped with a 1 mm raster of 34 x 34 holes (d = 0.7 mm). The front plate ("J2") carried the same raster but was made of multiple-step holes, i.e. 0.7 mm in diameter for 2.5 mm depth followed by 0.5 mm in diameter for the remaining 0.5 mm depth, serving as a stop for the micro capillaries (see below). A groove (width = 1 mm, depth = 0.7 mm) was cut into the wall of each raster plate for insertion of a conventional o-ring seal (d = 1 mm). Both raster plates were congruently fitted to each other by use of two stainless steel guide pins (Fig. 6 "K", d = 4 mm). Two layers of sealing film (Fig. 6 "L", Nescofilm, Bando Chemical Ind. Ltd., Kobe, Japan) were fixed between the raster plates to prevent leakage between the capillaries during vacuum suction of soil solution. A filter membrane of 0.2 μm pore size (Fig. 6 "M", d = 50 mm, Whatman GmbH, Dassel, Germany) was placed in front of the front raster plate to ensure sterile sampling of soil solution at each position of the raster. The entire set consisting of filter membrane, front raster plate, sealing films, and rear raster plate was inserted into the outer cylinder and fixed tightly by screwing the inner cylinder into the outer cylinder, pressing the raster plates against the circular stop of the outer cylinder. Due to the sealing films between both raster plates and the o-ring seal in the wall of each raster plate, the raster access port was watertight. The raster access ports could be inserted into the rhizotrone at arbitrary depths (0 - 30 mm) through the sealing adapter of the holes in the back plate. The rotatability and moving of the raster access ports allowed an optimized positioning of the micro capillary raster in close contact with roots (0.5 mm distance) in order to get cross and longitudinal transects of soil samples across and along roots, respectively.

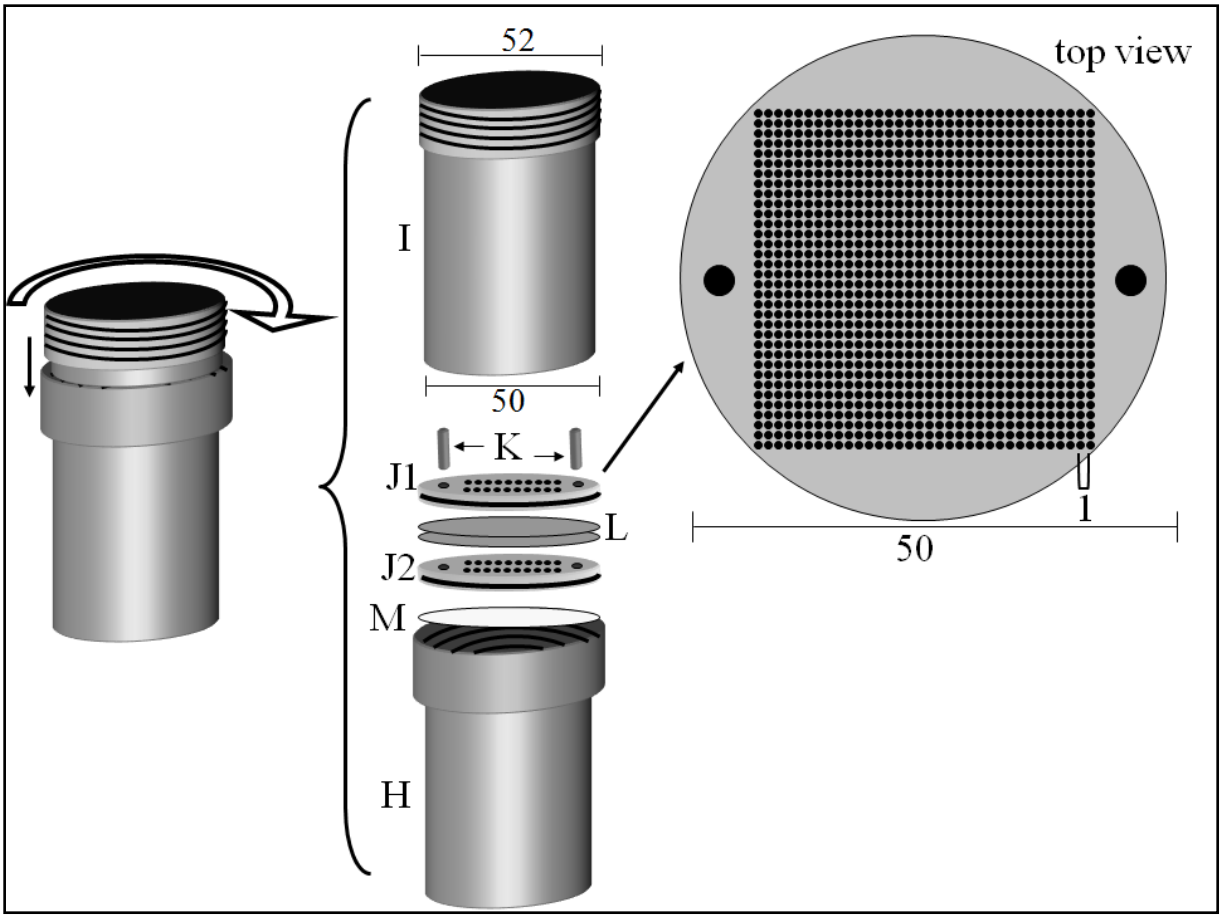

Figure 6. Drawing of a raster access port. A set consisting of filter membrane (M), front raster plate (J2), sealing films (L), and rear raster plate (J1) that was fitted together by two steel pins (K), was inserted into the outer cylinder (H) and fixed tightly by screwing the inner cylinder (I) into the outer cylinder, pressing the raster plates against the internal circular stop of the outer cylinder. The drawing is not to scale.

2.5.2. Vacuum sampling of soil solution

For minimal-invasive sampling of soil solution, a series of stainless steel capillaries (Fig. 5 "N", d_o = 0.6 mm, d_i = 0.4 mm, length = 30 cm, SWS Edelstahl GmbH, Emmingen, Germany) serving as microsuction cups were inserted in the raster plates penetrating the sealing film but stopped in the multi-step holes 0.5 mm in front of the sterile filter membrane that separates the soil from the raster plates. For prevention of blockage of the capillaries by intrusion of sealing film a steel wire (d = 0.4 mm) was inserted into each capillary prior to its insertion into the raster plates, which was removed after positioning of the capillary. Due to the elasticity of the sealing film it affixed to the steel capillaries maintaining its function as a watertight sealant.

Each steel capillary was connected to a vacuum sampling chamber (GÖTTLEIN *et al*. 1996) via 10 mm tubing connectors (Fig. 5 "O", d_i = 0.5 mm, Pharmed, Saint-Gobain Performance Plastics Verneret, Charny, France). The sampling chamber was constructed with 100 ports available (Fig. 5 "P"). A vacuum of - 300 hPa was applied to this chamber by a vacuum pump (Fig. 5 "Q", Laboport N 86 KT.18, KNF Neuberger GmbH, Freiburg, Germany). The vacuum was regulated by a manual valve (Fig. 5 "R") that was connected between the pump and the vacuum sampling chamber. The sampled soil solution (250 – 500 µl) was collected in standard 2 ml test tubes, positioned in the sampling chamber underneath of each of the 100 ports. The sampling time of one complete set of microsuction cups was short (30 – 45 minutes), highlighting the minimal-invasive character of this technique. After sampling of the soil solution, the test tubes were immediately closed and stored in a freezer (-20 °C) until they were used for capillary electrophoresis (CE) analysis.

2.6. CE analysis of soil solution for organic acids

The advantages of CE analysis are the need of only very small sample volumes (µl), high separation efficiency and high analyte sensitivity, all being essential prerequisites for the analysis of rhizosphere solution at high spatial resolution. In this study the soil solution samples were analyzed for organic acids using capillary electrophoresis with a salicylate electrolyte (BAZZANELLA *et al.* 1997). A capillary electrophoresis system G1600A (Agilent, Böblingen, Germany) installed at the Research Centre Jülich (*Institute of Chemistry and Dynamics of the Geosphere, ICG-3: Phytosphere/BioSpec*) was used, equipped with a built-in diode-array detector. The CE analysis itself was performed by Dr. Björn Thiele employed at the *ICG-3: Phytosphere/BioSpec*. Fused silica capillaries (Polymicro, Phoenix, USA) of 75 µm inner diameter and 64.5 cm of total length (56 cm to the detector) were used. The electrolyte solution contained 7.5 mM salicylic acid, 15 mM TRIS, 0.5 mM dodecyltrimethylammonium hydroxide and 0.3 mM $Ca(OH)_2$ and was freshly

prepared every day. The electrolyte was exchanged every 10th CE analysis during a series of samples. A voltage of 30 kV was applied during all separations, with temperature maintained at 25 °C. Injections were carried out hydrodynamically with a pressure of 50 mbar for 30 s followed by injection of a plug of electrolyte at 50 mbar for 5 s. The separated compounds were detected by indirect UV-detection at a wavelength of 360 nm (bandwidth 40 nm) and a reference wavelength of 232 nm (bandwidth 20 nm). Quantification was performed using external calibration with aqueous standard solutions (5, 10, 20 μM) and internal standardization using phenylacetic acid as internal standard. The rhizosphere samples (2 μl) were diluted with 16 μl deionized water and 2 μl 100 μM internal standard solution prior to analysis. The capillary was flushed with 0.1 N NaOH for 5 min, water for 1 min and electrolyte for 5 min before each analysis.

However, problems arose from measurement of acetate. Presence of organic acids in laboratory air, as impurities in chemicals, on glassware and on human skin is well known (PELDSZUS 2007). Thus, the accumulation of organic acids was tested in blank samples, revealing that the concentration of acetate increased from below detection limit up to 87.0 μM during performance of the analysis sequences. Hence, samples derived from the bulk soil and the rhizosphere were corrected for the drift in acetate concentration. Calibration lines for the organic acids investigated were linear in the range between 5 and 20 μM with excellent correlation coefficients (0.9965 – 0.9991). The limits of detection (LOD, 3σ) were about 0.5 μM.

2.7. Experimental design for sampling soil solution

In order to investigate the effect of plant roots on the dynamics of organic acids under submerged soil conditions and different soil pH, the test-compartments of the rhizotrone were filled with the same soil substrate but of different pH (compartment C = soil type E910 (pH 5.9), compartment B = soil type A600 (pH 3.9), compartment A = E400 (pH 5.5), Tab. 2, Fig. 7) up to the lower edge of the holes for the raster access

ports. The ports were positioned 1 mm off the acrylic front plate and then the test-compartments were topped up. Afterwards, the ports were pushed 0.5 mm closer to the front plate to ensure sampling of soil solution across and along a growing root to be seen from outside through the transparent window. The parent soil compartment was filled with E400 and treated in the same way as the test-compartments. During filling of the compartments a set of three temperature sensors (Pt 1000) was installed at three different depths (top, centre and bottom of the compartment) for monitoring soil temperature in each compartment. To maintain equal nutrient conditions in all soil compartments the rhizotrone was watered with Knop standard nutrient solution (Tab. 3) during the entire experiment. To simulate wetland conditions, the rhizotrone was kept waterlogged by use of the nutrient solution. Light conditions in the laboratory were kept constant at near photosynthetic saturation level of the investigated plant species (see chapter 3.2.) during a 14/10 h day – night cycle (HIT 400 W, NORKA GmbH & Co. KG, Hamburg, Germany). Mean air temperature varied between 21.8 ± 0.6 °C at night and 23.8 ± 1.6 °C during daytime. By use of the fluid coolers soil temperature at all depths was nearly constant at 19.85 °C throughout the experiment, and showed negligible diurnal variation (19.82 ± 0.22 °C at night-time, 19.88 ± 0.24 °C at daytime).

An individual plant of *Juncus effusus*, *Juncus inflexus* and *Juncus articulatus* were grown in separate rhizotrones for three weeks before the first sampling of the rhizospheric soil solution in the parent soil compartment (25 samples per species). Two weeks later a second series of rhizospheric soil solution was sampled in the test-compartment B (50 samples per species), since at this time no roots were growing along the raster plates within the other two test-compartments. However, samples from the bulk soil of the test compartment A and C were taken during this sampling period. During the measurements the steel capillaries were placed in different raster intervals (1 mm vs. 2 mm) for evaluation of the spatial resolution of this new sampling technique.

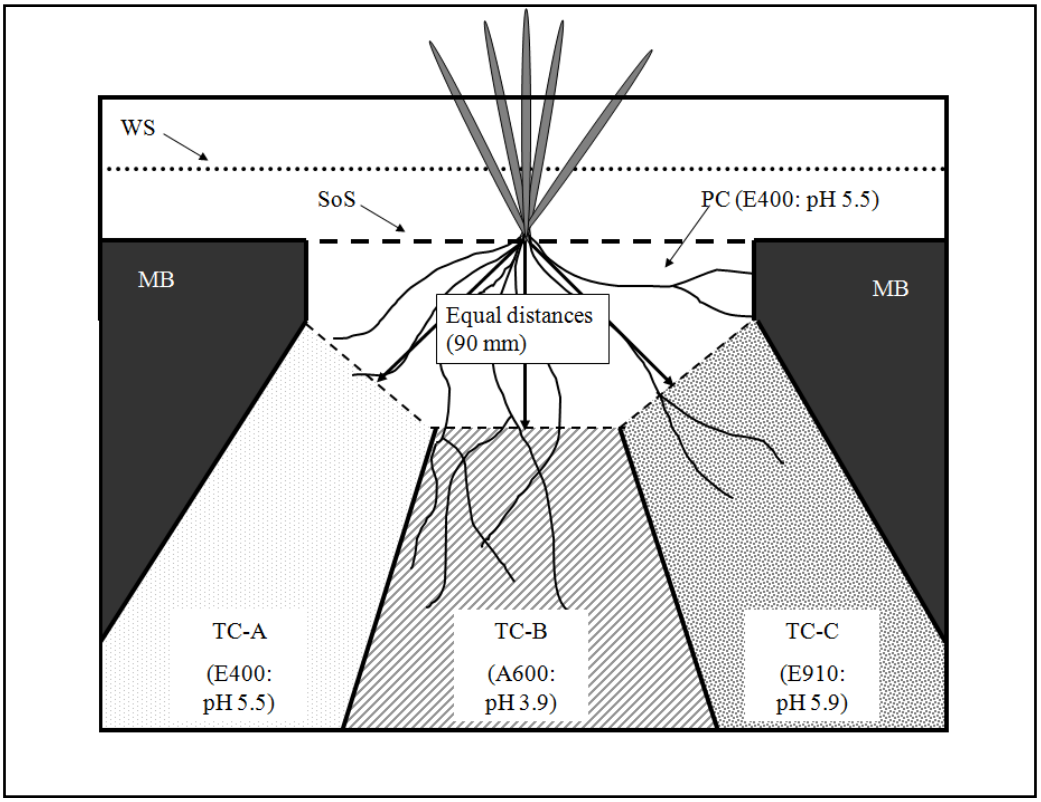

Figure 7. Three different soil types were filled into the different test-compartments (see Tab. 2 for soil characteristics). The parent soil compartment (PC) contained the same soil type as the test-compartment 'A' (TC-A, E400, pH 5.5). Test-compartment 'B' was filled soil type A600 (TC-B, pH 3.9) and the test compartment 'C' contained the soil type E910 (TC-C, pH 5.9). This system allowed a free-choice root ingrowth into the different compartments. To maintain equal soil volumes, two metal bodies (MB) were inserted into the rhizotrone. The water surface (WS) was always above the soil surface (SoS) to induce waterlogged soil conditions. The drawing is not to scale.

Table 2. Characteristics of the different soils used in the test-compartments 'A' to 'C' and in the parent compartment 'P' (data provided by Stender AG, Schermbeck, Germany). Nutrient content is given in mg l^{-1}.

	Soil characteristics		
Soil type	E910	E400	A600
Rhizotrone test-compartment	'C'	'P' and 'A'	'B'
dry matter (%)	59.1	47.0	40.1
pH ($CaCl_2$)	5.9	5.5	3.9
Ammonium (NH_4-N)	68	142	17
Nitrate (NO_3-N)	2	60	3
Phosphorus (P_2O_5)	68	255	2
Potassium (K_2O)	190	341	47

Table 3. Nutrient content of the Knop nutrient solution.

Nutrient	Concentration (mg l^{-1})
$Ca(NO_3)_2$	1000
$MgSO_4$	250
KH_2PO_4	250
KNO_3	250
$FeSO_4$	20

2.8. Principle of non-invasive optical pH and O_2 measurement

The optical measurement of pH and O_2 by planar optodes is based on the measurement of the fluorescence decay time of pH and O_2 -sensitive indicator dyes, which are permanently fixed in a polymer, ion and oxygen permeable matrix, drawn out to a sensor foil of constant thickness (10 μm). Proportionality exists between the analyte concentration (e.g. molecular oxygen) and the fluorescence decay time of the corresponding indicator. Thus, optical measurement of molecular oxygen is based on the effect of dynamic luminescence quenching by oxygen as the quenching molecule (Fig. 8). The collision between the O_2 sensitive luminescent indicator molecule (O_2 luminophore) in its excited state, and the quencher (molecular oxygen) results in radiation-less deactivation, and is called collisional or dynamic quenching. After collision, energy transfer takes place from the excited indicator molecule to oxygen which consequently is transferred from its ground state (triplet state) to its excited singlet state. There is a nonlinear decrease in luminescence with increasing concentration of molecular oxygen. The signal can be linearized by means of the Stern-Volmer equation (STERN & VOLMER 1919) which describes the dynamic fluorescence quenching by molecular oxygen (KLIMANT *et al.* 1995).

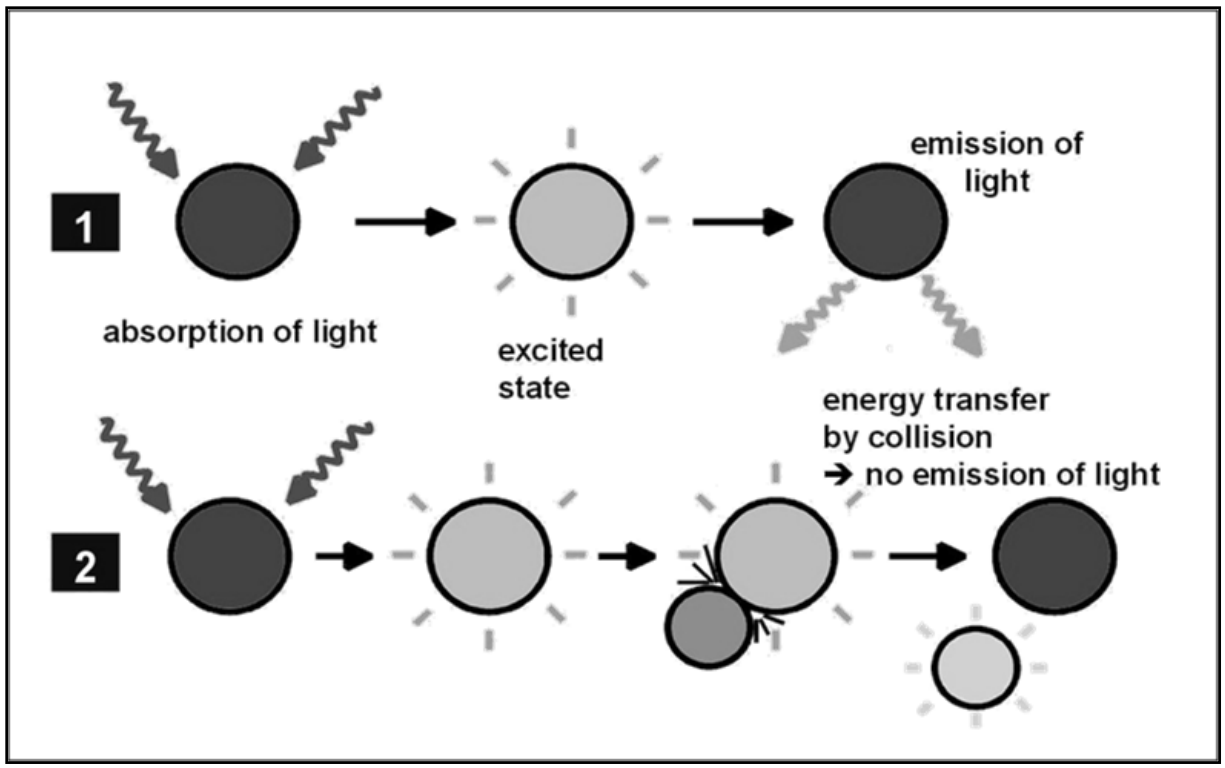

Figure 8. Principle of dynamic luminescence quenching of an excited oxygen-sensitive indicator dye (luminophore) by molecular oxygen. (1) Luminescence of the excited luminophore in absence of oxygen. (2) Luminescence quenching by energy transfer from the excited luminophore to oxygen as the quenching molecule (Figure provided by PreSens Precision Sensing GmbH, Regensburg, Germany).

However, the decay time of the pH-sensitive indicator dyes is in the nanosecond (ns) time scale, requiring a sophisticated and expensive instrumentation, which limits their use in sensor application. Therefore, a new measuring principle, the dual lifetime referencing method (DLR) was used (HUBER *et al*. 2001). This method integrates a couple of organic molecules (luminophores) with different decay times but similar excitation spectra. An analyte-insensitive μs-lifetime luminophore, termed as the reference standard, is combined with an analyte-sensitive ns-lifetime fluorophore, referred to as the indicator, and fluorescence intensity is converted into a phase shift. The phase angle Φ measured at a single modulation frequency reflects the luminescence decay time, provided that the decay is single-exponential. The phase angle Φ_m of the overall luminescence obtained at a single frequency depends on the ratio of intensities of the reference luminophore and the indicator fluorophore. The Φ_m can be represented as the superposition of the single sine-wave signals of the indicator fluorophore and the reference luminophore. The reference luminophore

gives a constant background signal while the fluorescence signal of the indicator depends on the analyte concentration. Hence, the average Φ_m directly reflects the analyte concentration. The modulation frequency is adjusted to the decay time of the reference dye (KLIMANT *et al*. 2001; GANSERT *et al*. 2006).

2.9. Experimental setup for single optical pH measurement

In order to evaluate the novel optode technology for the use in rhizospheric research, a pH-sensitive planar optode (sensor foil) of 85 mm length and 95 mm height was used (PreSens Precision Sensing GmbH, Regensburg, Germany). It was fixed inside a regular, watertight rhizotrone of rectangular dimensions (40 cm width, 30 cm height, 7 cm depth; V = 0.0084 m^3) in the middle of a removable transparent acrylic plastic front plate (Plexiglas, thickness: 4 mm; Röhm GmbH, Darmstadt, Germany). In principle, this rhizotrone was a simplified "one compartment" version of the compartmented rhizotrone described in chapter 2.5., without raster access ports for soil solution sampling. As investigated elsewhere, acrylic plastic shows no detrimental effect on growth and survivorship of roots (WITHINGTON *et al*. 2003). The pH optode was fixed onto the front plate by the use of silicone grease (Baysilone; Bayer AG, Leverkusen, Germany) to compensate for surface roughness and to prevent enclosure of air bubbles between the acrylic glass and the optode.

In order to test the suitability and the performance of this specific pH sensor within the optimum pH range of the sensor (i.e. pH 6 – 8), the rhizotrone was filled with sieved (2 mm mesh) eutric-calcric histosol (pH 8) and was kept submerged throughout the experiment.

The rhizotrone was fixed on a tiltable mount that could be slanted between an angle of 0° (upright) and 45° (Fig. 9). The experimental plant (*Juncus sp.*; see 2.1.*)* was inserted closely to the front plate in mid-position of the rhizotrone and pre-cultivated for 2 weeks. Until the end of the experiment, usually more than two dozen roots of

the investigated individual grew across the sensor foil and were investigated for changes in the pH field. With respect to the light saturation of photosynthesis (BLOSSFELD 2005; Chapter 3.2.), the plant received 14 h d^{-1} of saturating light (700 µmol photons m^{-2} s^{-1}, KL 2500 LCD; Walz GmbH, Effeltrich, Germany). Temperatures varied between 22 °C at night-time and 25 °C at daytime. Photosynthetic photon flux density (PPFD) at 10 cm above water table and close to the culms was measured by a quantum sensor (SKP 215; Skye Instruments Ltd., LlandrindodWells, Powys, UK). Temperature at the culm surface ($T_{culm\ surface}$; 10 cm above water table) and air temperature (T_{air}; 2 cm above water table) were measured by the use of conventional thermocouples. Temperature and PPFD were recorded at 5 min intervals using a data logger (1200 Squirrel; Grant Instruments Ltd., Barrington, Cambridge, UK). The temperature of the waterlogged soil was measured by the use of two temperature sensors (T_{soil}; Pt-1000) mounted diagonally opposite close to the planar optode. One of these temperature sensors was connected to a conventional fiber-optic oxygen meter (Microx TX 3; PreSens GmbH), used for temperature-compensated measurement of the local pO_2 in the soil and for monitoring radial oxygen loss (ROL) from single root surfaces as well. The second Pt-1000 temperature sensor was connected to the optical phase detection device of the planar pH optode (pH-1 mini; PreSens GmbH) to compensate the effect of small temperature variation on the accuracy of pH measurement.

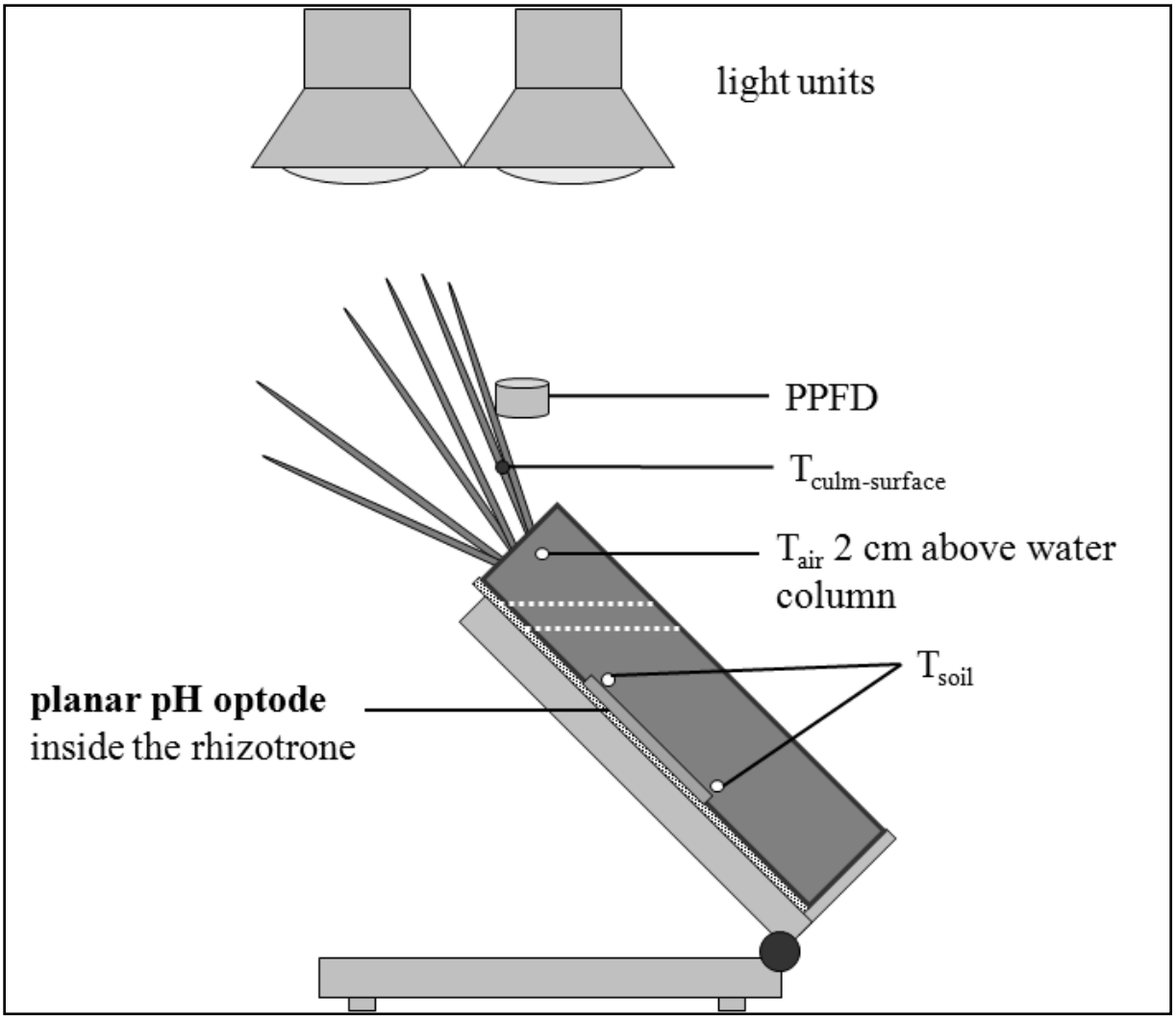

Figure 9. Scheme of the experimental design illustrating the tiltable mount, the watertight rhizotrone planted with *Juncus effusus* L. in submerged soil, and the positions of different sensors used to measure photosynthetic photon flux density (PPFD) and temperature conditions (T_{air}; T_{soil}; $T_{culm-surface}$). The position of the planar pH optode (85 x 95 mm) fixed at the inner side of the acrylic front plate is also shown. Horizontal dashed lines indicate the height of the water column above the soil surface (~ 2 cm). The diagram is not to scale. (BLOSSFELD & GANSERT 2007)

According to Henry's law of solubility of gases in water, the calibration of the Microx oxygen sensor was done by a two-point calibration in water of known O_2 concentration at a given temperature (T = 20 °C) in a water bath. The two calibration solutions were set by the use of a N_2/O_2 gas mixing unit (GMS 600; QCAL Messtechnik GmbH, Munich, Germany) to (1) oxygen-free water (0%) and (2) air saturated water (100%), defined as the concentration of dissolved O_2 in equilibrium with 21% O_2 concentration of the N_2/O_2 gas mixture (283 µmol O_2 l^{-1} water).

The radial oxygen loss from the root surfaces (ROL) was measured by attaching the glass fiber with its O_2-sensitive tip (d ~ 150 μm) to the surface of different exemplarily chosen roots nearby the pH sensor foil. The position of the O_2 sensor (O_2 optode) was kept constant while the root tip moved along the acrylic window over time. The O_2 concentration of seven different root surfaces was investigated with this technique. Measurements of O_2 partial pressure in the aqueous phase were necessary for evaluation of the oxic/anoxic conditions in the submerged soil and at the root surface in particular. To estimate the oxygen consumption rate of the oxygen-deficient bulk soil that is not influenced by roots, a temporal rise of the local pO_2 was applied by using a syringe with a needle (tip diameter 0.4 mm). The needle was inserted into the submerged soil closely to the oxygen sensor at a depth of 7 cm, and 6.6 ml of ambient air was injected.

2.9.1. Single optical measurement of pH

The optical measurements of pH were conducted non-invasively from outside the rhizotrone through the transparent front plate (Fig. 10). A polymer optical fiber, POF, (d = 2 mm), transferring the excitation light to the pH detecting planar optode and the returning optical signals to the detector, was connected to a single channel pH meter (pH-1 mini; PreSens GmbH). The wavelength of the excitation light was 470 nm. At that wavelength, the energy transport of the emitted light was 0.9 mW cm^{-2} nm^{-1} at a flux rate of 0.0035 pmol photons cm^{-2} s^{-1} nm^{-1} (PreSens GmbH). The pH meter was connected to a personal computer and controlled by a specific software (Comm Logging; PreSens GmbH), recording the data at each measuring spot at a 4 s interval. The tip of the POF, positioned about 1 mm off the front plate, was moved along the abscissa and the ordinate by use of two precision stepper motors. The tip of the fiber was modified by the application of a converging lens to focus the spotlight at the surface of the pH optode (d = 1.2 mm). The stepper motors moved the glass fiber in a line-scanning mode across a preselected section of the root–rhizosphere–

soil interface of growing roots. The movements of the stepper motors were controlled by a conventional interface and software (SMC 800; Conrad Electronic GmbH, Hirschau, Germany). The experimental setup optionally allowed the creation of large-scale or small-scale high-resolution quantitative two-dimensional images at any location over the total area of the planar pH optode. In order to maintain a constant measuring interval (15 min) at different sizes of the investigated sections of the root system, the spatial resolution ranged between 1.5 and 3.0 mm. Thus, the number of measurements per turn ranged between 120 and 225. For verification of the pH data derived from the planar optode, a pH mini-electrode (diameter 1.7 mm, MI-414–6 cm pH Combination Electrode; Microelectrodes, Inc., Bedford, NH, USA) connected to a pH meter (pH 340i; WTW, Weilheim, Germany) was used to measure pH at 12 identical positions in the soil.

The relationship between the measured Φ_m and the corresponding pH value is sigmoidal, and can mathematically be described by the Boltzman Equation:

$$\Phi_m = (\Phi_{min} - \Phi_{max})/\{1+ Exp[(pH_m – pH_0) / dpH]\} + \Phi_{max} \quad (2)$$

where Φ_{min} and Φ_{max} represent the minimum and maximum range of Φ. dpH and pH_0 give the slope and inflexion point of the sigmoidal curve, respectively, and pH_m is the corresponding pH value. Thus, Eqn. 2 is solved for pH_m:

$$pH_m = pH_0 + dpH * \ln[(\Phi_{min} - \Phi_{max}) / (\Phi_{min} - \Phi_{max})-1]. \quad (3)$$

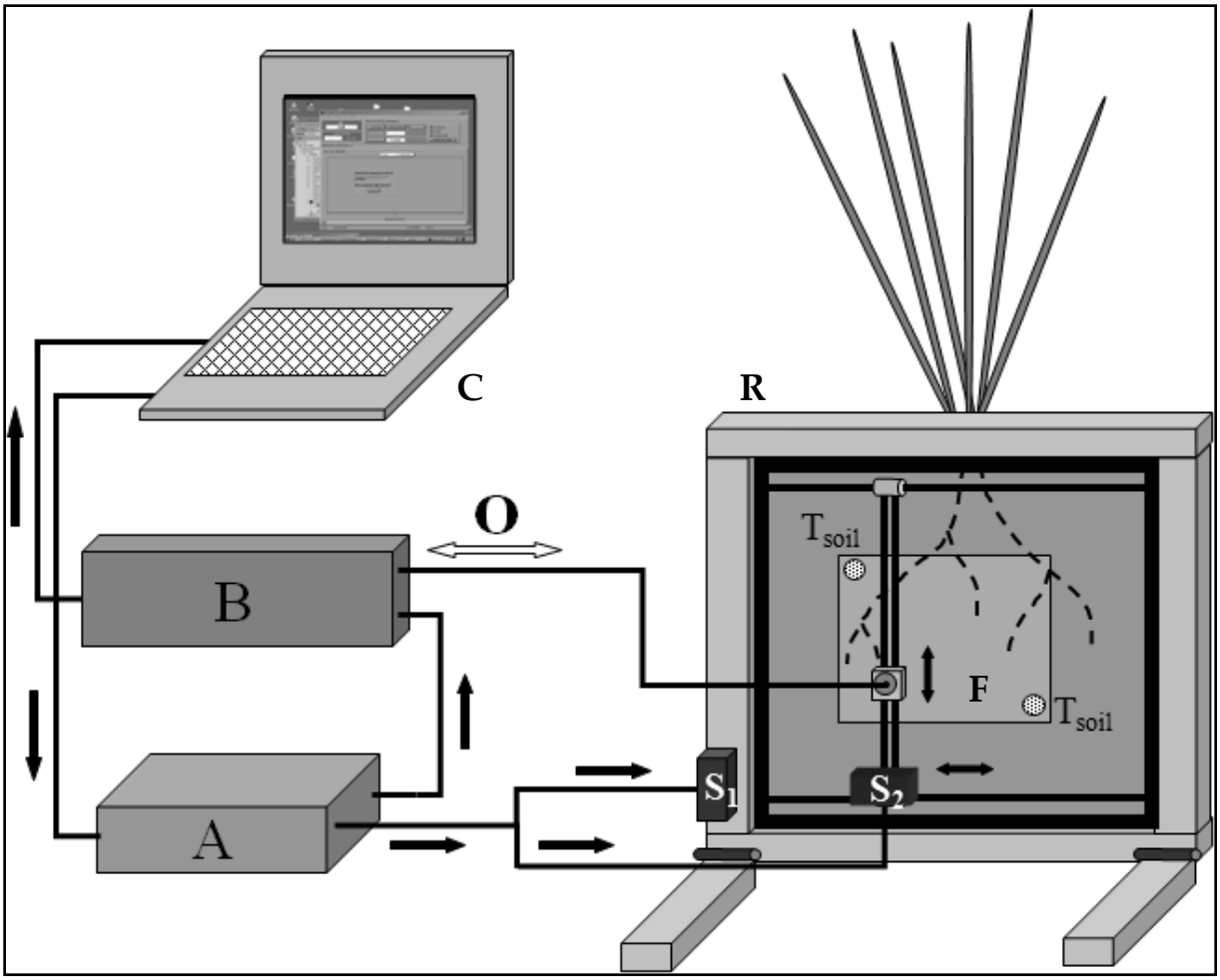

Figure 10. Scheme of the hardware components used for the optical non-invasive measurement of pH in the root–rhizosphere–soil interface of *Juncus effusus* L. with a planar optode (F). An optical fiber (O) is moved outside the rhizotrone (R) by two stepper motors (S1, S2) across the planar optode, which is fixed inside the rhizotrone. Both stepper motors are controlled by a specific interface (A), which triggers the fiber-optic detection device (B, i.e. pH-mini) after each movement of the optical fiber. The data transfer between the computer (C) and the different devices, and the trigger impulses as well, are indicated by black arrows. The optical data transfer is indicated by a double-headed white arrow. The soil temperature is measured at two positions inside R (T_{soil}). The diagram is not to scale. (BLOSSFELD & GANSERT 2007)

Calibration of the planar pH optode was done by the use of six different conventional pH buffer solutions, ranging from pH 4 to 9 (Riedel-deHaën; Sigma-Aldrich Laborchemikalien GmbH, Seelze, Germany). Six small-sized parts (4 x 4 mm) were cut from the original planar pH optode and were used as calibration replicates. Each part was fixed with conventional silicone grease to a same-sized plate of acrylic glass that was used as the front plate of the rhizotrone. The calibration temperature was kept constant in a temperature-controlled water bath (T_{cal} = 20 °C). For each pH buffer solution, the Φ_m of 10 measurements per replicate was recorded. The

arithmetic mean of all 60 measurements of each buffer solution was used as input data for a specific calibration software (pH Solver-v07; PreSens GmbH). The derived calibration values of the coefficients pH_0, dpH, Φ_{min} and Φ_{max} were used in Eqn. 3 for the calculation of the pH value. Recalibration at the end of the experiment was conducted in the same way. The effect of thermal variation on Φ_m during the experiments was compensated as follows:

$$pH_m = (pH_0 - pH_{0\text{-}T\text{-}comp}) + (dpH - dpH_{T\text{-}comp}) * \ln\{[(\Phi_{min} - \Phi_{minT\text{-}comp}) - (\Phi_{max} + \Phi_{maxT\text{-}comp})] / [\Phi_m - \Phi_{max} + \Phi_{maxT\text{-}comp})] - 1\} \quad (4)$$

where

$pH_{0\text{-}T\text{-}comp} = 0{,}01744 * (T_m - T_{cal})$

$dpH_{T\text{-}comp} = 0{,}00258 * (T_m - T_{cal})$

$\Phi_{minT\text{-}comp} = 0{,}05526 * (T_m - T_{cal})$

$\Phi_{maxT\text{-}comp} = 0{,}04402 * (T_m - T_{cal})$

T_m = measured temperature during experiment

T_{cal} = calibration temperature.

2.10. Simultaneous optical measurements of O_2 and pH by hybrid optodes

Oxygen-pH hybrid optodes are based on a one layer–two particle system. The pH indicator is covalently attached to ion permeable polymer particles, whereas the oxygen indicator is electrostatically bound to the oxygen permeable polymer nano-particles. These pH and oxygen sensitive particles are dispersed in an ion and oxygen permeable polymer layer (GANSERT *et al.* 2006). In hybrid optodes one of the major problems to overcome, is to avoid cross sensitivity of the different indicators. To overcome this problem, the multi-frequency approach has been applied for the oxygen-pH hybrid optode: Both indicator dyes have overlapping absorption and emission spectra. Thereby, simultaneous excitation of both indicator dyes with one light source is possible. One emission filter is chosen to pass the emission light from both indicators. According to this principle, an extended DLR sensor was designed (BORISOV *et al.* 2006). The only difference to the DLR principle described above (chapter 2.8.) is, that the reference dye is now sensitive to one of both analytes. Thus, for separation of information derived from both luminophores, phase shift measurements are performed at two different modulation frequencies (45 kHz and 30 kHz), and mathematical models are used for data separation. Signal discrimination is possible because the dyes, having different decay times, are modulated differently. The major advantage of multi-frequency measurement lies in a simplified and therefore much cheaper optical set-up (Fig. 11). As a peculiarity of the oxygen-pH hybrid optode, the O_2 indicator particles are not only used for determination of oxygen but also serve as a reference for short-lived fluorescence of the pH indicator. Simultaneous excitation of both indicators is performed by a blue 470 nm LED, and emission light of the indicators is filtered through an OG 530 long pass filter.

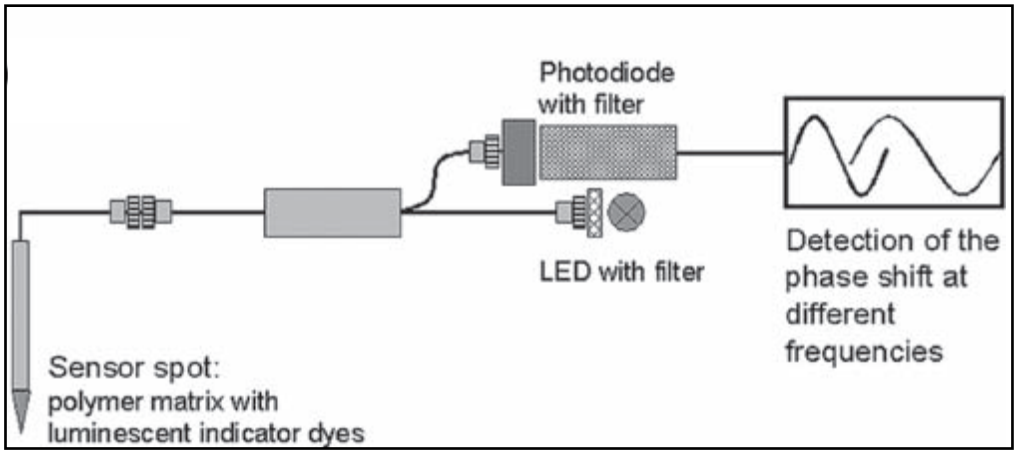

Figure 11. Optical system components for the multi-frequency measuring principle applied in hybrid optical chemical sensor technology. (GANSERT *et al.* 2006; GANSERT & BLOSSFELD 2008)

The calibration of the planar O_2-pH hybrid optode was done by a combination of the calibration methods described for the single planar pH optode and the Microx O_2-optode. But in this case the Φ_m of the hybrid sensor foil calibration replicates was measured for two modulation frequencies (45kHz and 30kHz) in six different pH buffer solutions (pH 4 to pH 9) at two different oxygen concentrations (0% and 100% air saturation) for each buffer solution. This resulted in four calibrations curves derived from six data points (Fig. 12). The calibration values of the coefficients pH_0, dpH, Φ_{min} and Φ_{max} were calculated in the same way as it was done for the single pH sensor. But due to the two different wavelengths and two different oxygen concentrations, four different values per coefficient were generated, indicated by different subscripts (45kHz-0%, 45kHz-100%, 30kHz-0%, 30kHz-100%).

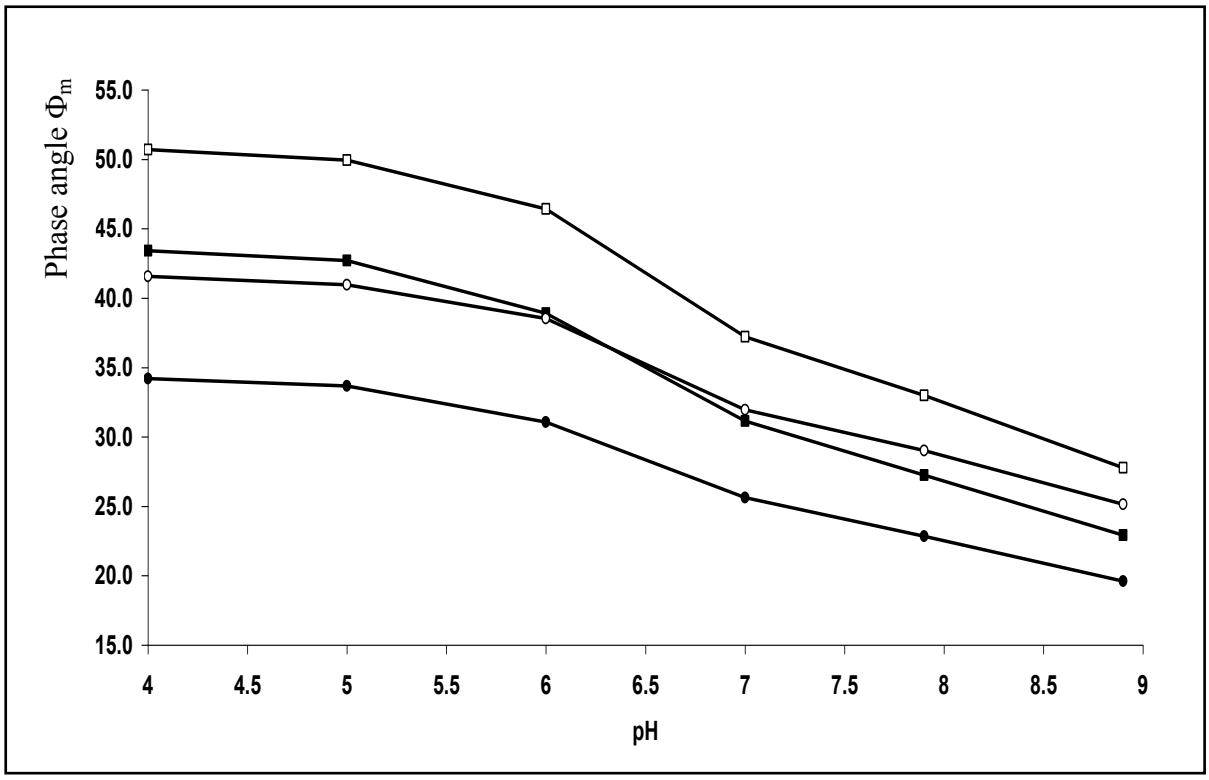

Figure 12. Calibration curves for an O_2-pH hybrid optode. Each curve reflects the phase angle Φ_m at different pO_2 and excitation wavelengths, depending on the pH value (filled boxes = 45kHz at 100% air sat., open boxes = 45kHz at 0% air sat., filled circles = 30kHz at 100% air sat., open circles = 30kHz at 0% air sat.).

Due to the fact that both analytes affected the emitted light signals of the hybrid sensor foil, the calculation of the pH-value and the oxygen concentration differed from that of single pH measurements. In the hybrid measurements the retrieved phase signals for each frequency and the calibration coefficients were used as variables in the following equations (provided by PreSens):

$$pH = pH0 + dpH * \ln((\Phi_A - \Phi_B) / (\Phi_{m\text{-}freq45khz} - \Phi_A) - 1) \quad (5)$$

$$O_2 = 100 * (k_0 / \Phi_{m\text{-}freq30kHz} - 1) / (k_0 / k_{100} - 1) \quad (6)$$

Where:

$\Phi_{m\text{-}freq45kHz}$ = measured phase angle at 45kHz

$\Phi_{m\text{-}freq30kHz}$ = measured phase angle at 30kHz

$$\Phi_A = \Phi_{min\text{-}45kHz\text{-}0\%} / (O_2 / 100 * (\Phi_{min\text{-}45kHz\text{-}0\%} / \Phi_{min\text{-}45kHz\text{-}100\%} - 1) + 1) \quad (7)$$

$$\Phi_B = \Phi_{max\text{-}45kHz\text{-}0\%} / (O_2 / 100 * (\Phi_{max\text{-}45kHz\text{-}0\%} / \Phi_{max\text{-}45kHz\text{-}100\%} - 1) + 1) \quad (8)$$

$$k_0 = (\Phi_{min\text{-}30kHz\text{-}0\%} - \Phi_{max\text{-}30kHz\text{-}0\%}) / (1 + EXP((pH - pH_0) / dpH)) + \Phi_{max\text{-}30kHz\text{-}0\%} \quad (9)$$

$$k_{100} = (\Phi_{min\text{-}30kHz\text{-}100\%} - \Phi_{max\text{-}30kHz\text{-}100\%}) / (1 + EXP((pH - pH_0) / dpH)) + \Phi_{max\text{-}30kHz\text{-}100\%} \quad (10)$$

This calculation of the pH value and the O_2 concentration caused recursions, due to the use of Eqn. 7 to 10 as input variables in Eqn. 5 and 6. These recursions were necessary to include the dependencies of oxygen concentration and pH value on the two measured phase angles at the two different modulation frequencies. The results of the recursions were calculated by the use of a conventional spreadsheet program (Microsoft Excel 2007) using a maximal iteration number of 1000 iterations in combination with a maximum change of the calculated values of 0.001 units.

2.10.1. Experimental setup for simultaneous optical O_2 and pH measurements

The experimental setup for the simultaneous optical measurements of O_2 and pH in the rhizosphere was designed similar to the single optical pH measurements with only small adaptations of the system. All plants were grown under the same environmental conditions as described in chapter 2.9. Just as for the single pH measurements, a pH-1 mini (PreSens) was connected to the stepper motor device for detecting pH and pO_2 in the soil. But contrarily to the single pH measurements, a planar pH-O_2 sensitive hybrid optode (PreSens) for sensing pH and oxygen dynamics in the soil, as well as the new type of compartmented rhizotrone was used (see chapter 2.5.).

Another major difference was that the rhizotrone compartments were filled with commercially available soils of a more acidic soil pH range (Stender AG, pH 4 – 6; Tab. 2) than in the experiments described before (pH 8), according to investigate the

plant-soil interaction under the specific strong reducing conditions, that were similar to the conditions of most wetland soils (KIRK 2004). The following soil pattern was used: compartment A was filled with E910-soil, compartment B with A600-soil and compartment C with E400-soil. The parent soil compartment was filled with E400-soil during all experiments (see Tab. 2 for soil specifications).

To check, if an oxidative acidification is prior to all other possible proton generating process in this study (e.g. H^+ excretion during NH_4^+ uptake), an additional experiment was conducted: At the end of a regular experiment with *J. effusus*, all culms were cut 1cm above the water surface and the rhizotrone top was covered with a polystyrene seal. This seal had an inlet for a continuous inflow of well defined air mixtures, provided by a N_2/O_2 gas mixing unit (see chapter 2.9.) and an outlet to prevent an overpressure within the system. The oxygen concentration of the airspace above the culms was monitored by the use of an O_2 micro-optode, pierced through the polystyrene seal (Microx; see chapter 2.9.).

This system allowed manipulation of the ambient air conditions within the rhizotrone, and thus to manipulate the oxygen concentrations within the rhizosphere without any photosynthetically derived effects. During this experiment, the artificial atmospheric oxygen concentration was reduced stepwise from 100% air saturation to 60%, 30% and finally 0% air saturation within four and a half hours. The anoxic phase was kept constant for 150 minutes and afterwards the artificial atmospheric oxygen concentration was raised within four and a half hours stepwise to 30%, 60% and finally 100% air saturation again. During this experiment, the rhizospheric pH value and oxygen concentrations were continuously measured with a planar pH-O_2 sensitive hybrid optode.

2.11. Color contour plots of measured pH and O_2 concentrations

For visualizing the axial and radial gradients of pH and O_2 concentrations along the roots and across the root–rhizosphere–soil interface, the collected database was transformed into a XYZ format (x-position, y-position and measured pH value).The colour contour plots were created by the use of the SigmaPlot software (Systat Software, Inc., San Jose, CA, USA).

3. Results

3.1. Soil moisture gradient experiment

Morphological and anatomical leaf parameters were differently influenced in the three species by soil moisture and interspecific interactions. The rather differentiated trends, detailed in the following, are depicted quantitatively in Figure 13.

3.1.1. Biometric leaf parameters of *J. effusus* in mono- vs. competition culture

The *J. effusus* monoculture experiment (Tab. 4) revealed that the average leaf dry matter content (LDMC) of *Juncus effusus* significantly decreased at increased soil moisture levels from dry (0.28 g g^{-1}) to wet conditions (0.23 g g^{-1}). However, at waterlogged soil conditions the LDMC was significant higher (0.25 g g^{-1}) than at wet soil conditions. In contrast, the average specific leaf length (SLL) of *J. effusus* was significantly higher at wet soil conditions (184.1 cm g^{-1}) compared to all other soil moisture levels, which did not differ significantly from each other due to high standard deviations. The average leaf porosity was positively correlated with increasing soil moisture level (70.2 – 83.2%), whereas the average leaf length was correlated with the soil moisture following a bell shaped curve. The peak was at low and medium moisture levels (74.5 – 75.1 cm) and the minimum values were recorded at dry (59.0 cm) and waterlogged moisture levels (61.9 cm), respectively. There was no correlation between the average leaf dry weight and the different soil moisture conditions.

Within the competition study (Tab. 4) the LDMC of *J. effusus* significantly decreased from low moisture levels (0.36 g g^{-1}) to waterlogged soil levels (0.27 g g^{-1}). However, in comparison to the monoculture, the LDMC was not significantly changed except for low (+37.6%) and wet soil conditions (+18.6%). In contrast, the SLL of *Juncus effusus* significantly increased within the competition experiment from low

soil moisture (127.2 cm g^{-1}) to wet soil conditions (181.6 cm g^{-1}). But compared to the monoculture, the SLL changed significantly at low soil moisture levels only (-29.0%). Due to the different soil moisture levels the average leaf porosity was significantly higher at wet (78.4%) and waterlogged (81.6%) than at low- (71.7%) and medium moisture levels (67.8%). There was a significant competition effect on the average leaf porosity at low (-6.9%) and medium soil moisture (-12.4%) and at wet soil levels (-5.8%). The correlation between average leaf length and the soil moisture levels during competition revealed a maximum at medium soil moisture levels (79.2 cm) and a decline of the leaf length towards dry and waterlogged soil levels. The minimum was recorded for dry soil levels (14.6 cm). In relation to the monoculture, the average leaf length significantly decreased at dry (-75.2%) and low soil moisture levels (-22.0%), but also significantly increased at wet (+8.9%) and waterlogged soil conditions (+13.1%). Within the competition basins, the average leaf dry weight was significantly affected only at dry soil levels (0.11 g). At this soil moisture level, the leaf dry weight was significantly reduced compared to the other moisture levels. Furthermore, the leaf dry weight was significantly reduced (-70.6%) compared to this particular soil level during monoculture. However, there was also a significant increase of the leaf dry weight at waterlogged soil levels (+22.3%), in comparison to the monoculture.

Table 4. Key growth parameters of *Juncus effusus* during monoculture and competition (different characters indicate significant differences between values of the same column (t-test, p<0.1, n=10), bold numbers indicate significant differences of investigated parameter at particular soil moisture during competition (t-test, p<0.1, n=10)).

	average leaf dry matter content		average specific leaf length		average leaf porosity		average leaf length		average leaf dry weight	
	g g^{-1}		cm g^{-1}		%		cm		g	
moisture level	mono-culture	competi-tion	mono-culture	competi-tion	mono-culture	competi-tion	mono-culture	competi-tion	mono-culture	competi-tion
dry	0.28 ± 0.02 a	0.36 ± 0.08 a/b	163.2 ± 15.9 a	129.5 ± 24.2 a	70.2 ± 2.0 a	69.3 ± 10.1 a/b/c	59.0 ± 2.2 a	**14.6 ± 8.6** a	0.37 ± 0.05 a	**0.11 ± 0.05** a
low	0.26 ± 0.01 b	**0.35 ± 0.03** b	179.1 ± 15.0 a	**127.2 ± 20.3** a	77.0 ± 4.0 b	**71.7 ± 0. 7** a	74.5 ± 3.7 b	**58.2 ± 3.9** b	0.42 ± 0.05 b	0.46 ± 0.05 b
medium	0.25 ± 0.01 c	0.28 ± 0.02 a	174.6 ± 25.1 a	170.8 ± 15.8 b	77.8 ± 5.1 b	**67.8 ± 5.7** a	75.1 ± 6.0 b	79.2 ± 2.5 c	0.42 ± 0.11 a/b	0.47 ± 0.04 b
wet	0.23 ± 0.01 d	**0.27 ± 0.00** a	184.0 ± 21.6 b	181.6 ± 20.7 b	83.2 ± 2.4 c	**78.4 ± 0.7** b	69.1 ± 4.7 c	**75.2 ± 4.1** c/d	0.38 ± 0.07 a/b	0.42 ± 0.06 b
waterlogged	0.25 ± 0.01 c	0.27 ± 0.01 a	169.4 ± 9.4 a	156.0 ± 10.3 a/b	82.6 ± 2.5 d	81.6 ± 0.5 c	61.9 ± 7.3 a	**70.0 ± 2.8** d	0.37 ± 0.06 a/b	**0.45 ± 0.01** b

3.1.2. Biometric leaf parameters of *J. inflexus* in mono- vs. competition culture

The *J. inflexus* monoculture study (Tab. 5) revealed that the LDMC of *J. inflexus* was negatively correlated with soil moisture, from dry (0.30 g g^{-1}) to waterlogged soil conditions (0.27 g g^{-1}). But there was no significant difference in LDMC between the medium soil moisture, wet and waterlogged soil conditions. Furthermore, the SLL of *Juncus inflexus* decreased significantly from dry (186.3 cm g^{-1}) to the waterlogged soil level (146.1 cm g^{-1}), too. The average leaf porosity was significantly higher at the wet (69.0%) and medium soil moisture levels (68.5%) than at the dry (61.2%) and low soil moisture levels (64.9%), whereas the average leaf porosity at waterlogged soil conditions (67.6%) differ only from the average leaf porosity at dry soil conditions. The maximal average leaf length was recorded at low soil moisture levels (78.6 cm) and minimum values were found at waterlogged soil levels (62.6 cm). The average leaf dry weight was maximal at low soil moisture conditions (0.45 g) and decreased from this soil moisture level towards dry (0.35 g) and waterlogged soil conditions (0.40 g).

The competition study (Tab. 5) proved that the LDMC of *Juncus inflexus* was not correlated with the different soil moisture levels in these basins. Moreover, the LDMC was nearly constant at 0.25 g g^{-1}. Only at medium soil moisture levels the LDMC was 0.01 g g^{-1} lower than at the other moisture levels. However, the LDMC was significantly reduced at all soil moisture levels in comparison to the monoculture. In contrast, the SLL of *J. inflexus* significantly decreased within the competition basins from low soil moisture (222.5 cm g^{-1}) to wet soil levels (148.4 cm g^{-1}). But in comparison to the monoculture, the SLL was significantly increased only at low (+26.8%) and medium soil moisture conditions (+ 14.9%). The average leaf porosity of *Juncus inflexus* was positively correlated with soil moisture during the competition. The minimum was 60.1% at low soil moisture conditions, which was significantly lower than the maximum of 75.0% at waterlogged soil conditions. In contrast to the monoculture, the leaf porosity was significantly increased at dry

(+6.6%), wet (+5.7%) and waterlogged soil conditions (+10.9%). There was a bell shaped curve correlation between average leaf length and the soil moisture levels during the competition experiment. The maximum was measured at medium soil moisture levels (83.9 cm). The minimum was measured at dry soil levels (50.3 cm) with a high standard deviation (± 18.9 cm). The competition effect on the average leaf length was restricted to medium soil moisture (+15.5%), wet (+26.7%) and waterlogged soil conditions (+17.0%), in comparison to the monoculture. The average leaf dry weight was positively correlated with soil moisture during the competition itself. The maximum was measured at waterlogged soil conditions (0.50 g), which was significantly higher than the minimum at dry soil conditions (0.29 g). Due to the competition effect, the leaf dry weight was significantly lower at low soil moisture levels than during monoculture (-23.6%). However, there was a significant positive competition effect on the leaf dry weight at wet (+18.8%) and waterlogged soil conditions (+25.6%).

Table 5. Key growth parameters of *Juncus inflexus* during monoculture and competition (different characters indicate significant differences between values of the same column (t-test, p<0.1, n=10), bold numbers indicate significant differences of investigated parameter at particular soil moisture during competition (t-test, p<0.1, n=10)).

	average leaf dry matter content		average specific leaf length		average leaf porosity		average leaf length		average leaf dry weight	
	g g^{-1}		cm g^{-1}		%		cm		g	
moisture level	mono-culture	competi-tion	mono-culture	competi-tion	mono-culture	competi-tion	mono-culture	competi-tion	mono-culture	competi-tion
dry	0.30 ± 0.01 a	**0.25 ± 0.01** a	186.3 ± 8.9 a	177. 9 ± 29.7 a/b/c	61.2 ± 2.2 a	**65.2 ± 2.2** a	64.3 ± 7. 5 a	50.3 ± 18.9 a	0.35 ± 0.05 a	0.29 ± 0.10 a
low	0.27 ± 0.01 b	**0.25 ± 0.01** a/b	175.4 ± 15.2 a/b	**222.5 ± 12.7** b	64.9 ± 4.2 b	60.1 ± 4. 8 a	78.6 ± 4.7 b	77.0 ± 3.9 a/b	0.45 ± 0.07 b	**0.35 ± 0.00** a
medium	0.28 ± 0.01 b/c	**0.24 ± 0.01** b	188.1 ± 18.8 a	**216.1 ± 12.5** b	68. 5 ± 2.4 c	66.0 ± 7.2 a/b	75.1 ± 6.0 b	**83.9 ± 3.6** c	0.39 ± 0.05 a/c	0.39 ± 0.04 a
wet	0.29 ± 0.01 c	**0.25 ± 0.00** a/b	169.9 ± 13.1 b	180.7 ± 11.4 c	69.0 ± 2.2 c	**72.9 ± 1.0** b	65.4 ± 5.7 a	**82.9 ± 3.1** b/c	0.39 ± 0.05 a/c	**0.46 ± 0.04** b
waterlogged	0.28 ± 0.00 c	**0.25 ± 0.01** a	146.1 ± 8.5 c a	148.4 ± 8.5 a	67.6 ± 2.3 b/c	**75.0 ± 2.0** b	62.6 ± 6.8 a	**73.3 ± 6.1** a	0.40 ± 0.04 b/c	**0.50 ± 0.07** b

3.1.3. Biometric leaf parameters of *J. articulatus* in mono- vs. competition culture

The *J. articulatus* monoculture experiment (Tab. 6) revealed the LDMC of *J. articulatus* was minimal at wet soil conditions (0.18 g g^{-1}), but maximal at dry (0.21 g g^{-1}) and waterlogged soil conditions (0.22 g g^{-1}). In contrast, the SLL of *Juncus articulatus* followed a bell shaped curve with a maximum at wet soil conditions (270.7 cm g^{-1}). The minimum SSL was recorded for the waterlogged (176.6 cm g^{-1}) and for the dry soil level (179.8 cm g^{-1}). The average leaf porosity was not correlated with the different soil moisture levels, except for a significant reduction at dry soil conditions. The average leaf length was highest at medium soil moisture levels (32.0 cm), whereas the minimum was at dry soil levels (22.1 cm). During monoculture, there was a significant difference in average leaf dry weight between wet and waterlogged soil conditions, only.

In the competition study (Tab. 6), the LDMC of *J. articulatus* was not affected by the different soil moisture levels. Only at waterlogged soil conditions, the LDMC was significantly increased (0.24 g g^{-1}), compared to the other soil moisture levels. Additionally, there was a significant competition effect compared to the monoculture only at the waterlogged soil levels (+9.2%). In contrast, the SLL of *Juncus articulatus* significantly decreased from dry (292.5 cm g^{-1}) to wet (230.5 cm g^{-1}) and waterlogged soil levels (165.1 cm g^{-1}). There was a pronounced and significant increase of SLL in the competition experiment compared to the monoculture, particularly at dry (+62.7%), low (+30.5%) and medium soil moisture levels (+48.2%), respectively. The average leaf porosity was almost not affected by soil moisture during the competition experiment and there was no significant difference in leaf porosity between the competition and the monoculture experiment. There was a correlation between average leaf length and the soil moisture levels within the competition study, with a maximum at medium soil moisture levels (47.2 cm). The minimum leaf length was measured at dry soil levels (17.6 cm) with a high standard deviation (± 10.8 cm). In comparison to the monoculture, the leaf length was significantly increased due to the

competition from low soil moisture (+62.9%) to waterlogged soil conditions (+17.8%). During competition, the average leaf dry weight significantly increased from dry (0.06 g) to waterlogged soil conditions (0.18 g). There was also a significant positive competition effect on leaf dry weight at wet (+46.8%) and waterlogged soil levels (+24.4%), compared to the monoculture experiment.

Table 6. Key growth parameters of *Juncus articulatus* during monoculture and competition (different characters indicate significant differences between values of the same column (t-test, p<0.1, n=10), bold numbers indicate significant differences of investigated parameter at particular soil moisture during competition (t-test, p<0.1, n=10)).

	average leaf dry matter content		average specific leaf length		average leaf porosity		average leaf length		average leaf dry weight	
	g g^{-1}		cm g^{-1}		%		cm		g	
moisture level	mono-culture	competi-tion	mono-culture	competi-tion	mono-culture	competi-tion	mono-culture	competi-tion	mono-culture	competi-tion
dry	0.21 ± 0.02 a/c	0.19 ± 0.01 a	179.8 ± 15.2 a/c	**292.5 ± 36.3** a	65.1 ± 2.5 a	66.3 ± 1.6 a	22.1 ± 4.4 a	17.6 ± 10.8 a	0.11 ± 0.04 a/b	0.06 ± 0.04 a
low	0.19 ± 0.02 a/b	0.19 ± 0.01 a	210.3 ± 31.7 a	**274.5 ± 17.0** a	69.0 ± 5.4 a/b	69.0 ± 7.3 a/b	25.4 ± 2.4 a	**41.3 ± 4.0** b/c	0.13 ± 0.03 a/b	0.15 ± 0.01 b
medium	0.19 ± 0.01 a/b	0.17 ± 0.02 a	228.7 ± 30.2 a/b	**338.9 ± 61.1** a	69.9 ± 4.2 b	70.1 ± 3.0 a/b	32.0 ± 1.2 b	**47.2 ± 4.2** b	0.17 ± 0.09 a/b	0.14 ± 0.03 b/c
wet	0.18 ± 0.02 b	0.21 ± 0.02 a/b	270.7 ± 57.3 b	230. 5 ± 10.3 b	69.9 ± 4.7 b	64.8 ± 7.3 a/b	31.3 ± 3.6 b	**40.2 ± 2.9** c	0.12 ± 0.02 a	**0.17 ± 0.01** b/c
waterlogged	0.22 ± 0.01 c	**0.24 ± 0.01** b	176.6 ± 25.09 c	165.1 ± 13.2 c	70.5 ± 1.9 b	69.5 ± 1.1 b	25.8 ± 1.4 a	**30.4 ± 1. 8** a	0.15 ± 0.02 b	**0.18 ± 0.01** c

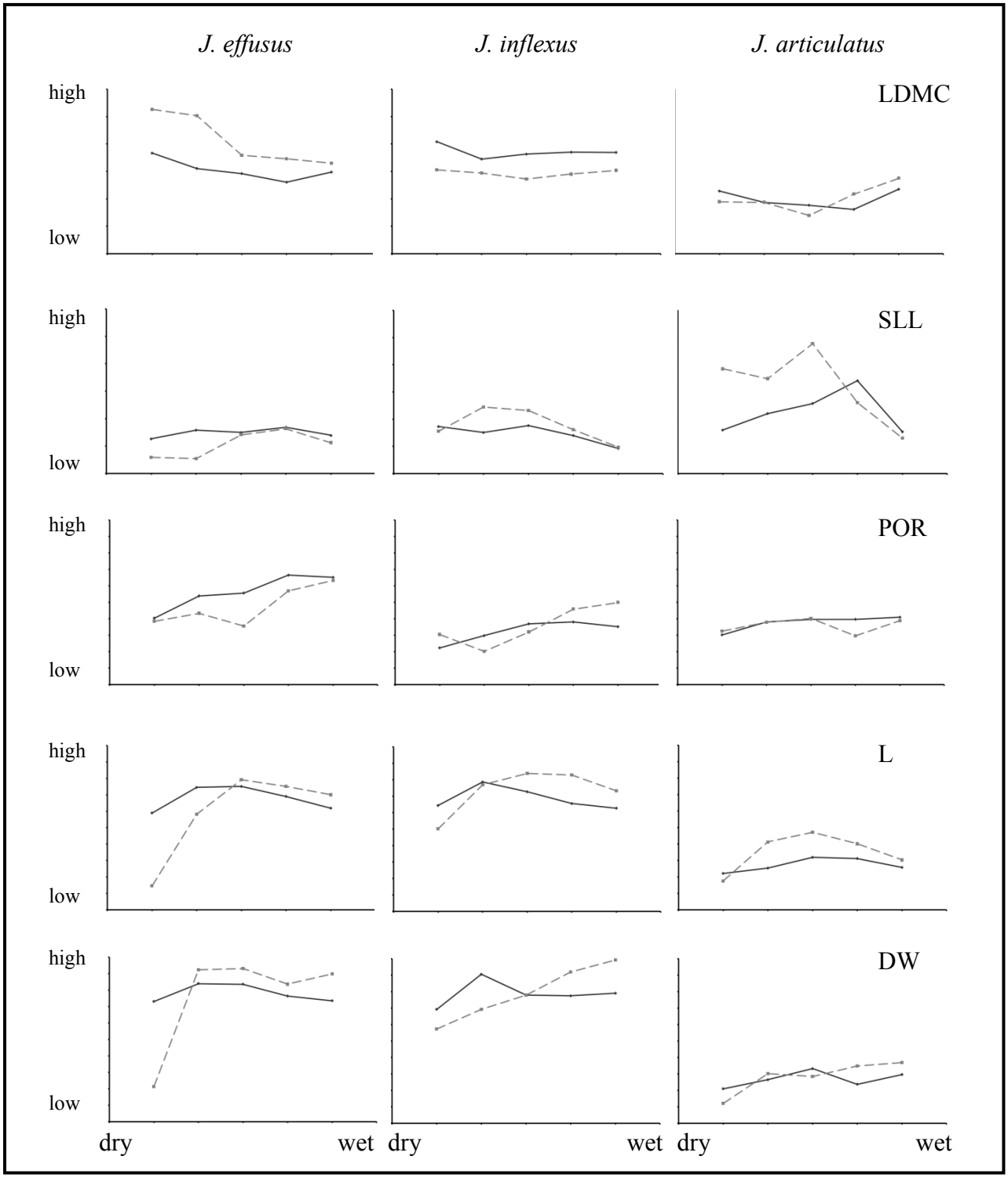

Figure 13. Qualitative response of biometric leaf parameters (leaf dry matter content = LDMC; specific leaf length = SLL; leaf porosity = POR; average leaf length = L; average leaf dry weight = DW) of *J. effusus*, *J. inflexus* and *J. articulatus* related to increased soil moisture during monoculture (dark lines) and competition treatments (light dashed lines).

The summary of the qualitative results of the soil moisture gradient experiments, as depicted in Figure 13, demonstrate that within the competition basins, all biometric leaf parameters of *J. effusus* were strongly affected under dry to medium soil moisture conditions and lesser affected under wet soil conditions, compared to the monoculture. In contrast, the biometric leaf parameters of *J. inflexus* were altered during the competition throughout the entire soil moisture range, compared to the monoculture study. Interestingly, not all biometric leaf parameters of *J. articulatus* were changed during competition. Especially leaf dry matter content, average leaf dry weight and leaf porosity were only slightly changed compared to the monoculture. Whereas specific leaf length and average leaf length were strongly increased during competition.

3.2. CO_2 and H_2O Gas exchange

To allow a correct comparison of the measured gas exchange rates, the chlorophyll content of the leaves was spectroscopically quantified by a 0.05m Tris-buffered 80% acetone extraction (PORRA 2002). These extractions revealed that the culms of *Juncus articulatus* have higher chlorophyll contents of up to 5.33 ± 1.52 mg g^{-1} compared to the other two species which do not differ from each other (*J. effusus* = 0.81 ± 0.41 mg g^{-1}, *J. inflexus* = 1.09 ± 0.37 mg g^{-1}, Tab. 7). In *J. effusus* and *J. inflexus* the average chlorophyll content was increased in the culm tips compared to the culms bases by 152.9% and 98.6%, respectively. For *J. articulatus* the increase was 57.5%. Even though there is a difference in the chlorophyll content, the chlorophyll a/b ratio in the culm tips is comparable in all investigated species. However, *Juncus effusus* has a slightly higher chlorophyll a/b ratio in the culm bases than the other two investigated species.

Table 7. Average chlorophyll content per culm dry weight and average chlorophyll a/b ratio at two different positions of the culms (base, tip; n=10).

	average chlorophyll content	**chlorophyll a/b ratio**	**average chlorophyll content**	**chlorophyll a/b ratio**
	culm tip		culm base	
	mg g^{-1} DW		mg g^{-1} DW	
Juncus effusus	0.81 ± 0.41	2.78 ± 0.63	0.32 ± 0.08	3.46 ± 0.73
Juncus inflexus	1.09 ± 0.37	2.64 ± 0.21	0.55 ± 0.42	2.28 ± 0.50
Juncus articulatus	5.33 ± 1.52	2.31 ± 0.05	3.39 ± 1.13	2.28 ± 0.09

Porometric gas exchange measurements showed that for *Juncus effusus* the maximum photosynthetic rates (A_{max}) reached 7.5 µmol CO_2 m^{-2} leaf area (LA) s^{-1}, and the light saturation (> 90% of A_{max}) of *J. effusus* was above 700 µmol photons m^{-2} s^{-1} (Fig. 14a). Light compensation point for *J. effusus* was below 30 µmol photons m^{-2} s^{-1}. For *Juncus inflexus* A_{max} was recorded at nearly 8.0 µmol CO_2 m^{-2} s^{-1}, and the light saturation of *J. inflexus* was above 800 µmol photons m^{-2} s^{-1} (Fig. 14b). Light compensation point for *J. inflexus* was below 20 µmol photons m^{-2} s^{-1}. In contrast to this, A_{max} of the investigated *Juncus articulatus* was recorded at 11.6 µmol CO_2 m^{-2} s^{-1} and the light saturation was reached at about 800 µmol photons m^{-2} s^{-1} (Fig. 14c). The light compensation point was reached at 40 µmol photons m^{-2} s^{-1}.

Temperature optimum (> 90% of A_{max}) of photosynthesis was between 19 °C and 32 °C for *Juncus effusus* (Fig. 15a). And for *J. inflexus* the temperature optimum of photosynthesis ranged between 24 °C and 39 °C (Fig. 15b), whereas it was between 23 °C and 28 °C for *J. articulatus* (Fig. 15c). The temperature range of net CO_2 gain of all investigated species reached from about 12 °C to 40 °C.

In *J. effusus*, stomatal conductance (g_s) limited photosynthesis below 0.5 mol H_2O m^{-2} s^{-1} (Fig. 16a). In contrast, g_s limited A in *J. inflexus* below 0.4 to 0.6 mol H_2O m^{-2} s^{-1}

(Fig. 16b). And for *J. articulatus*, g_s limited A already below 1.0 mol H_2O m^{-2} s^{-1} (Fig. 16c).

Transpiration rate (E) of *J. effusus* was limited by g_s below approximately 0.6 mol H_2O m^{-2} s^{-1} and reached maximal rates of 4.0 mmol m^{-2} LA s^{-1} (Fig. 17a). Whereas E of *J. inflexus* was limited by g_s below 0.8 mol H_2O m^{-2} s^{-1}. The maximal transpiration rates for this species were reached at 4.5 mmol m^{-2} LA s^{-1} (Fig. 17b). In contrast, E of *J. articulatus* was already limited by g_s below 1.4 mol H_2O m^{-2} s^{-1}. The maximal rates for this species were reached at 6.0 mmol m^{-2} LA s^{-1} (Fig. 17c).

Stomatal conductance of *J. effusus* was stable up to a vapor pressure deficit (VPD) of 1.7 to 2.8 kPa (Fig. 18a), higher VPD caused stomatal closure. In *J. inflexus* g_s was even stable until a VPD of 3.7 kPa was reached (Fig. 18b), whereas stomatal closure of *J. articulatus* already occurred above a VPD of 1.6 kPa (Fig. 18c).

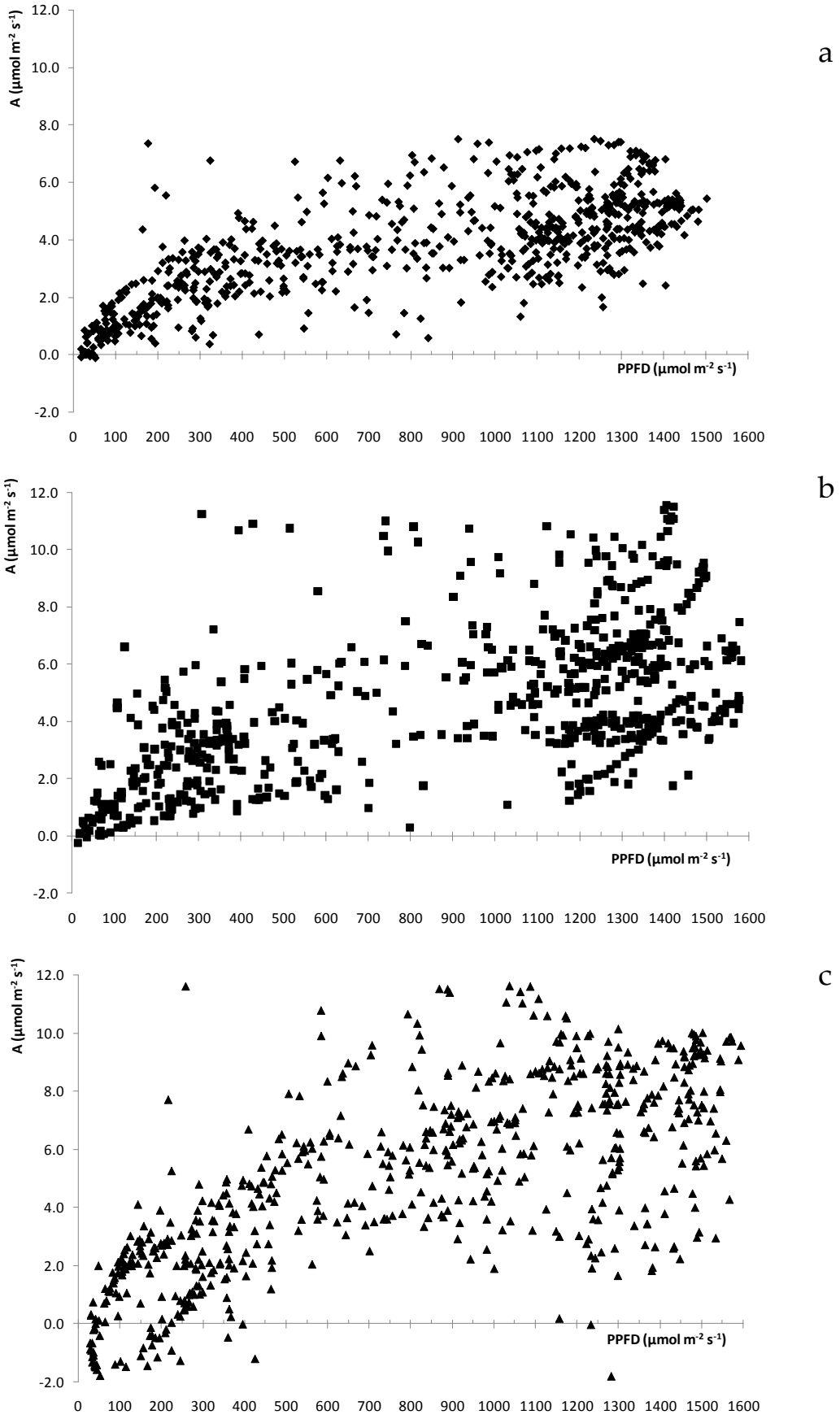

Figure 14. Photosynthetic rate (A) as a function of photosynthetic photon flux density (PPFD) of all data from diurnal courses for *J. effusus* (a), *J. inflexus* (b) and *J. articulatus* (c). Highest values of the cloud of scatter points indicate the dependency, lower values are due to limiting co-variant factors.

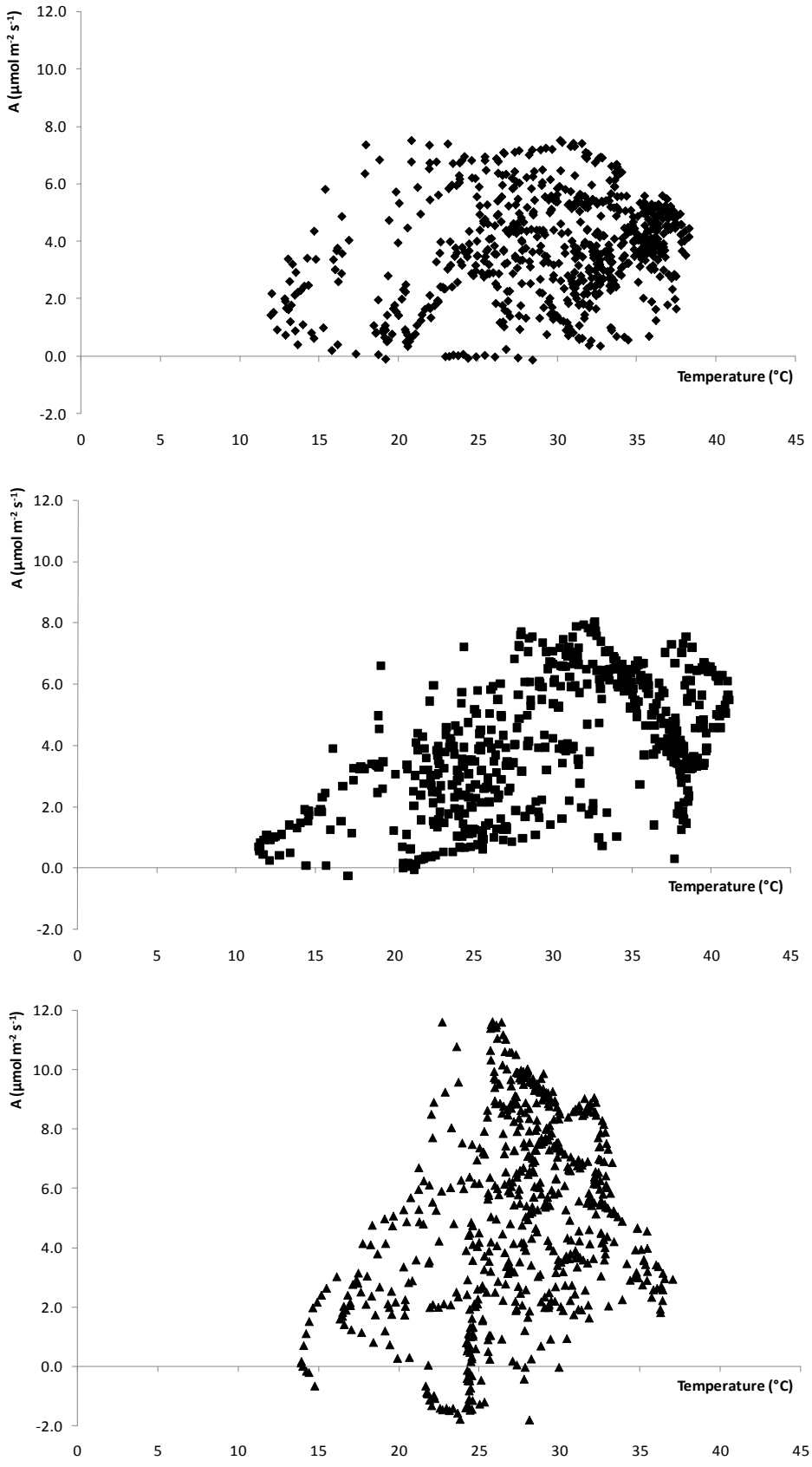

Figure 15. Photosynthetic rate (A) as a function of leaf surface temperature (T) of all data from diurnal courses for *J. effusus* (a), *J. inflexus* (b) and *J. articulatus* (c). Values below 20 °C may result from co-variant factor limitation of insufficient PPFD at early morning, values above 30 °C from co-variant factor limitation of high leaf-air VPD. For further details see Fig. 11.

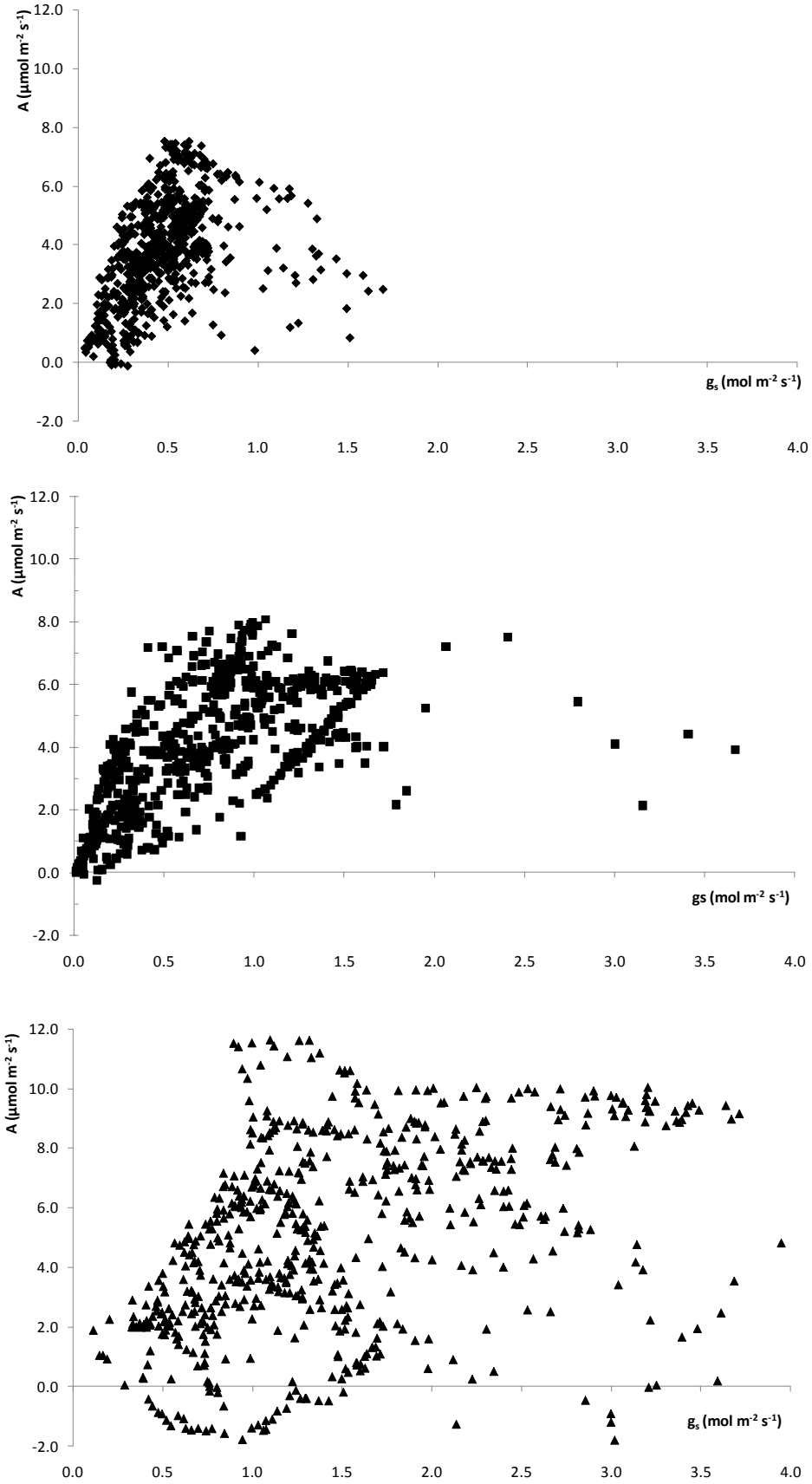

Figure 16. Photosynthetic rate (A) as a function of stomatal conductance (g_s) of all data from diurnal courses for *J. effusus* (a), *J. inflexus* (b) and *J. articulatus* (c). For further details see Fig. 11.

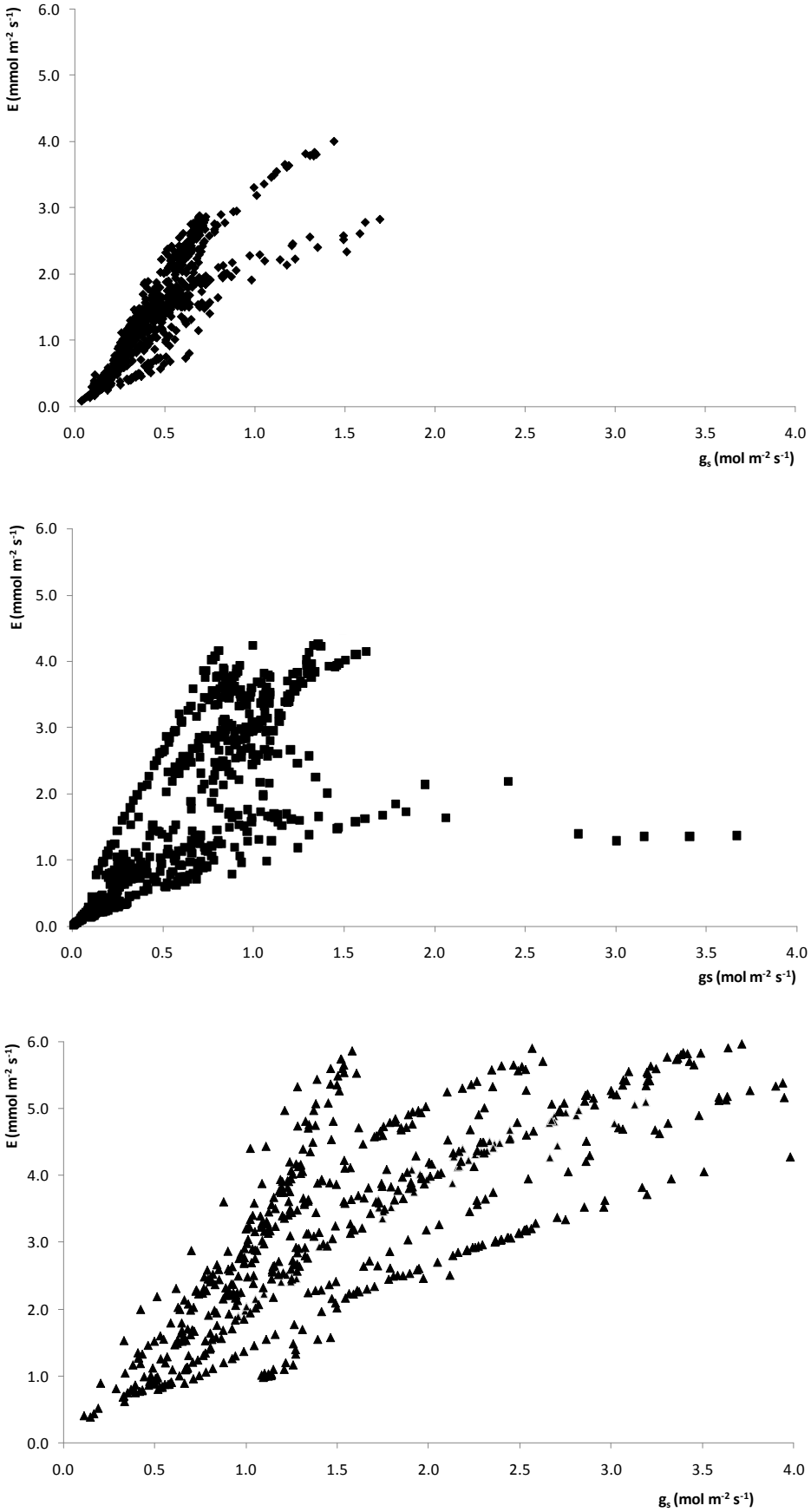

Figure 17. Transpiration rate (E) as a function of stomatal conductance (g_s) of all data from diurnal courses for *J. effusus* (a), *J. inflexus* (b) and *J. articulatus* (c). For further details see Fig. 11.

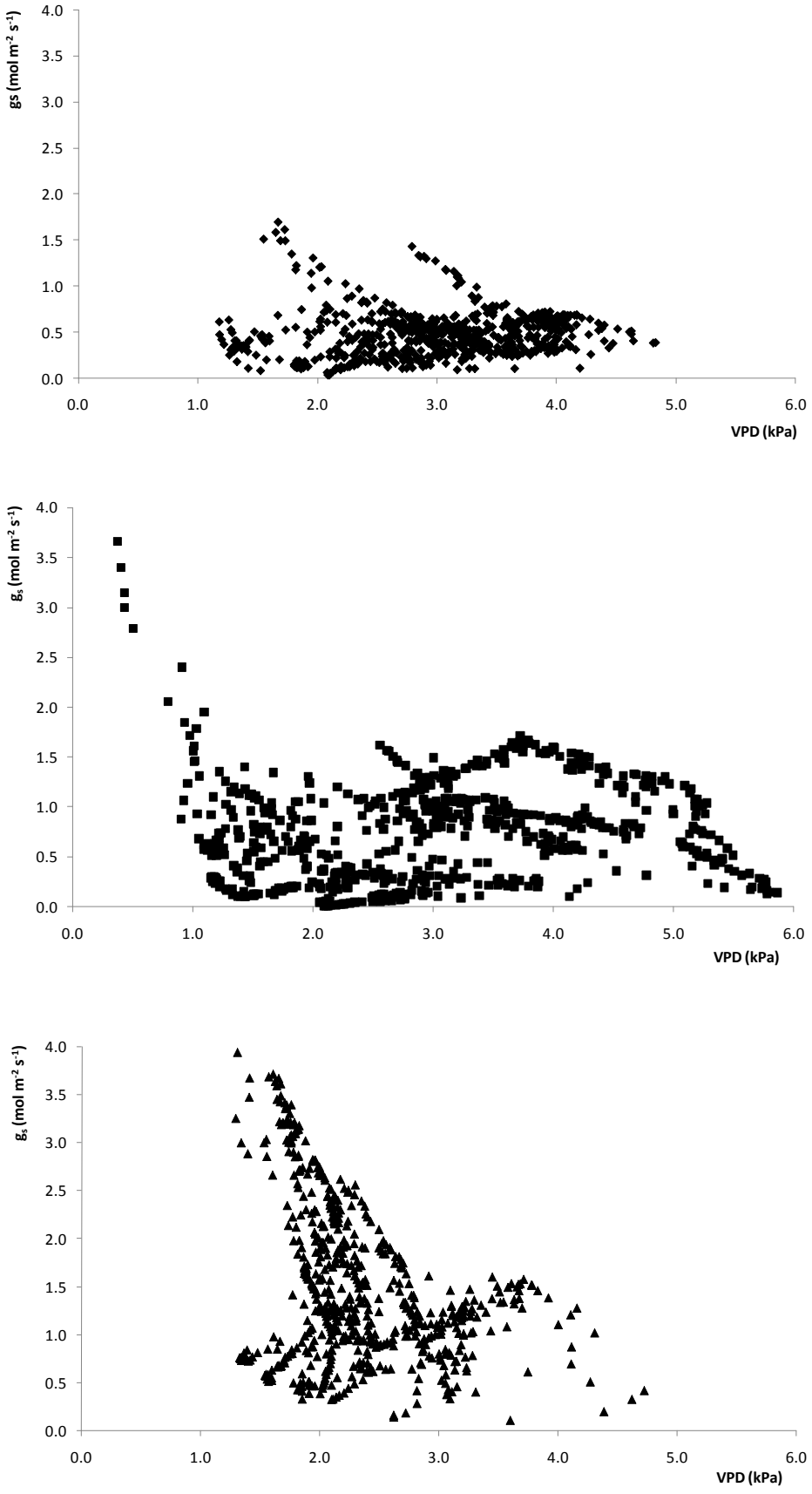

Figure 18. Stomatal conductance (g_s) as a function of vapor pressure deficit (VPD) of all data from diurnal courses for *J. effusus* (a), *J. inflexus* (b) and *J. articulatus* (c). For further details see Fig. 11.

3.3. Aerenchyma internal oxygen measurements

During days of high radiation (Fig.19, PPFD > 800 μmol photons m^{-2} s^{-1}) and temperatures above 30 °C, the culm internal oxygen concentration decreased in all investigated plant species compared to the night time average by 5 – 7% at noon due to elevated respiratory activity (Fig. 20). In the evenings and during the night, culm internal oxygen concentration reached a constant level at 90.6 ± 1.2% of ambient air (*J. effusus*), or 101.5 ± 1.3% (*J. inflexus*) and 102.7 ± 1.7% of ambient air (*J. articulatus*), when oxygen diffusion from outside just balanced the diminished respiratory activity at lower temperatures. Interestingly, equilibration of the culm atmosphere with the ambient air oxygen concentration never occurred for *J. effusus*. In contrast to *J. articulatus*, the oxygen concentration within the culms of *J. inflexus* decreased during the night time again from ambient conditions to minimal values of 97.5% ambient air. During dawn the internal oxygen concentration of *J. inflexus* rose back to ambient conditions until it declined again at noon. The negative relationship between ambient air temperature and internal oxygen concentration, especially within the culms of *J. effusus*, was most prominent, when the ambient temperature quickly dropped below 30 °C, then the internal oxygen concentration rapidly rose back to the night time average (Fig. 20; 28.07.2007 12:00h).

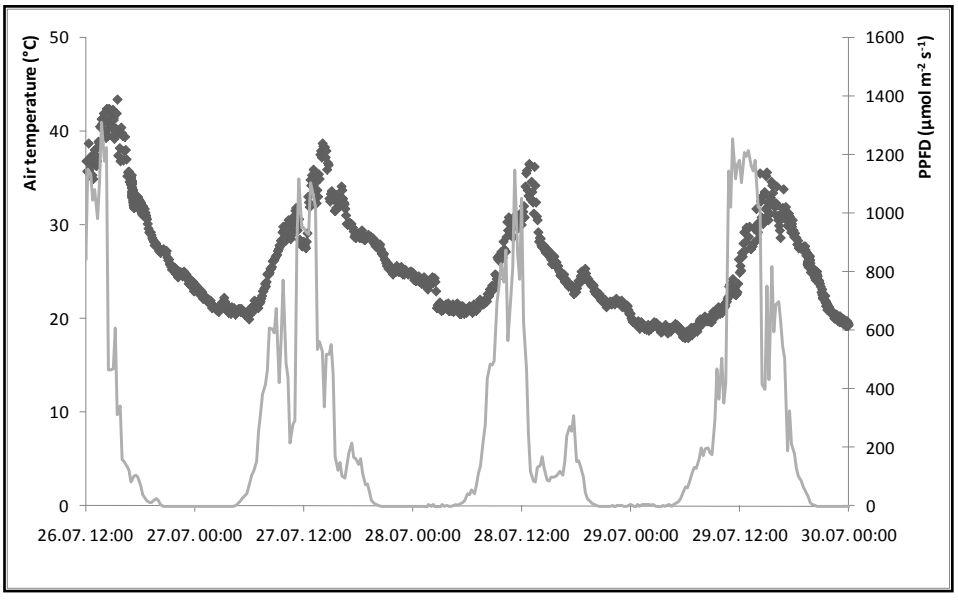

Figure 19. Diurnal courses of ambient radiation (grey line) and air temperature (bold line) during the course of the culm internal oxygen measurements.

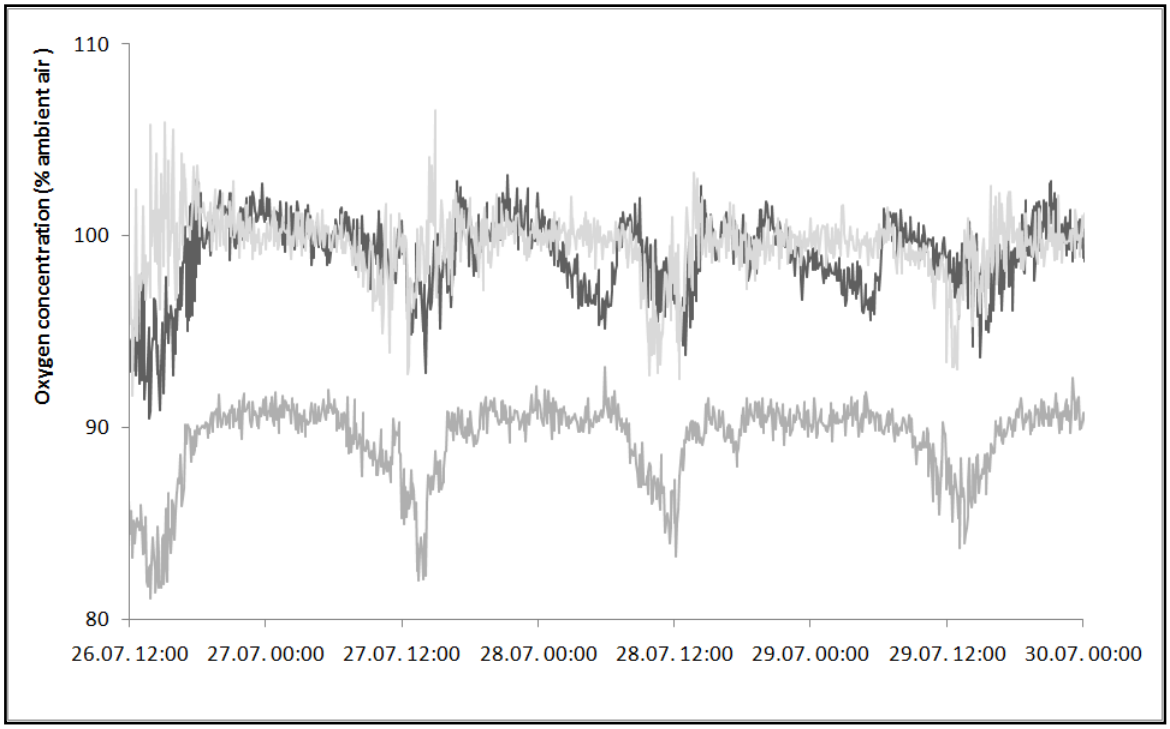

Figure 20. Diurnal turns of internal oxygen concentration in the pith of *J. effusus* (grey line below 95% ambient air), *J. articulatus* (light grey line above 95% ambient air) and *J. inflexus* (dark grey line).

Further investigation of the relationship between oxygen concentration change (ΔO_2) and temperature revealed that during daytime at temperatures higher than 25 °C the internal oxygen concentration of *J. effusus* decreased by up to 8.9% compared to the night time level (Fig. 21a). In *J. inflexus* the internal oxygen concentration was stable until 30 °C, and decreased at higher temperatures in the same manner as it was measured in *J. effusus* up to a deficit of 9.2% compared to ambient air during daytime compared to the night time level (Fig. 21b). But the scatter of the internal oxygen concentration changes in the culms of *J. inflexus* was stronger than in *J. effusus*. In contrast, the internal oxygen concentration changes in the culms of *J. articulatus* started to scatter even stronger than the other two investigated species at ambient air temperatures above 25 °C (Fig. 21c). This spreading of ΔO_2 values was coupled also with a decreasing tendency of the cloud of scatter points above ambient air temperatures of 30 °C. This value spreading of the internal oxygen concentration changes in the culms of *J. articulatus* increased even further with increasing temperatures and the maximum spread of ΔO_2 (± 8 % of ambient air) was reached at 40 °C. A fitting of the data clouds by the Arrhenius function (GANSERT & BURGDORF

2005; SCHOPFER & BRENNICKE 2006) was only possible for *J. effusus* (R^2 = 0.6312; Fig. 21a), whereas this fitting was prohibited by the broad scatter of data points measured for *J. inflexus* and *J. articulatus*.

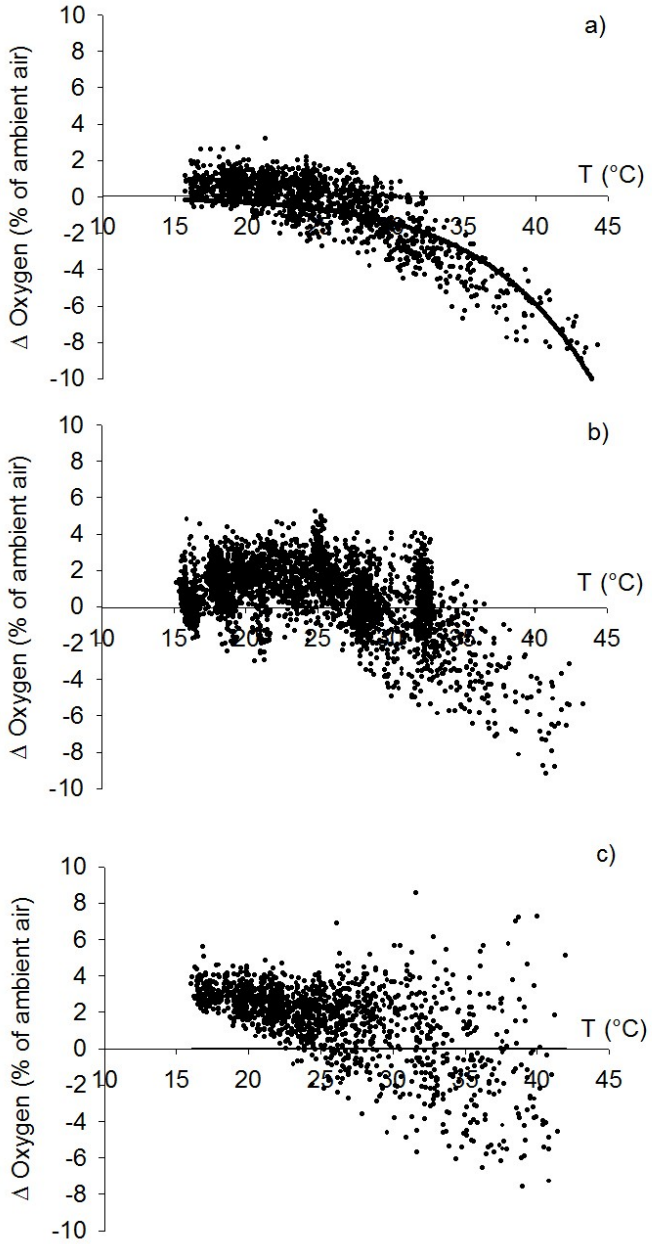

Figure 21. Differences in oxygen concentrations of the aerenchyma between daytime values and the average night time level. The latter was 90.6% of ambient air for *J. effusus* (a), 101.5% for *J. inflexus* (b) and 102.7% for *J. articulatus* (c). Bold line represents the modified Arrhenius equation "f" for the bulk of data (R^2 = 0.6312, f = k*1e10*EXP(-a*1000/(8.31441*(x+273.15))); k = -3.39564e+009; a = 1.12471e+002).

In contrast, under laboratory conditions with less extreme temperatures the culm internal aeration dynamics were reversed compared to the field experiments. A light induced increase of the culm internal oxygen concentration, probably from photosynthetic oxygen production, was detectable in all of the investigated plant species. Figure 22 shows exemplarily the change of internal oxygen concentration for *J. effusus* under laboratory conditions. The average internal oxygen concentration of *J. effusus* varied around ambient conditions during daytime (98.2 ± 1.2% of ambient air) and dropped to 92.1 ± 1.5% ambient air during night time. Similar conditions were measured in the culms of *J. inflexus* and *J. articulatus*. During daytime the average culm internal oxygen concentration of *J. inflexus* was 101.2 ± 2.8% of ambient air and *J. articulatus* showed even higher internal oxygen concentrations of 104.7 ± 3.7% ambient air. During night time an internal oxygen concentration of 95.1 ± 1.2% ambient air was measured in the culms of *J. inflexus* and 94.9 ± 2.0% ambient air in the culms of *J. articulatus*, respectively. Not only the general temperature level, but also the temperature changes in the laboratory were rather small (overall daytime average 24.8 ± 0.4 °C, overall night time average 22.6 ± 0.5 °C).

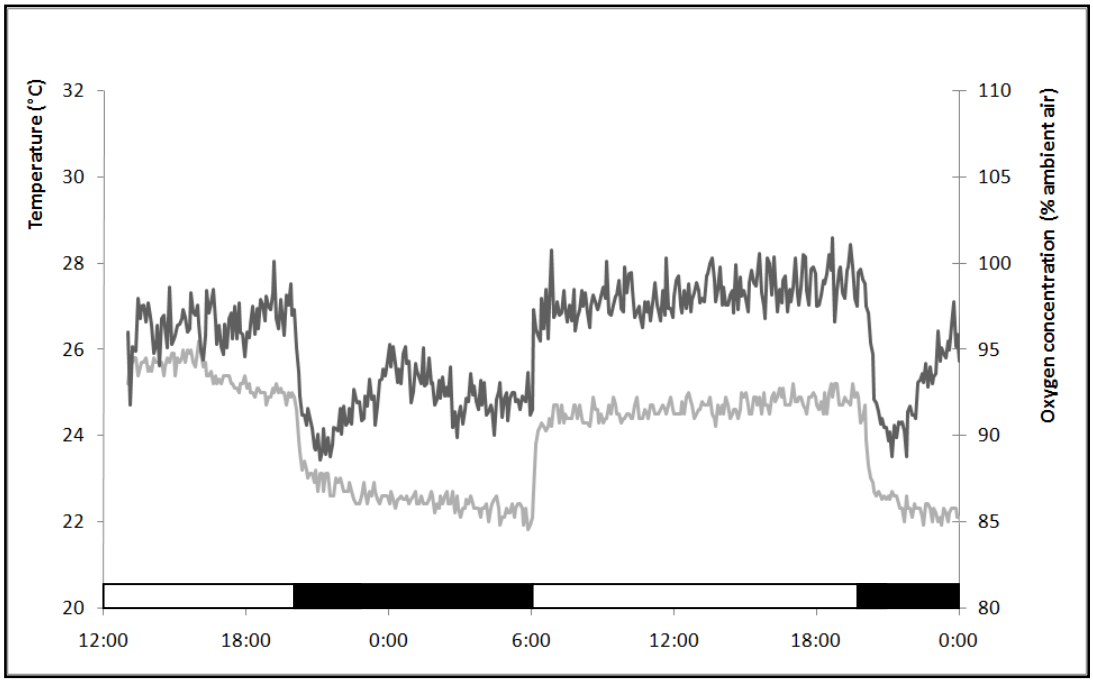

Figure 22. Diurnal turns of internal oxygen concentration (dark line) in the pith of *J. effusus* under laboratory conditions. Light grey line represents air temperature. Filled areas indicate night phases and open areas indicate day phases.

3.4. Determination of carboxylic acids by Capillary Electrophoresis (CE) analysis

3.4.1. Organic acids in the bulk soil

The suitability of the CE method is demonstrated for a bulk soil solution derived from test-compartment 'B' (Fig. 23). Despite considerable amounts of inorganic anions (e.g. carbonate, nitrate, sulphate, chloride, etc.) as matrix compounds the organic acids oxalate, formate, acetate, and lactate, could clearly be discriminated. Other common organic acids that often occur in soil e.g. citrate were not detectable.

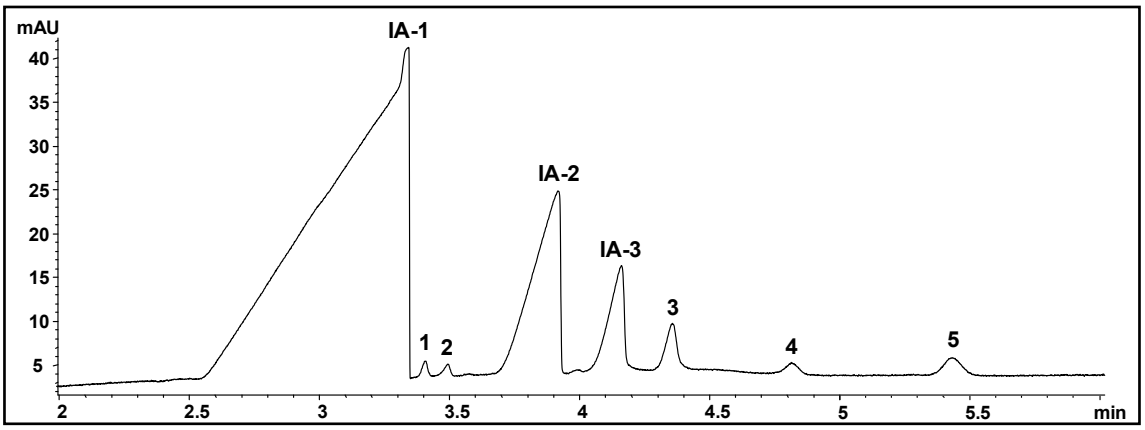

Figure 23. Electropherogram obtained from a bulk soil solution of the test compartment 'B' (pH 3.9). Peaks: (1) oxalate, (2) formate, (3) acetate, (4) lactate, (5) phenylacetic acid (internal standard), (IA-1) nitrate/ sulphate/ chloride, (IA-2) phosphate, (IA-3) carbonate.

In the *J. inflexus* experiment, the concentration of organic acids in the bulk soil of the parent soil compartment and the test-compartment 'C' added up to 96.0 µM or 91.2 µM respectively. But their concentration nearly doubled to 161.3 µM in the bulk soil of the test-compartment 'B' (Tab. 8). Moreover, the concentration of formate and oxalate increased under acidic soil conditions, whereas the concentration of lactate decreased. Interestingly, acetate was not detectable in the parent soil of the *J. inflexus* experiment, but high quantities were detected in the bulk soil of the acidic test-compartment 'B' (42.4 µM) and lower quantities (8.0 µM) in the test-compartment 'C' (Tab. 8). In comparison, the total amount of organic acids in the bulk soil was 76.6 µM in the parent soil compartment of *J. effusus* and 88.6 µM in the test-compartment

'C'. On the other hand the total amount of organic acids in the parent soil compartment of *J. articulatus* was 89.4 μM and 75.9 μM in the test-compartment 'C'. Thus, the total amounts of the organic acids in the bulk soil of the parent soil and the test-compartment 'C' in the *J. effusus* and *J. articulatus* experiments were lower but in a comparable range. However, strong differences between the experiments arose in the test-compartment 'B'. In contrast to the *J. inflexus* experiment, the total amount of organic acids in the test-compartment 'B' were strongly reduced in the case of *J. effusus* (92.2 μM) and increased in the case of *J. articulatus* (208.2 μM). Furthermore, the composition of organic acids in the bulk soil in the *J. effusus* and *J. articulatus* experiments was also quite different. In these cases no formate but acetate was present in the parent soil compartment, compared to the *J. inflexus* experiment. In both cases the bulk soil acetate concentration increased under the acidic soil conditions of test-compartment 'B' (Tab. 8). Additionally, formate was only present at very low concentrations (6.3 μM) in the case of *J. articulatus* in the test-compartment 'B'. However, formate was not detectable at all in any compartment in the case of *J. effusus*. Another interesting fact is, that the bulk soil lactate concentration increased under the acidic soil conditions (test-compartment 'B') in the *J. articulatus* experiment (116.5 μM), whereas it was the opposite in the case of *J. effusus* (14.6 μM; Tab. 8). This pattern was reversed for the bulk soil oxalate concentration, i.e. the oxalate concentration decreased under acidic soil conditions in the case of *J. articulatus* down to 15.5 μM and increased to 36.4 μM in the case of *J. effusus*.

Table 8. Distribution of organic acids in the bulk soil of the parent soil compartment 'P' (i.e. the same soil as in test-compartment 'A') and the test-compartments 'B' and 'C' of the three investigated species. Limit of detection (LOD) was reached at 0.5 µM.

	Mean concentration of organic acids (µM), n=10								
Organic acid	*J. inflexus*			*J. effusus*			*J. articulatus*		
	'P'/'A'	'B'	'C'	'P'/'A'	'B'	'C'	'P'/'A'	'B'	'C'
oxalate	10.4 ± 7.1	36.9 ± 9.4	9.0 ± 6.7	23.3 ± 5.0	36.4 ± 19.3	29.6 ± 6.5	24.1 ± 10.9	15.5 ± 9.1	21.1 ± 4.0
formate	25.6 ± 7.7	45.2 ± 13.7	27.1 ± 11.4	< LOD	< LOD	< LOD	< LOD	6.3 ± 3.6	< LOD
lactate	50.0 ± 26.3	36.8 ± 24.3	47.1 ± 18.0	21.8 ± 12.5	14.6 ± 4.4	31.7 ± 19.0	45.1 ± 24.7	116.5 ± 54.4	37.8 ± 21.5
acetate	< LOD	42.4 ± 26.0	8.0 ± 5.2	31.5 ± 7.7	41.2 ± 20.2	27.3 ± 15.2	20.2 ± 6.0	69.9 ± 35.3	17.0 ± 5.1

3.4.2. Organic acids in the rhizosphere

Again, as measured for the bulk soil, only four different organic acids were detectable in the rhizosphere of the investigated species: oxalate, formate, lactate and acetate. Other organic acids that were commonly found in the rhizosphere of plants growing in unsaturated soil like citrate or malate were not found in the rhizospheric soil solution of this study.

Compared to the bulk soil, the CE analysis of the rooted soil showed a strong impact of the roots on the distribution of the organic acids. For example, a cross transect of 1 mm-intervals across three roots of *Juncus inflexus* growing in the parent soil compartment showed that the highest concentration of lactate occurred 2 mm off the root surface (96.2 and 77.3 µM at positions 1 and 5 respectively, Fig. 24), while at the root surface lactate was significantly reduced to 28.1 µM and 17.7 µM (Fig. 24, positions 3 and 9). Reduction of organic acid concentration at the root surface was also observed on root 2, where formate dropped from 39.5 to 20.7 µM followed by an increase to 26.4 µM at a distance of 2 mm from the root surface (Fig. 24 , positions 7 -

11). However, root 1 showed a less pronounced radial profile of formate concentration. Even though oxalate concentrations were close to the detection limit, roots had a decreasing effect on oxalate, too. Compared to the bulk soil (Tab. 8), the total concentration of organic acids at the root surface of *J. inflexus* was decreased by more than 50% (Fig. 24, positions 3 & 9). In general similar impacts of plant roots on the concentration of organic acids were detected also for *J. effusus* and *J. articulatus*, but there were also some differences. First of all there was no formate detectable in the rhizospheric soil solution samples of *J. effusus and J. articulatus*, but in contrast to *J. inflexus* acetate was detectable. Especially in the case of *J. effusus* the concentration of acetate was strongly reduced at the root surfaces and their proximate environment (Fig. 25, positions 1 to 6). In fact, acetate concentration was below detection limit at the root surfaces (sampling positions 2 and 5). The acetate concentration increased again up to 47.7 µM at distances farther than 2 mm off the root surface. This pattern was also typical for the rhizosphere of *J. articulatus* (Fig. 26), but in general the acetate concentration in the proximate environment of the roots (± >2 mm) was higher than in the case of *J. effusus*. In both experiments *(J. effusus* and *J. articulatus),* the oxalate concentrations were rather stable and varied between 17.9 µM and 24.6 µM in the case of *J. effusus* (Fig. 25), and between 18.0 and 33.6 µM in the case of *J. articulatus* (Fig. 26). In contrast to the situation in the *J. inflexus* experiment, the lactate concentration in the *J. effusus* experiment showed no root induced decline and was never higher than 28.9 µM (Fig. 25). But on the other hand, the lactate concentration declined in the *J. articulatus* experiment from 78.3 µM at position 8 (3 mm off the root surface) to below the detection limit at the root surface (Fig. 26). Compared to the total organic acid content in the bulk soil, the total organic acid content at the root surface of *J. effusus* and *J. articulatus* was reduced up to 52% and 47%, respectively (Tab. 8; Fig. 25 pos. 2 & 5; Fig. 26 pos. 5).

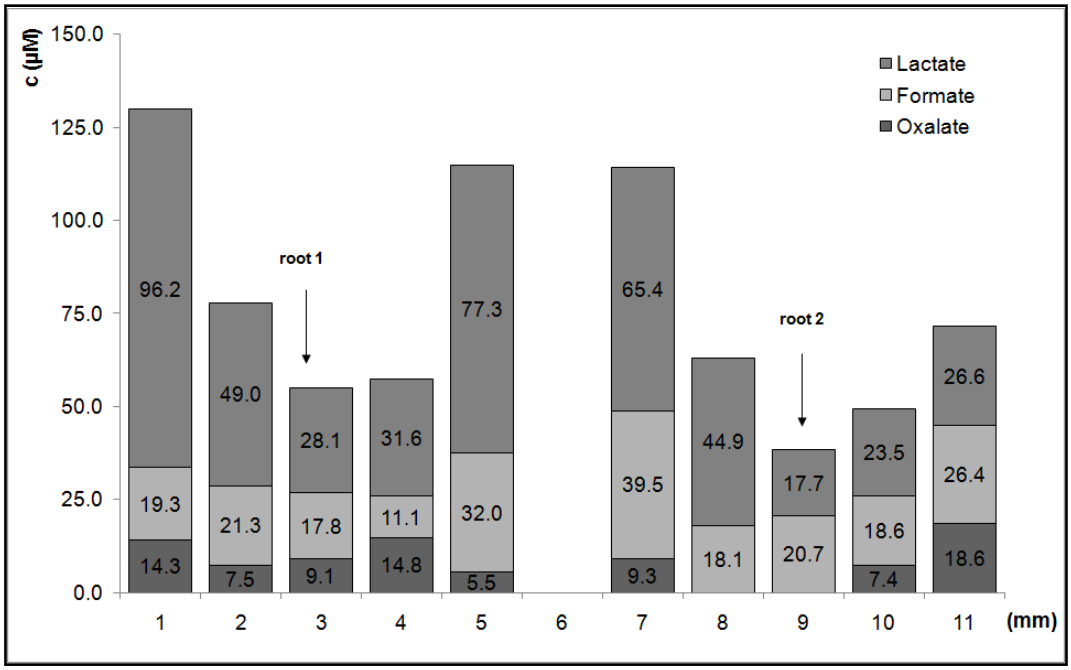

Figure 24. Distribution pattern of organic acids in a linear transect across the rooted soil (parent soil compartment, *J. inflexus*). Abscissa indicates sampling position in mm. The concentrations of the organic acids were stacked up per each sampling point. The numbers in each part of the columns indicate the single concentrations of the different organic acids per sampling point. The position of the two root surfaces (root 1-2) are indicated by arrows pointing at the corresponding column.

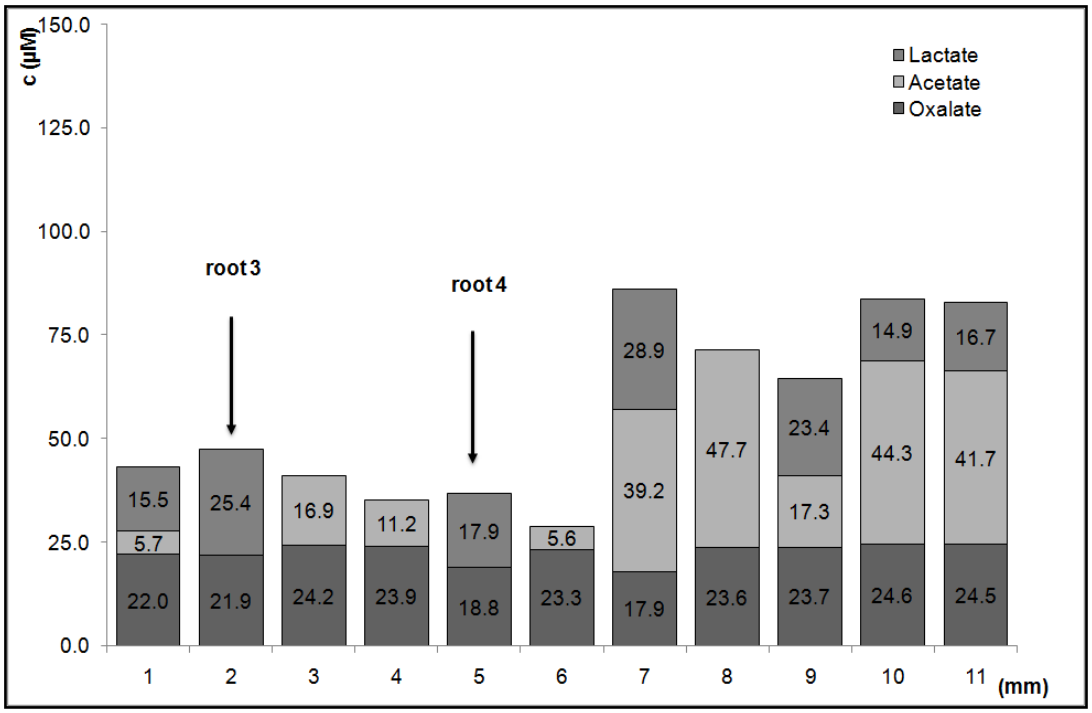

Figure 25. Distribution pattern of organic acids in a linear transect across the rooted soil (parent soil compartment, *J. effusus*). Abscissa indicates sampling position in mm. The concentrations of the organic acids were stacked up per each sampling point. The numbers in each part of the columns indicate the single concentrations of the different organic acids per sampling point. The position of the two root surfaces (root 3-4) are indicated by arrows pointing at the corresponding column.

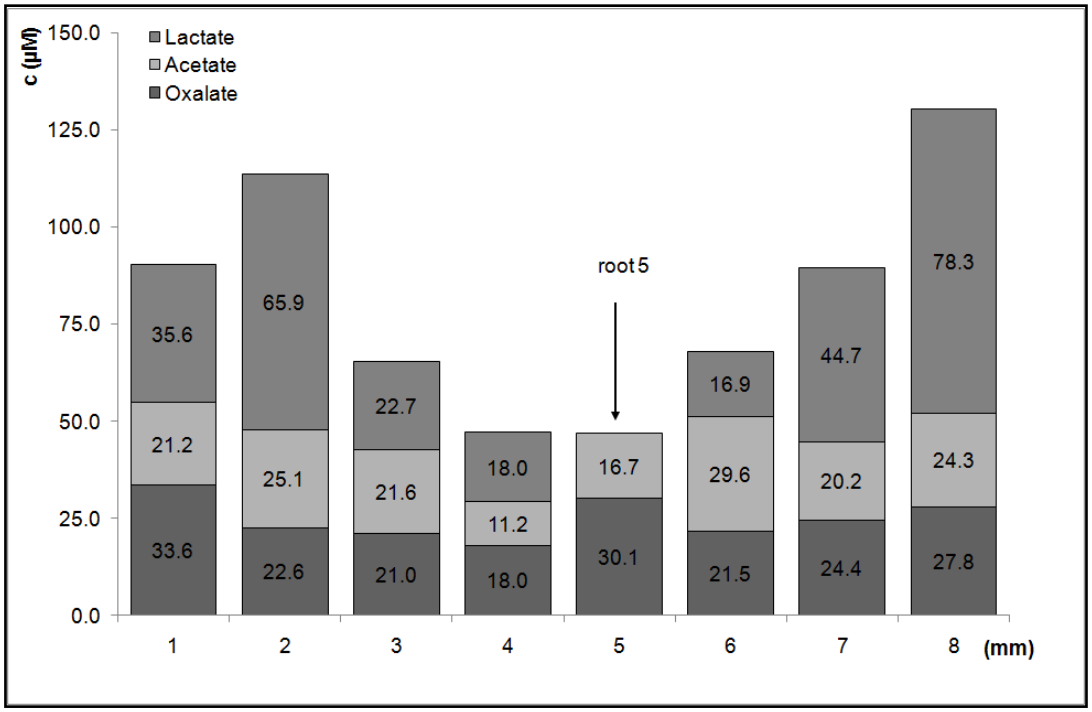

Figure 26. Distribution pattern of organic acids in a linear transect across the rooted soil (parent soil compartment, *J. articulatus*). Abscissa indicates sampling position in mm. The concentrations of the organic acids were stacked up per each sampling point. The numbers in each part of the columns indicate the single concentrations of the different organic acids per sampling point. The position of the root surface (root 5) are indicated by arrows pointing at the corresponding column.

In the acidic test-compartment 'B' profiles of organic acids across two growing roots of *J. inflexus* (6 and 7) were measured at a 2 mm-interval (Fig. 27). The data showed that besides lactate, formate and oxalate, acetate was present at considerable concentrations in the soil. Regarding root 6, the acetate concentration was highest at 2 and 4 mm off the root surface (Fig. 27, position 8: 176.0 µM) and it decreased to very low concentrations at the root surface (Fig. 27, position 4: 3.4 µM). The concentrations of lactate and formate also decreased towards this root of *J. inflexus*, but the variation was less pronounced as it was observed for acetate. With respect to oxalate, the data did not indicate a clear effect of the roots on the concentration of this organic acid. Interestingly, the effect of root 7 on the distribution of the organic acids showed a striking difference from all the other roots (Fig. 27 position 22). For this root, no decline of the concentration of any organic acid from the proximate soil towards the root surface was detectable. Figure 26 also illustrates, that near the roots 6 and 7 (± 2

mm) grown in the acid substrate, the mean concentrations of oxalate and formate (29.4 ± 9.2 µM and 33.4 ± 9.2 µM) were considerably higher compared to the data derived from the roots 1 and 2 that grew in the less acidic parent soil compartment (Fig. 24 oxalate: 8.7 ± 6.1 µM, formate: 22.5 ± 8.1 µM). Compared to the bulk soil, the total organic acid content at the root surface of *J. inflexus* was reduced by up to 55% (Tab. 8).

The data retrieved from the acidic test-compartment 'B' of the *J. articulatus* experiment showed only a transect through the bulk soil, due to missing root growth in the test-compartments (see also chapter 3.8.). Interestingly, the proportion of the single organic acids in this acidic soil was different from what was found in the same soil during the *J. inflexus* experiment. In the case of the *J. articulatus* experiment, lactate was the predominant organic acid with a maximum concentration of 177.4 µM (Fig. 28, position 8). Formate on the other hand, was almost not abundant in the acidic soil during the *J. articulatus* experiment, whereas the acetate concentration varied strongly along the transect. The maximum acetate concentration was found at position 6 (92.4 µM; Fig. 28). Also, the total amount and the composition of the organic acids in the acid test-compartment from the *J. effusus* experiment were also very different from the other two experiments. For example lactate was only a minor abundant organic acid, detected at only two sampling positions of this transect, with a maximum concentration of 17.6 µM (Fig. 29, position 14). On the other hand, formate was not detectable at all in this transect. The predominant organic acids of this transect were acetate and oxalate with maximum concentrations of 84.6 µM and 43.3 µM respectively (Fig. 29, positions 4 & 12). The impact of the root surface was not as prominent as it was detected for the other two species (Fig. 29, position 8). Moreover, the positions 2 and 16 of this transect show even lower total amounts of organic acids than position 8 although no root was visible at these positions. Due to this, the total organic acid content at the root surface was only 25% lower than the average total organic acid content of the bulk soil (Tab. 8).

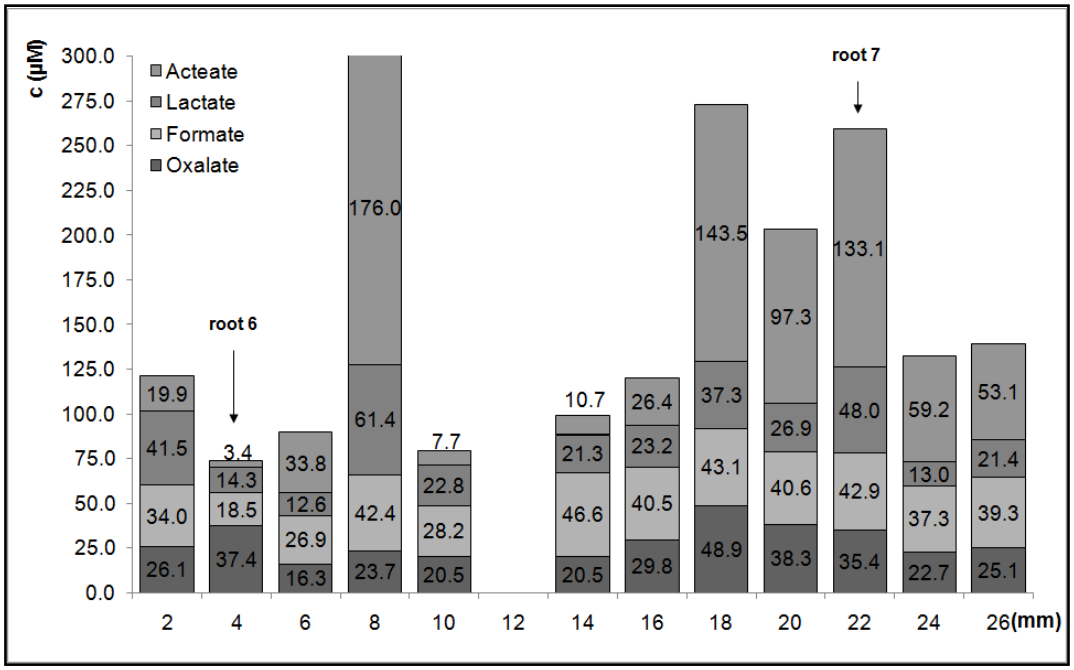

Figure 27. Distribution pattern of organic acids in a linear 2mm-transect across the rooted soil (test compartment B, *J. inflexus*). Abscissa indicates sampling position in mm. The concentrations of the organic acids were stacked up per each sampling point. The numbers in each part of the columns indicate the single concentrations of the different organic acids per sampling point. The position of the two root surfaces (root 6 and 7) are indicated by arrows pointing at the corresponding column.

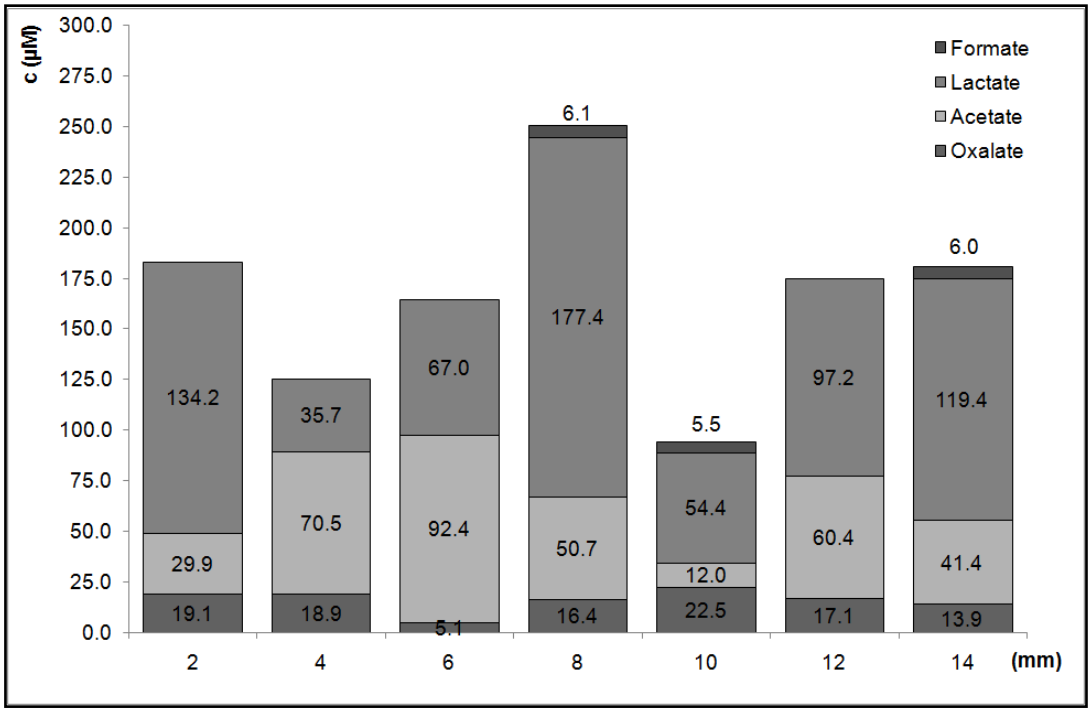

Figure 28. Distribution pattern of organic acids in a linear 2mm-transect across the rooted soil (test compartment B, *J. articulatus*). Abscissa indicates sampling position in mm. The concentrations of the organic acids were stacked up per each sampling point. The numbers in each part of the columns indicate the single concentrations of the different organic acids per sampling point.

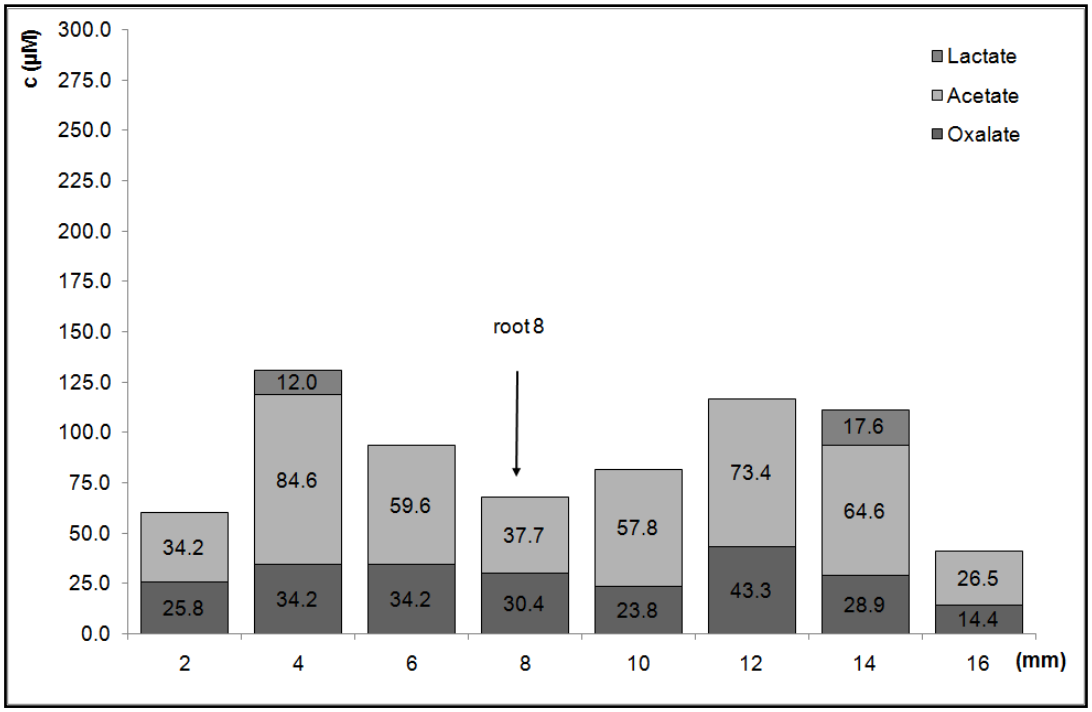

Figure 29. Distribution pattern of organic acids in a linear 2mm-transect across the rooted soil (test compartment B, *J. effusus*). Abscissa indicates sampling position in mm. The concentrations of the organic acids were stacked up per each sampling point. The numbers in each part of the columns indicate the single concentrations of the different organic acids per sampling point. The position of the root surface (root 8) is indicated by an arrow pointing at the corresponding column.

3.5. Technical qualification of the planar optodes

Long-term measurements with the planar optodes showed a very high stability of the pH and O_2-sensitive indicator dyes. Comparison of this optical measuring technique with different pH and oxygen measuring techniques (i.e. pH-electrodes, O_2-analyzer in combination with a gas mixing unit; for further information see chapter 2.9.) during the calibration and recalibration processes ensured and proved the accuracy of the planar optodes during the measurements.

For the single pH measurements, the calculation error of pH (Eqn. 3) ranged between 0.01 and 0.06 pH-units across the range of pH 4 to pH 9. The recalibration of the planar single pH optode showed almost no drift of the phase angle Φ, especially in the range of the measurements between pH 6.5 and pH 8.0. Maximum drift of the Φ occurred at pH 9 with an up shift of Φ by 1.03°, corresponding to a downshift of 0.2

pH units compared with the precalibration (Fig. 30a). At pH values below 6.5, the recalibration showed a downshift of maximal 0.62°, corresponding to an upshift of 0.4 pH units compared with the precalibration (Fig. 30a).

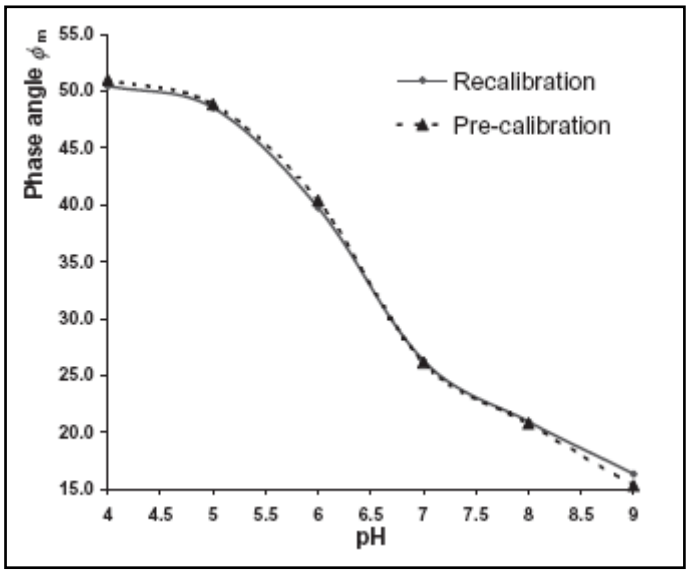

Figure 30a. Calibration curves of the planar pH optode at the beginning of the experiment (pre-calibration) and at the end of the experiment (recalibration). The measured phase angle Φm reflects the pH as shown in Eqn 3.

On the other side, the continuous use of the planar pH-O_2 hybrid optode for more than eight weeks during each experiment revealed a very good fit of the iteration model (Eqns. 5 & 6). The errors of this iteration model for pH and oxygen calculation ranged between 0.01 to 0.09 pH units and 0.09% to 4.24% of air saturation, respectively. The indicator dyes of the pH-O_2 hybrid sensors were not as stable as the indicator dye of the single pH sensor, so that a recalibration was necessary after each experiment. The drift of Φ ranged from 0.42° to 3.57°, depending on ph and oxygen concentration (Fig. 30b). To compensate this drift, a linearized adaptation model of the calibration coefficients (Φ_{max}, Φ_{min}, pH_0, dpH) during the experiment was developed. For this, the preliminary calibration coefficients were gradually changed over time by adding or subtracting an individual calculated increment until they finally equaled the results of the recalibration at the last days of the experiments. This resulted in different calibration coefficients per day which were used for the iteration models.

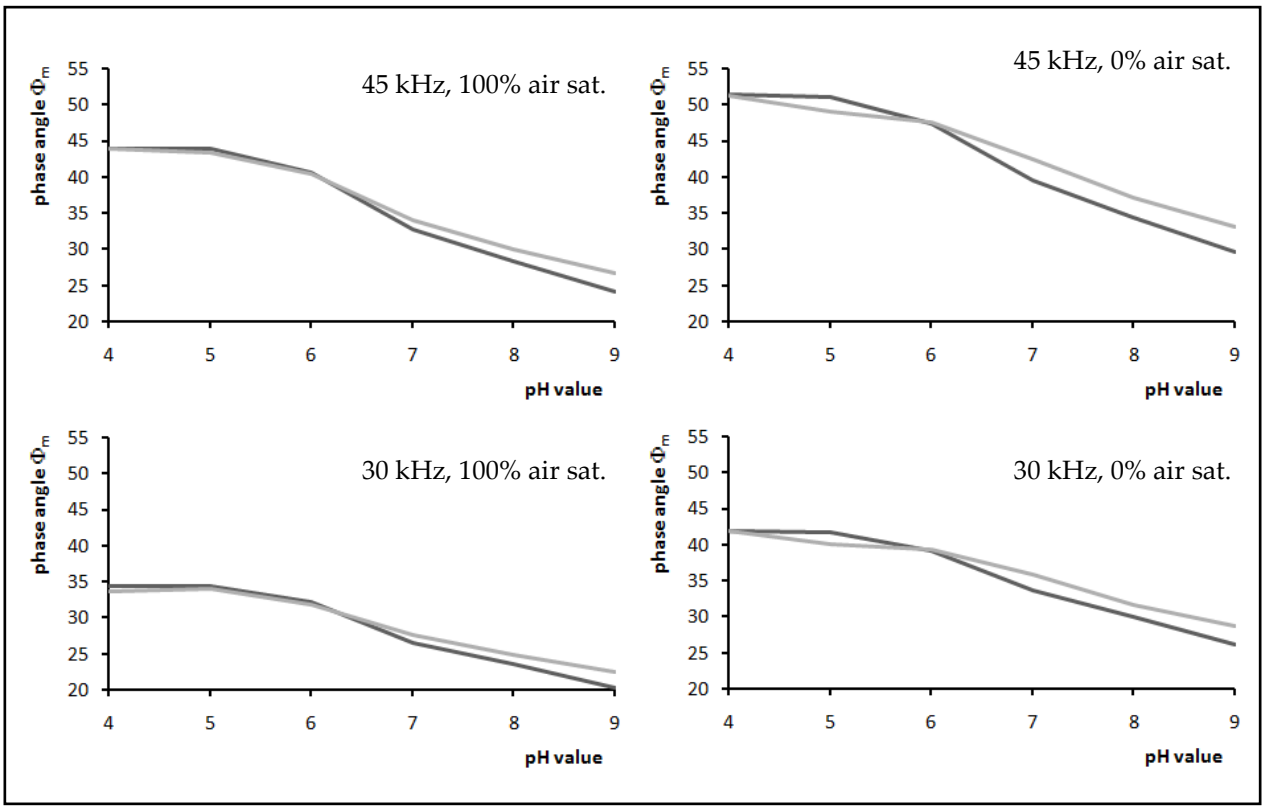

Figure 30b. Calibration curves of the planar O_2-pH hybrid optode at the beginning of the experiment (black lines) and at the end of the experiment (grey lines). Calibration curves were done for the pH range 4 – 9 at two different wavelengths (30 kHz and 45 kHz) and two different oxygen concentrations (100% air saturation and 0% air saturation).

3.6. Soil oxygen and ROL measured with O_2 fiber optodes

The soil oxygen concentration was measured with O_2 fiber optodes in parallel to the first non-invasive pH measurements with *J. effusus* as the test organism (see next chapter). The measurements revealed that the soil oxygen concentration (eutric-calcric histosol; bulk soil pH = pH 8; for further information see chapter 2.9.) varied barely around 0.18 - 0.88 µmol O_2 l^{-1}, if no root was present (Fig 32). But as soon as the root tips of *Juncus effusus* passed the sensor tip, the ROL of the growing roots raised the oxygen concentration from the base level (about 0.88 µmol O_2 l^{-1}) up to an oxygenation level of 70 µmol O_2 l^{-1} (Fig. 31, highest observed ROL). However, no effect of illumination on ROL was observed. The root specific oxygenation level is highly variable, and its maximum is reached when the elongation zone passes the O_2 sensor tip. A decrease of the oxygen concentration back to the nearly anoxic

conditions of the bulk soil started 3 – 5 days after the beginning of ROL, when the differentiation zone had passed the O_2 sensor tip.

A locally restricted artificial oxygenation of the bulk soil without roots nearby with ambient air instantaneously raised the oxygen concentration to 187 µmol O_2 l^{-1} (Fig. 32). After merely 70 min, 90% (168.3 µmol O_2 l^{-1}) of the locally added oxygen (t_{90}) was consumed by either soil microbes or abiotic oxidation of reduced soil compounds, corresponding to an O_2 consumption rate of about 40 nmol O_2 s^{-1}. After 8.5 h, the added oxygen was completely consumed.

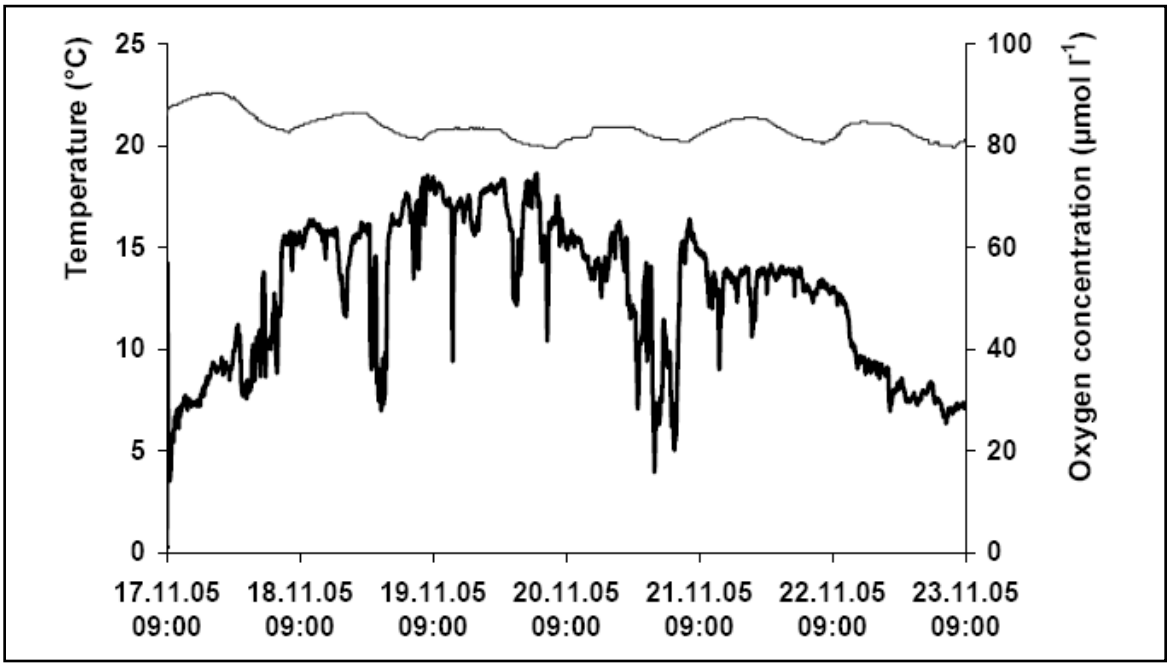

Figure 31. Soil temperature (hairline) and dissolved oxygen concentration (bold line) at the root surface during week 7 and 8 of the experiment. At the beginning of this measurement, the oxygen optode was positioned at the root tip. During the following days, the different root zones passed the sensor. (BLOSSFELD & GANSERT 2007)

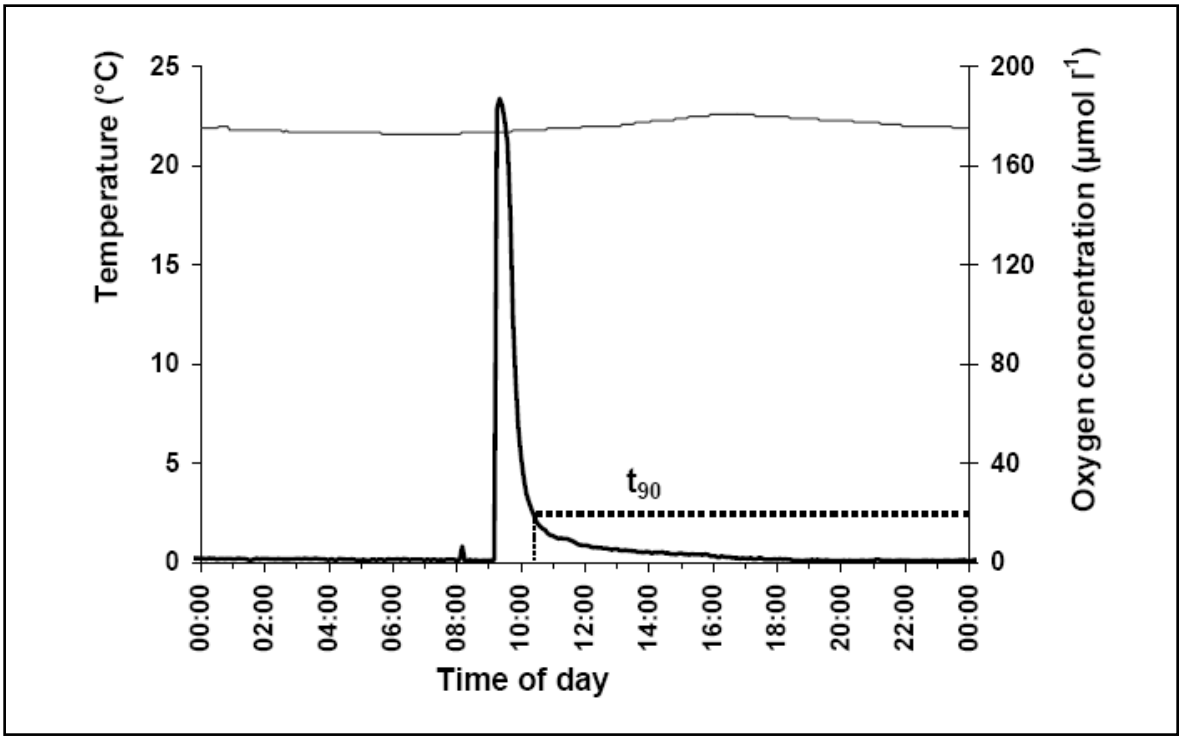

Figure 32. Soil temperature (hairline) and oxygen concentration (bold line) after a local oxygen impulse of ambient air applied by a syringe on day 43 of the experiment. Ninety per cent of the added oxygen (167.3 µmol O_2 l^{-1}) was consumed after 70 min (t_{90}). (BLOSSFELD & GANSERT 2007)

3.7. Root-induced variation of pH, measured with a planar single pH optode

As stated in the chapter before, *Juncus effusus* was used as the living test organism for qualifying the performance of the planar single pH optode under submerged soil conditions. The non-invasive pH measurements proved that the roots of *J. effusus* caused considerable changes of soil pH, revealing both pronounced daily patterns and acidification of the soil substrate in the long term. Fig. 33 shows a 24 h series of repetitive measurements of the same area of the planar optode (11.52 cm^2, 14.2% of the total size of the sensor foil). This series illustrates the growth of two roots of *J. effusus* and the related changes of the pH induced by these roots on day 12 of the whole experiment (indicated as D1). Within one day (D1, 0830 h–D2, 0830 h), one root grew 16.2 mm across the planar optode, corresponding to an average growth rate of 0.675 mm h^{-1} (depicted as root I left in Fig. 33). The second root growing across the sensor foil was observed first on day 2 of the experiment at 0400 h. Both growing

roots induced acidification of the submerged soil by about one pH unit (pH 8.5 to 7.5).The major influence of root-induced acidification during this 24 h period was restricted to the rhizosphere, while the bulk soil remained unchanged (blue to purple colors). The main acidification occurred during daytime between 0800 and 2200 h (illumination period). Thirty minutes before illumination of the plant shoots started (Fig. 33, D2, 0730 h), the pH in the rhizosphere of the roots was 0.5 units higher than 30 min after illumination of the plant (D2, 0830 h). Then, a pronounced pH gradient of decreasing acidification from the roots towards the bulk soil could be measured. The displayed segmentation of root pH (root I, Fig. 33) is caused by the interpolation formula of the SigmaPlot software (Systat Software, Inc.) rather than by a root specific pH pattern (D2, 0830 h). During night-time, the acidification of the soil substrate by the roots decreased, indicated by an increase of pH by up to 0.4, especially at the root tips but also up to 9 mm behind the root tips (Fig. 33: root I, D2, 0400–0730 h).

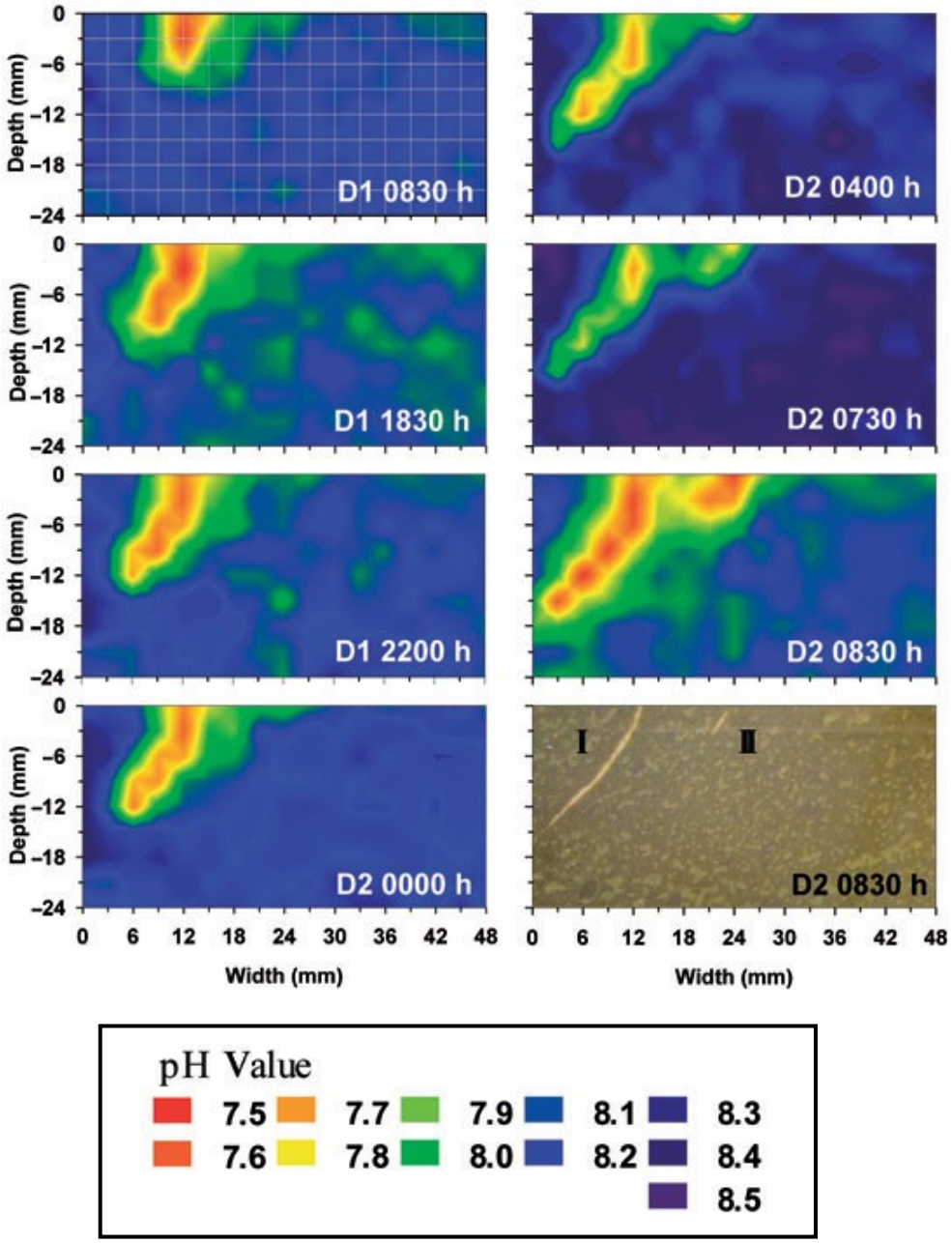

Figure 33. Visualization of a 24 h series of pH profiles across growing roots of *Juncus effusus* L. The figure illustrates snapshots at different times during the time series from day 1 (D1) to day 2 (D2). The crossing points of the grid (top left) indicate the positions of fiber-optic pH measurements. Illumination started at 0800 h and ended at 2200 h each day. The colors indicate different pH values. The digital photo (bottom right) shows the investigated section of the planar optode at the end of the time series with two roots growing across the pH optode (roman numerals indicate different roots). (BLOSSFELD & GANSERT 2007)

Long-term investigations over eight weeks of plant growth in the alkaline-submerged soil showed that at the root surface, no reduction of pH below 7.0 occurred. However, the data revealed a strong heterogeneity of the acidification pattern between mature main roots and adjacent lateral roots (Fig. 34). The lateral roots at the depths of -7.5 (I) and -18.0 to -21.0 mm (II and III) lowered the pH of their rhizosphere by about 0.1–0.2 units compared to the nearby parts of the parent main root (depicted left in Fig. 34, D49, 1400 h). In contrast, acidification by two lateral roots growing from the same main root at the depths of -22.5 (IV) and -27.0 mm (V) was much less pronounced. However, these different pH values (mature versus lateral roots) converged over a period of 12 d. Another aspect of temporal heterogeneity is the fact that mature roots, including their lateral roots, stopped the excretion of e.g. protons and thus the acidification of the soil (Fig. 35, roots I–IV), while the adjacent younger main roots showed a pronounced acidification. These newly grown roots reduced the pH of their rhizosphere up to 0.7 units compared to the rhizosphere of the older roots.

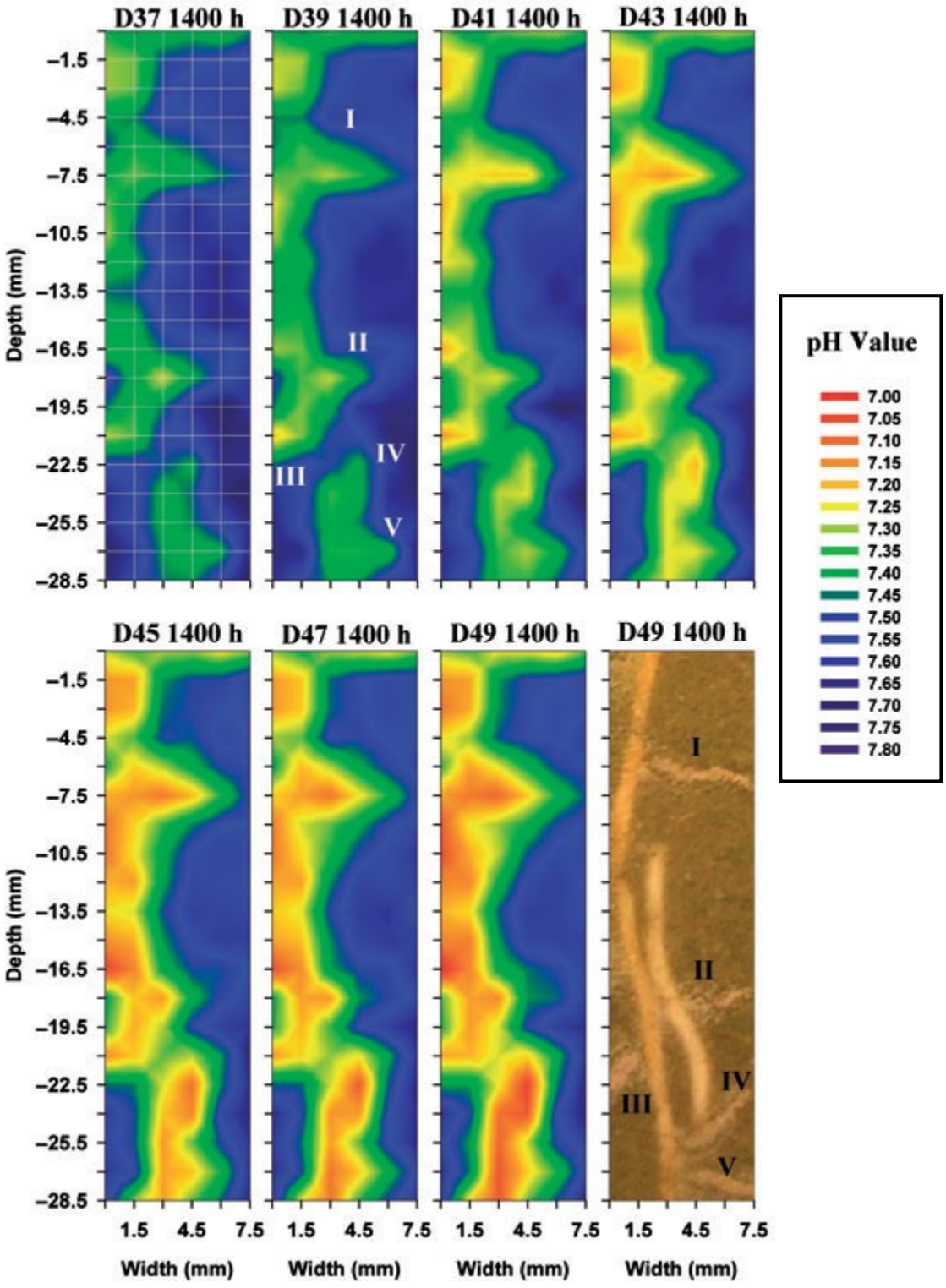

Figure 34. Time series of continuous pH measurement over a 13 d period (D37–D49) of a small section of the planar optode, illustrating the pH shift induced by two growing roots. All images visualize a snapshot of the pH of the investigated section at 1400 h in a 2 d interval. The heterogeneity of pH between main roots and lateral roots (I–V) can be clearly seen. The digital photo shows the investigated section, revealing the location of the two main roots. The root to the left exhibits several lateral roots, indicated by roman numerals. (BLOSSFELD & GANSERT 2007)

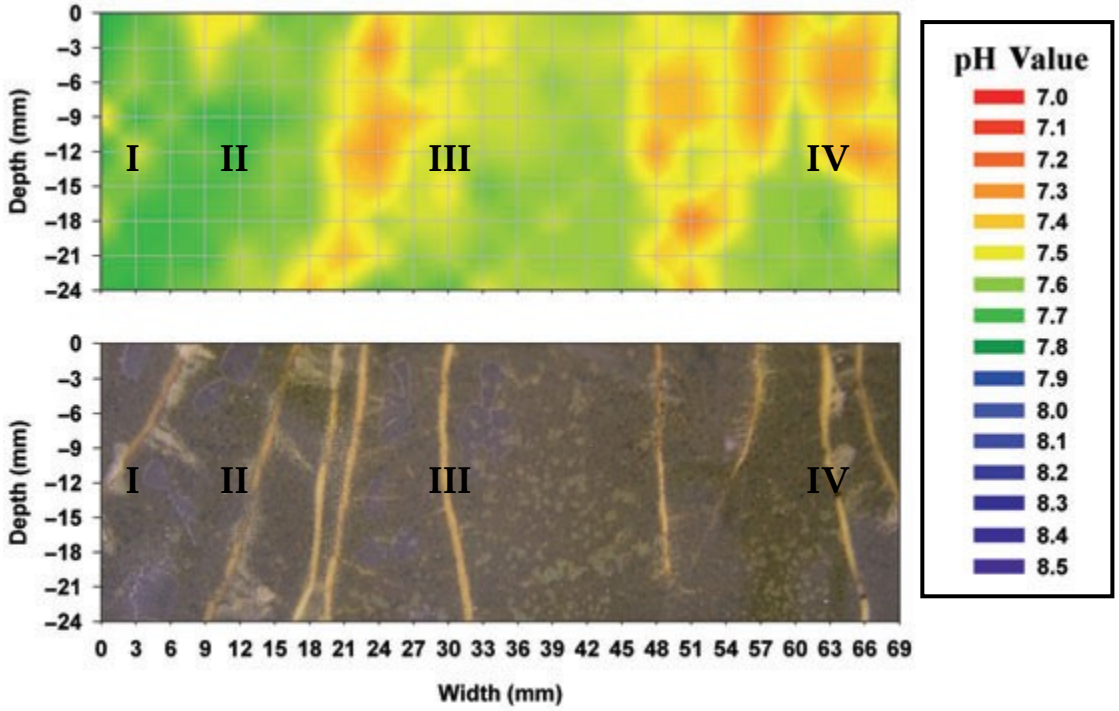

Figure 35. Image of the acidification pattern of the roots of *Juncus effusus*, 5 weeks after the onset of root growth across the sensor foil. The younger roots exhibit a stronger proton release than the elder roots (labeled by roman numerals). (BLOSSFELD & GANSERT 2007)

3.8. Root-induced variation of soil pH and O_2 concentration, measured with a planar pH-O_2 hybrid optode

As described in chapter 2.10.1., the planar pH-O_2 hybrid optodes were used in a combination with a free-choice split-root rhizotrone, where in contrast to the single pH measurements (chapter 3.7.), the different compartments were filled with soil substrate of varying pH (i.e. pH 4 – pH 6), to mimic the common pH range of natural wetlands. By use of these different acidic soil substrates and the permanent submergence of the soils, the biogeochemistry of each rhizotrone compartment was governed by individual reducing soil conditions (driven by the E_h-pH-stability field of water; Fig. 1). Due to these different physico-chemical soil conditions within the separate compartments and the setup for free-choice root in-growth, not all investigated plants rooted in all rhizotrone compartments.

In the tables 9a-c the key measured data on pH and oxygen dynamics of all plants and soil types are presented. The data highlights the maximal radial oxygen loss

from the main roots and the lateral roots as well (max. ROL main roots/ max. ROL lateral roots). Interestingly, in the case of *J. articulatus*, no ROL from lateral roots was detectable. Besides this, the average oxygen concentration of the bulk soil is presented (avg. O_2 bulk soil) as well as the impact of the growing roots on the oxygen concentration of the bulk soil (O_2 impact bulk soil), i.e. the increase of the bulk soil oxygen concentration due to the root activity. Additionally, the average rhizospheric pH value (avg. pH rhizosphere) and the average bulk soil pH value (avg. pH bulk soil), as well as the root induced change of the bulk soil pH value (pH impact bulk soil) are given in these tables. The maximal oxidation time, i.e. the duration of the oxygenation of a single spot in the soil that is passed by the growing root tip, is also given in these tables.

Table 9a. Effects of roots of *Juncus effusus* on rhizospheric and bulk soil pH and O_2 concentration (*Juncus effusus* roots did not grow into E 910 soil compartment). For details refer to the text.

soil type	number of grown roots	max. ROL main root	max. ROL lateral roots	avg. O_2 bulk soil	O_2 impact bulk soil	avg. pH rhizosphere	avg. pH bulk soil	pH impact bulk soil	max. oxidation time
		µmol O_2 l^{-1}	µmol O_2 l^{-1}	µmol O_2 l^{-1}	µmol O_2 l^{-1}				h
A 600	5	174.1	198.1	32.6 ± 15.1	+6.2	4.52 ± 0.67	5.11 ± 0.16	0	31
E 910	-	-	-	-	-	-	-	-	-
E 400	16	159.4	167.3	22.5 ± 10.7	+2.8	5.49 ± 0.47	5.92 ± 0.18	0	28

Table 9b. Effects of roots of *Juncus inflexus* on rhizospheric and bulk soil pH and O_2 concentration (*Juncus inflexus* roots did not grow into E 910 soil compartment).

soil type	number of grown roots	max. ROL main root	max. ROL lateral roots	avg. O_2 bulk soil	O_2 impact bulk soil	avg. pH rhizosphere	avg. pH bulk soil	pH impact bulk soil	max. oxidation time
		µmol O_2 l^{-1}	µmol O_2 l^{-1}	µmol O_2 l^{-1}	µmol O_2 l^{-1}				H
A 600	8	164.5	184.7	38.3 ± 12.9	+10.1	4.75 ± 0.27	4.93 ± 0.26	-0.15	49
E 910	-	-	-	-	-	-	-	-	-
E 400	27	170.3	179.7	20.6 ± 14.5	+16.3	5.31 ± 0.16	5.41 ± 0.17	-0.16	40

Table 9c. Effects of roots of *Juncus articulatus* on rhizospheric and bulk soil pH and O_2 concentration (*Juncus articulatus* roots did not grow into E 910 and A 600 soil compartment).

soil type	number of grown roots	max. ROL main root	max. ROL lateral roots	avg. O_2 bulk soil	O_2 impact bulk soil	avg. pH rhizosphere	avg. pH bulk soil	pH impact bulk soil	max. oxidation time
		µmol O_2 l^{-1}	µmol O_2 l^{-1}	µmol O_2 l^{-1}	µmol O_2 l^{-1}				h
A 600	-	-	-	-	-	-	-	-	-
E 910	-	-	-	-	-	-	-	-	-
E 400	9	101.3	n.d.	11.4 ± 4.5	+8.9	5.63 ± 0.06	5.44 ± 0.09	-0.08	∞

The use of the novel planar pH-O_2 hybrid optodes revealed, that the roots of all three investigated plant species strongly oxidized the rhizosphere (Fig. 36 to Fig 38, Tab. 9). While the root tips approached, the oxygen concentration was raised from nearly anoxic conditions of maximal 38.3 µmol O_2 l^{-1} (Tab. 9b) to moderate and strong oxidative conditions of up to 170.3 µmol O_2 l^{-1} (corresponding to an air saturation of about 60%), in the case of *J. inflexus* (Tab. 9b). The highest rhizospheric oxygen concentration for *J. effusus* and *J. articulatus* root tips were 174.1 and 101.3 µmol O_2 l^{-1}, corresponding to an air saturation of about 62% and 35% (Tab. 9a & c).

However, *Juncus effusus* and *Juncus inflexus* showed an oxygen release pattern, which was contrary to the oxygen release pattern of *Juncus articulatus*: For *J. effusus* and *J. inflexus*, oxygen release was restricted to the elongation zone of the root tips, whereas the roots of *J. articulatus* showed a ROL along the entire root surface (Fig. 36 - 38). Fig. 36 shows a series of repetitive measurements of the same section of the planar hybrid optode (4.08 cm^2, 25.5% of total sensor foil). This series illustrates the growth of a root of *J. effusus* and the related changes of the pH and O_2 concentration by this root on day 11 of the whole experiment (indicated as D1). Within 10 hours (D1, 1040 h – D1, 2040 h), the root grew 8.2 mm across the planar hybrid optode, corresponding to an average growth rate of 0.82 mm h^{-1}. Due to the root growth and the restriction of the ROL to the elongation zone, the oxygenation of this particular section of the submerge soil was only temporary. After 10h of root growth and ROL

(Fig. 36, D1 2040 h), the maximal oxygenation for this soil section was reached. In the following hours, the ROL ceased from the basal parts of the roots towards the direction of the moving root tip (Fig. 36, D2 0500 h – D2 0900 h). As a result, the oxidative zone (halo) around the root tips moved in a cone-shaped form through the strongly hypoxic soil.

The figure 39 shows exemplarily a detailed time course of the measured pH value and oxygen concentration at an exemplarily chosen data point of the investigated section. The root tip of *J. effusus* passed this point at nearly 1200h on day 1, which caused a strong increase of the measured oxygen concentration at this position. As soon as the elongation zone passed the investigated measuring spot, i.e. the elongation zone of the growing root tip was transformed into the root hair zone at this spot, the oxygen concentration dropped to bulk soil conditions again (D2 0600h). The same pattern of temporary oxygenation of the soil was observed for *J. inflexus* (Fig. 40). However, the duration of the oxidation was increased due to a slower root growth rate of *J. inflexus* (6.5 mm h^{-1}) by about 50% (Tab. 9b). In contrast to the roots of *J. effusus* and *J. inflexus*, the roots of *J. articulatus* continuously released oxygen into the soil; hence the rhizospheric oxygen concentration was permanently higher than bulk soil levels, but lower than the rhizospheric oxygen concentration of *J. effusus* and *J. inflexus* roots (Fig 41).

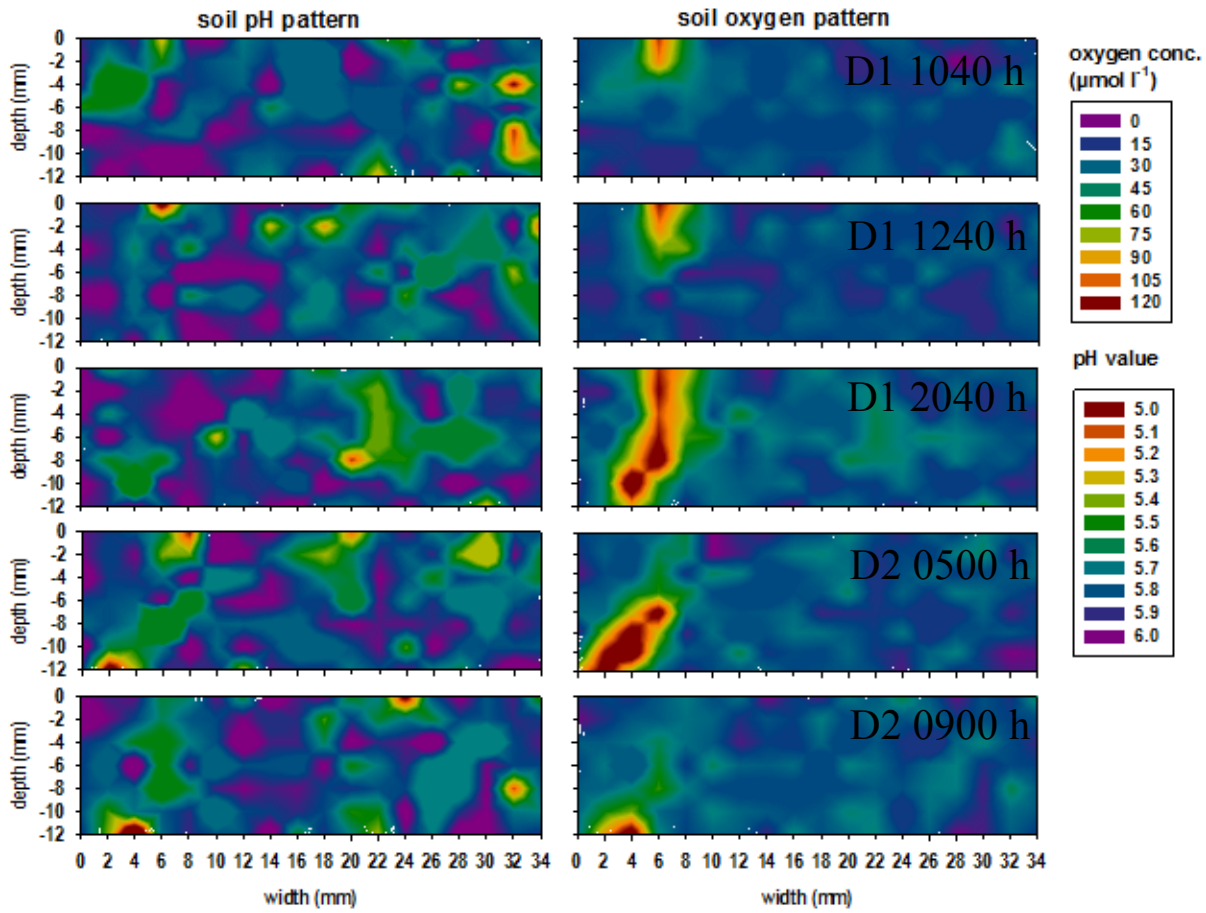

Figure 36. Visualization of a series of pH and O_2 profiles across a growing root of *Juncus effusus*, rooting in E400-soil. The figure illustrates snapshots at different times during the time series from day 1 (D1) to day 2 (D2). Illumination started at 0800 h and ended at 2200 h each day. The colors indicate different pH and O_2 values.

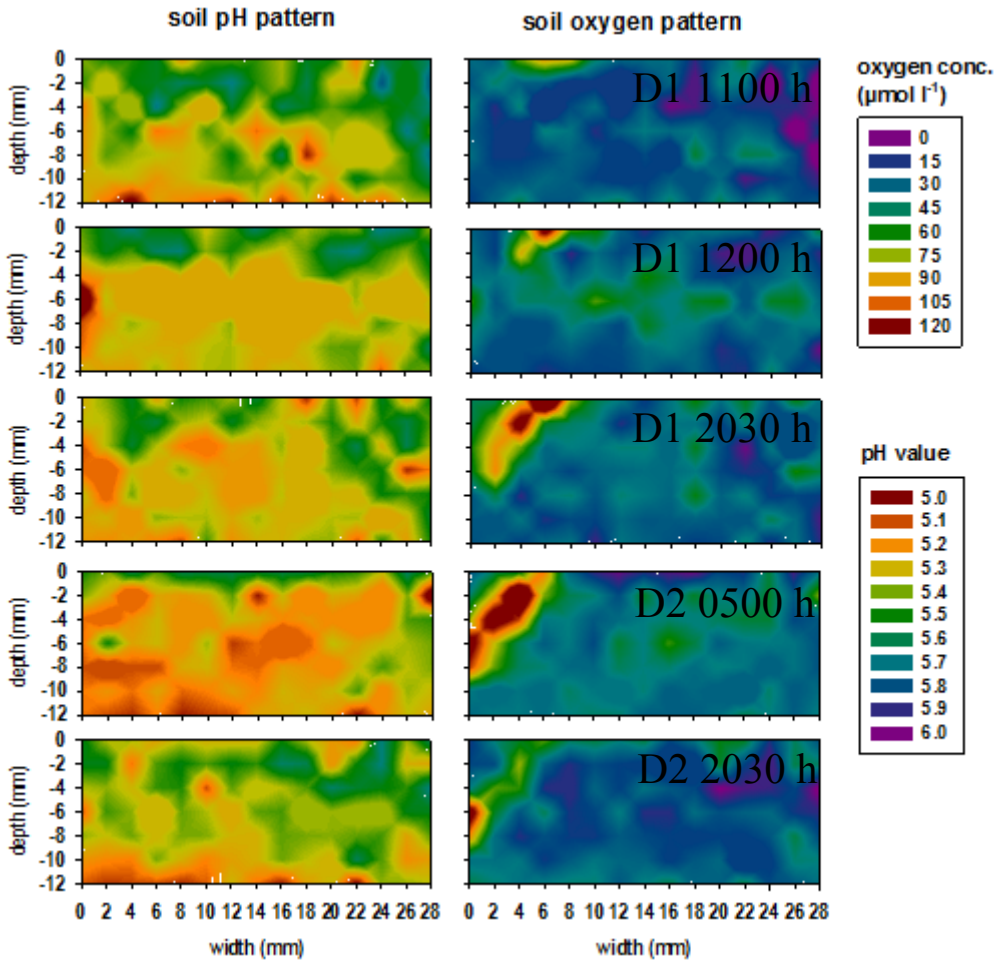

Figure 37. Visualization of a series of pH and O_2 profiles across a growing root of *Juncus inflexus*, rooting in E400-soil. The figure illustrates snapshots at different times during the time series from day 1 (D1) to day 2 (D2). Illumination started at 0800 h and ended at 2200 h each day. The colors indicate different pH and O_2 values.

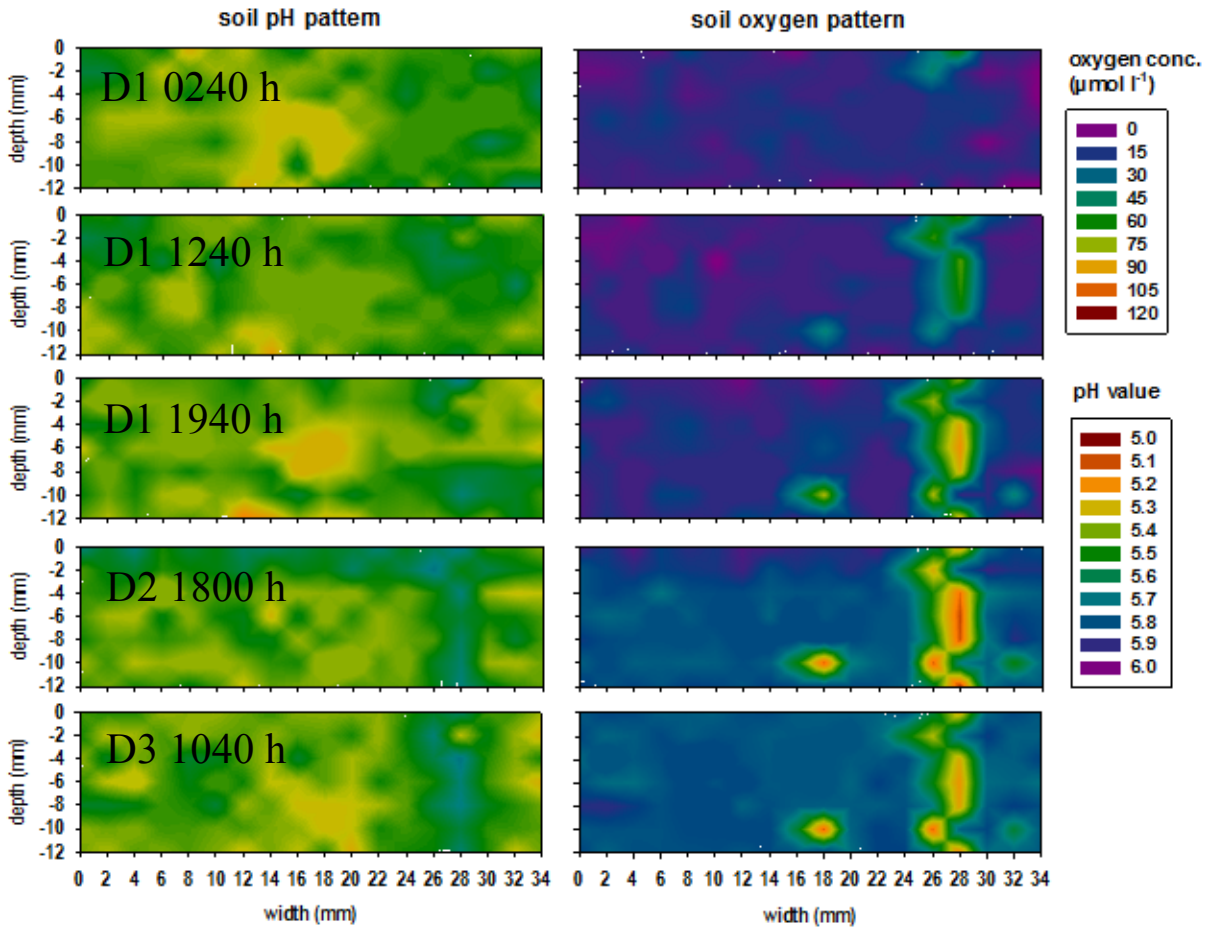

Figure 38. Visualization of a series of pH and O_2 profiles across a growing root of *Juncus articulatus*, rooting in E400-soil. The figure illustrates snapshots at different times during the time series from day 1 (D1) to day 3 (D3). Illumination started at 0800 h and ended at 2200 h each day. The colors indicate different pH and O_2 values.

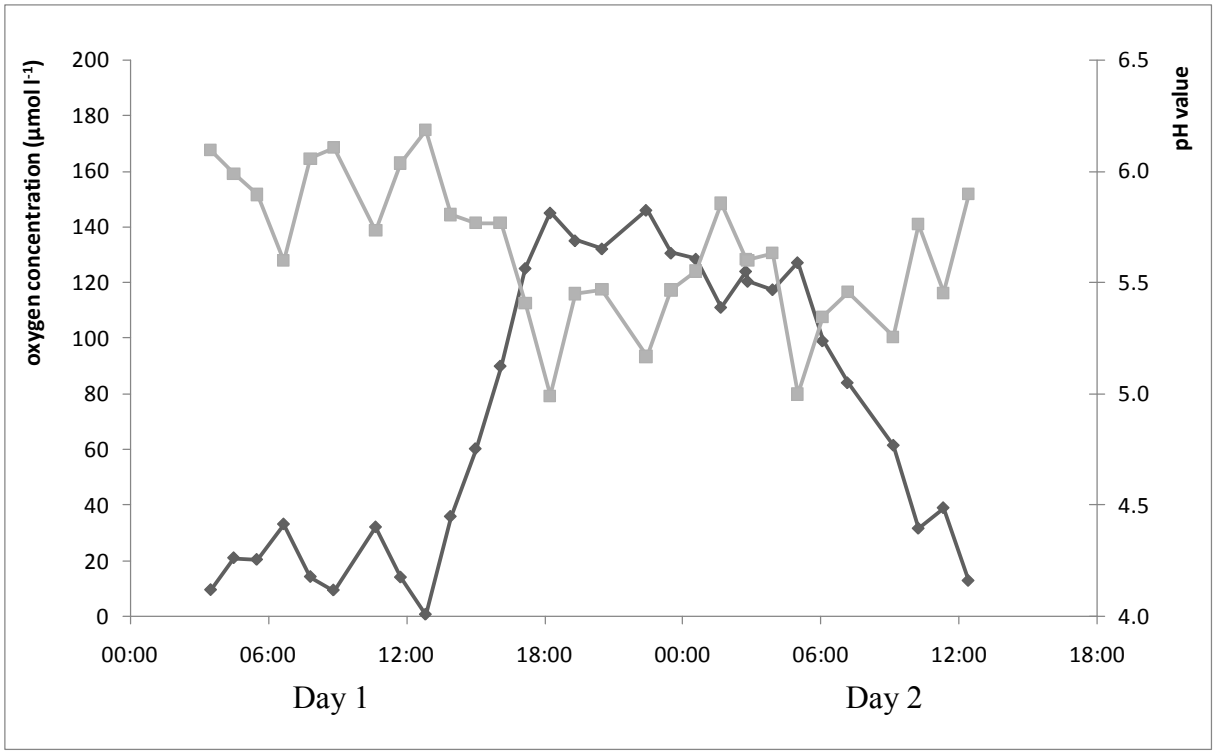

Figure 39. Detailed time course of the O_2 (dark grey line) and pH (light grey line) profile of a single measuring spot from *Juncus effusus* rooting in E400-soil (position -8/0 in figure 32).

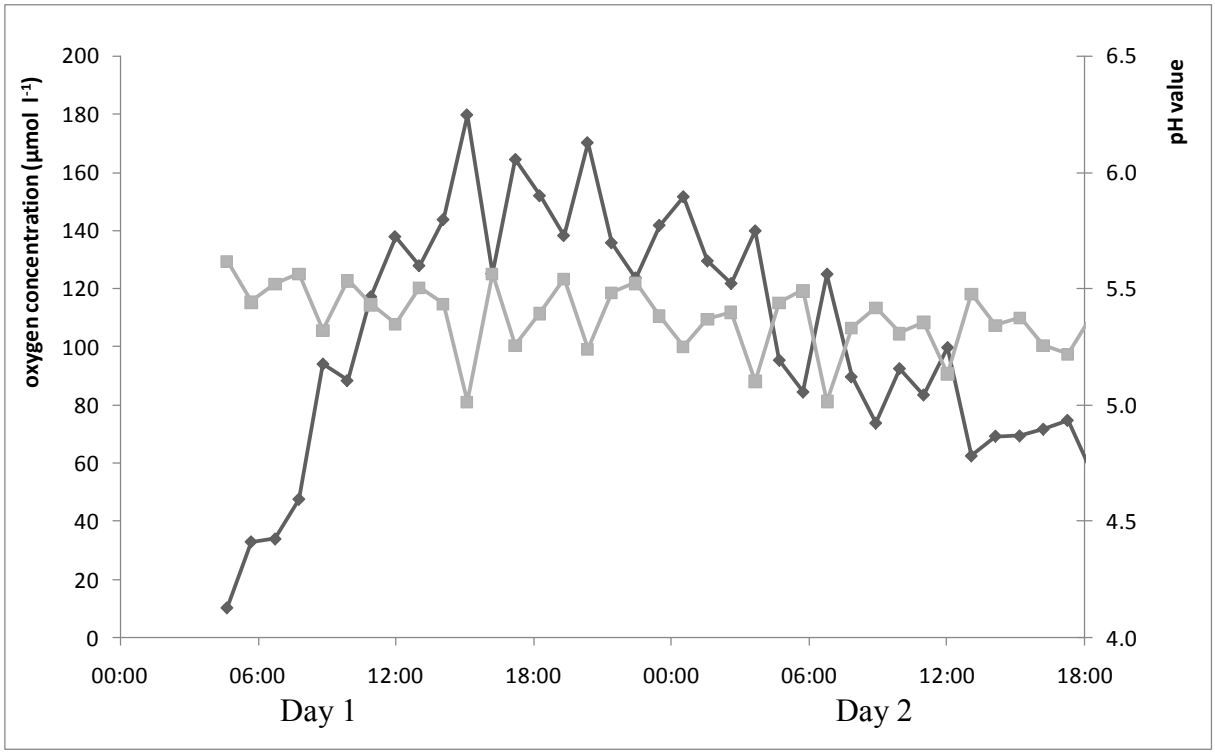

Figure 40. Detailed time course of the O_2 (dark grey line) and pH (light grey line) profile of a single measuring spot from *Juncus inflexus*, rooting in E400-soil (position 0/6 in figure 33).

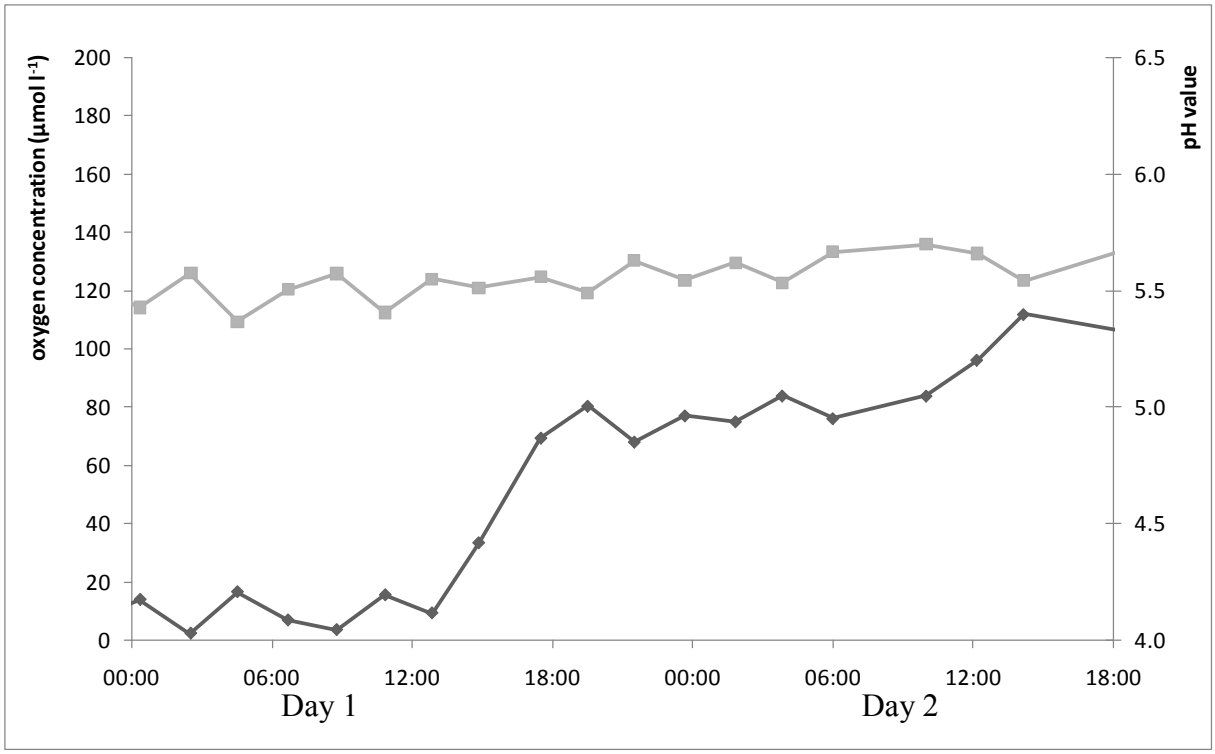

Figure 41. Detailed time course of the O_2 (dark grey line) and pH (light grey line) profile of a single measuring spot from *Juncus articulatus*, rooting in E400-soil (position -12/28 in figure 34).

The impact radius of this root induced soil oxygenation was restricted to a maximum of 4mm off the root surface in the case of *J. effusus* and *J. inflexus* but 2mm in the case of *J. articulatus*. However, the average oxygen content of the bulk soil was changed according to presence or absence of the roots. An increase of the average bulk soil oxygen content from 20.6 ± 14.5 to 36.9 ± 14.5 µmol O_2 l^{-1} was detected during the transit of the root tip in the case of *J. inflexus* (Fig. 37). In contrast, the increase of the oxygen content of the bulk soil of *J. effusus* from 22.5 ± 10.7 to 25.3 ± 10.2 µmol O_2 l^{-1} during the transit of the root tip was not that prominent (Fig. 36). The oxygen concentration in the bulk soil of *J. articulatus* increased continuously during the first 48 hours after the transit of the root tip from 11.4 ± 4.5 up to a steady value of 20.3 ± 4.4 µmol O_2 l^{-1} (Fig. 38).

Additionally, with the formation of lateral roots, the roots of *Juncus inflexus* and *Juncus effusus* released large amounts of oxygen into the soil again. This second phase of radial oxygen loss was even more prominent than the oxygenation by the root tips,

due to fact that this oxygenation by the lateral roots was permanent. This rhizospheric oxygenation by the lateral roots showed a pronounced diurnal rhythm and reached the highest oxygen concentration levels compared to the oxygenation by the root tips (Tab. 9a & b). Figure 42 exemplarily illustrates the formation of the lateral roots of *Juncus inflexus*, accompanied by a strong radial oxygen loss into the soil. The effect of the diurnal rhythm was remarkably pronounced: On day 2 0640h the artificial illumination was off and the average oxygen concentration was about 30 µmol l^{-1} lower than on the same day at 1050h, where the illumination was on for nearly 3 hours. Furthermore the extent of the oxidative zone was increased by 50%.

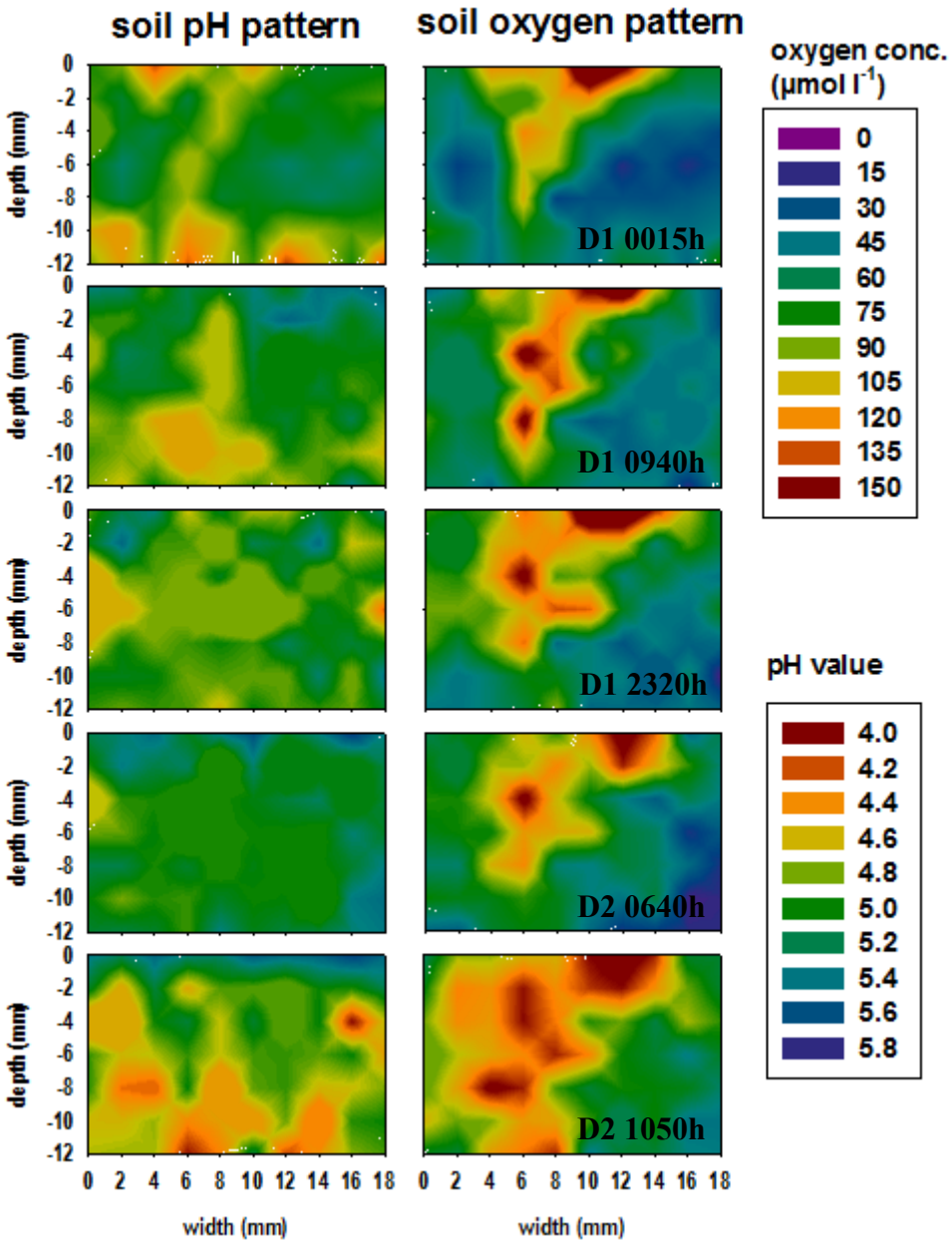

Figure 42. Visualization of a series of pH and O_2 profiles across the lateral roots of *Juncus inflexus* L, rooting in A600-soil. The figure illustrates snapshots at different times during the time series from day 1 (D1) to day 2 (D2). Illumination started at 0800 h and ended at 2200 h each day. The colors indicate different pH and O_2 values.

From the pH measurements in non-rooted soils it could be proven, that the uninfluenced bulk soil pH value was reciprocally proportional correlated to the soil oxygen concentration. This relationship was depending on the soil type that was used (Fig 43). Depending on the soil type used, the negative slope of the linear regression of the pH-O_2 relationship increased from -0.0101 pH units per µmol l^{-1} O_2

(A600-Soil) to -0.0149 and -0.0326 µmol l^{-1} O_2 (E400 and E910-Soil). These results confirmed the data retrieved by bulk soil measurements in vegetated soils.

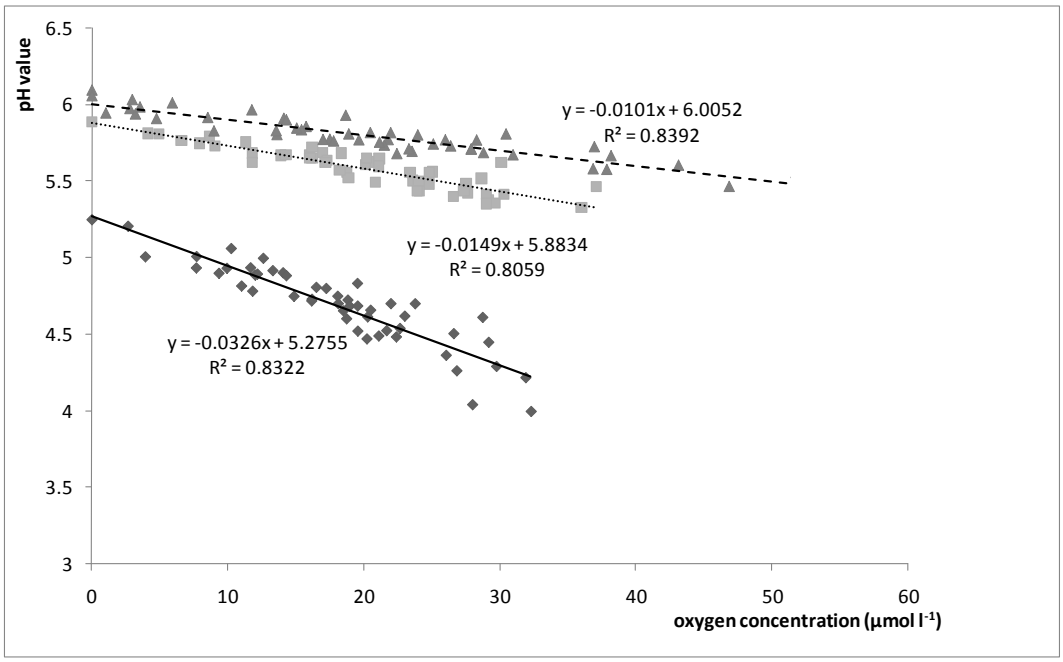

Figure 43. Effect of different un-rooted soil types on the oxidative acidification. Dark grey diamonds = A600-soil. Bold line = linear regression of A600-soil. Light grey squares = E400 soil. Dotted line = linear regression E400-soil. Grey triangles = E910-soil. Dashed line = linear regression E910-soil.

In contrast to the findings in alkaline soil substrate gained by the use of the planar single pH optode (initial bulk soil pH = pH 8; Figs. 32 - 35), no continuous acidification along the roots growing in this more acidic soil substrates (initial bulk soil pH = pH 4 – 6) was observed for any of the three investigated plant species. Nevertheless, a temporary rhizospheric acidification was detected for the roots of *J. effusus* (Fig. 36). This rhizospheric acidification by the roots of *J. effusus* was coupled to the rhizospheric oxygenation (Fig. 44). During the transit of the elongation zone, the average rhizospheric pH value dropped from 5.92 ± 0.18 to 5.49 ± 0.47 and rose back to the initial value afterwards (Fig. 39). Interestingly, the average bulk soil pH was not affected by the presence or absence of the roots of *J. effusus* (Tab. 9a).

Figure 47 illustrates exemplarily for one single measuring spot (position -8/6 in Fig. 36) the relationship between rhizospheric pH value and oxygen concentration:

Previous to the transit of the root tip, pH value and oxygen concentration were reciprocally proportional linked together, as it was described for the situation in the bulk soil (bulk soil reaction). During the first hours of transition of the root tip (red line), the pH value was constant although the oxygen concentration increased steadily, but above an oxygen concentration of 90 µmol l^{-1} the pH value suddenly decreased. When the elongation zone of the root tip began to form and the rhizospheric oxygen concentration peak was reached, pH value and oxygen concentration were reciprocally proportional linked together again. When the elongation zone passed by and the rhizospheric oxygen concentration steadily decreased to the initial value, this pH-O_2-loop turned back to the bulk soil reaction (green line).

In contrast to *J. effusus*, the average rhizospheric pH value of *J. inflexus* roots was not lowered by the oxygen release along the elongation zone (pH 5.31 ± 0.16) compared to the situation shortly before the approach of the root tip (pH 5.30 ± 0.12, Figs. 37 & 45). However, the pH value of the surrounding bulk soil was acidified by 0.16 pH units to an average pH value of 5.25 ± 0.17 during the transit of the root tips (Tab. 9b). During the approach of the root tip, the oxygen concentration quickly increased, but the rhizospheric pH value was varied only between pH 5.5 and pH 5.1 (Fig. 48). During the transit of the elongation zone, the oxygen concentration decreased slowly in a saw tooth pattern, resulting in a reciprocal saw tooth pattern of the pH value of the rhizosphere similar to the bulk soil reaction (Fig. 48, green line). Additionally to the oxidative acidification by the root tips, the effect of the ROL from lateral roots of *J. effusus* and *J. inflexus* on the rhizospheric and bulk soil pH was also very strong (Tab. 9a/b). Due to the effect of the diurnal rhythm of the oxygenation by the lateral roots, the pH value of the surrounding soil was strongly reduced during daytime (Fig. 42).

The roots of *J. articulatus* did not acidify, but alkalinized the rhizosphere (pH = 5.63 ± 0.06) compared to the bulk soil (pH = 5.49 ± 0.06), although the rhizospheric oxygen

concentration was five-fold higher than the bulk soil oxygen concentration (Figs. 38 & 46). Interestingly, the bulk soil pH value was lowered during the growth of the root by 0.08 pH units to an average pH value of 5.41 ± 0.09, compared to the initial pH value of the bulk soil (Fig. 41). Due to the constant oxygen release by the roots of *J. articulatus*, the pH-O_2 relation in figure 49 was not characterized by a pH-O_2 loop pattern; moreover the rhizospheric pH value and oxygen concentration were kept in a narrow stationary frame between pH 5.5 – 5.7 and an oxygen concentration of 80 – 120 µmol l^{-1} as soon as the root has passed by.

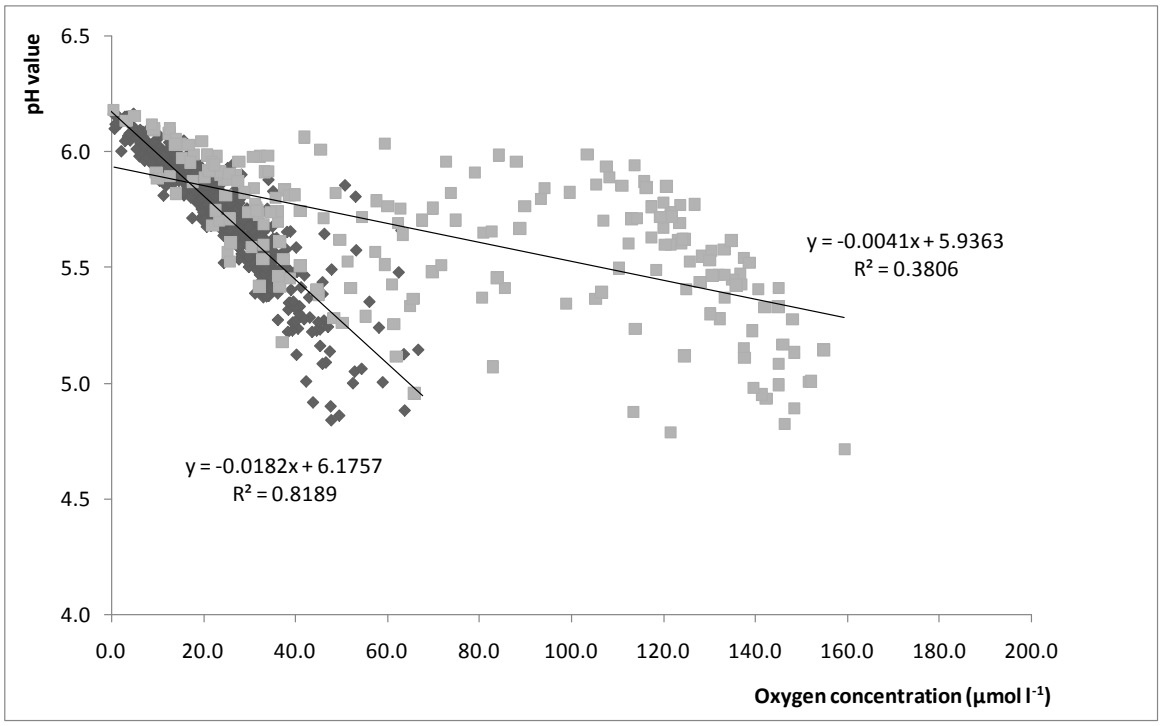

Figure 44. Effect of ROL from the root tips of *J. effusus* on the oxidative acidification in E400 soil. Dark grey diamonds = bulk soil. Hairline = linear regression of bulk soil. Light grey squares = rhizospheric soil. Bold line = linear regression of rhizospheric soil.

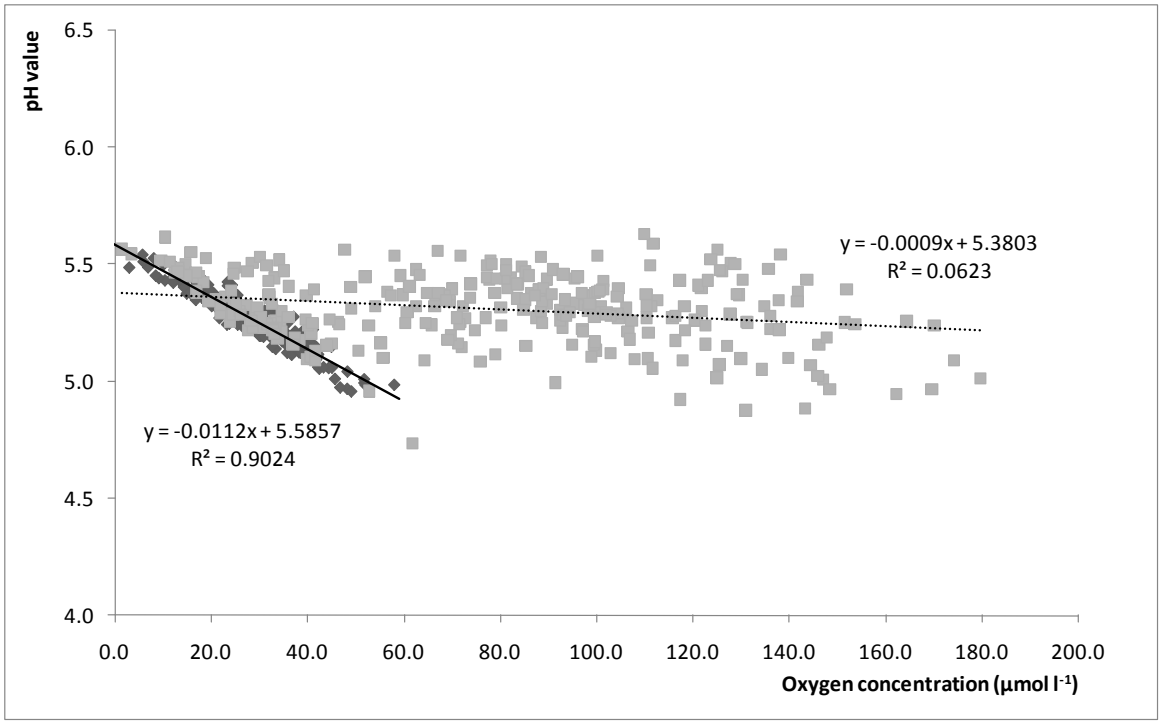

Figure 45. Effect of ROL from the root tips of *J. inflexus* on the oxidative acidification in E400 soil. Dark grey diamonds = bulk soil. Hairline = linear regression of bulk soil. Light grey squares = rhizospheric soil. Bold line = linear regression of rhizospheric soil.

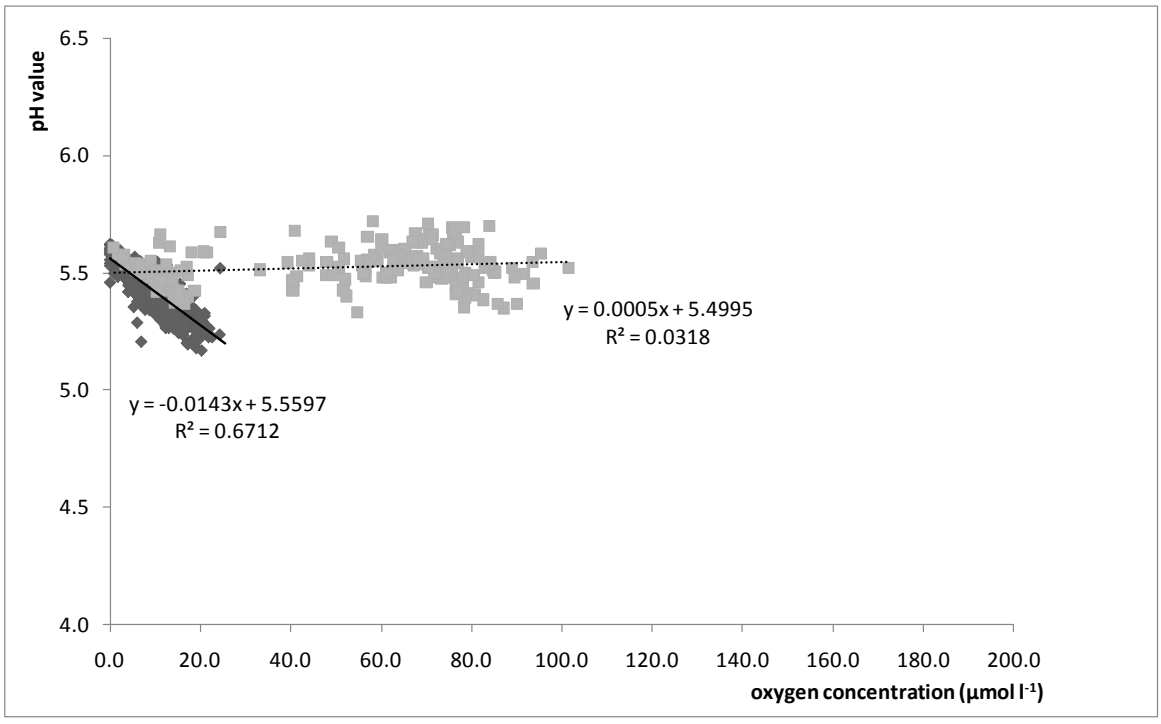

Figure 46. Effect of ROL from the root tips of *J. articulatus* on the oxidative acidification in E400 soil. Dark grey diamonds = bulk soil. Hairline = linear regression of bulk soil. Light grey squares = rhizospheric soil. Bold line = linear regression of rhizospheric soil.

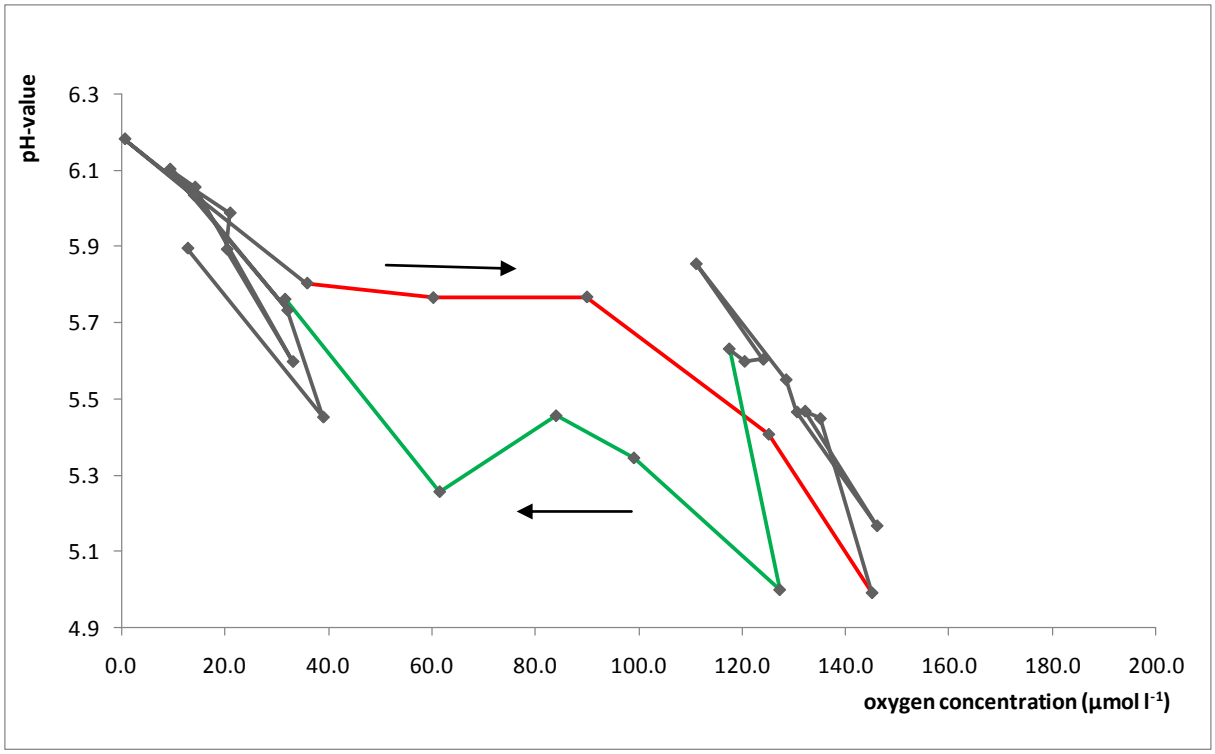

Figure 47. Time course of a single measuring spot of *Juncus effusus*, rooting in E400-soil (position -8/6 in Fig. 36). Red line represents the approach of the root tip towards this measuring spot and the green line represents the transition of the root tip. Arrows indicate chronology of the measuring spots.

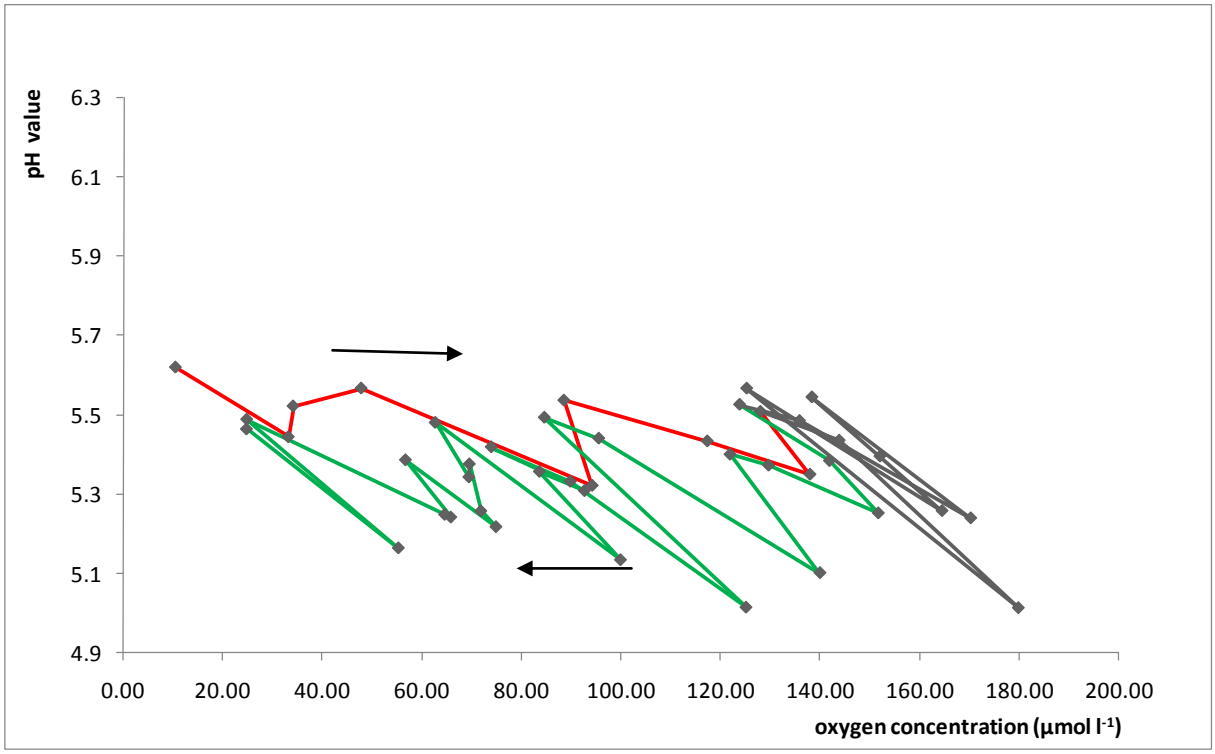

Figure 48. Time course of a single measuring spot of *Juncus inflexus*, rooting in E400-soil (position 0/6 in Fig. 37). Red line represents the approach of the root tip towards this measuring spot and the green line represents the transition of the root tip. Arrows indicate chronology of the measuring spots.

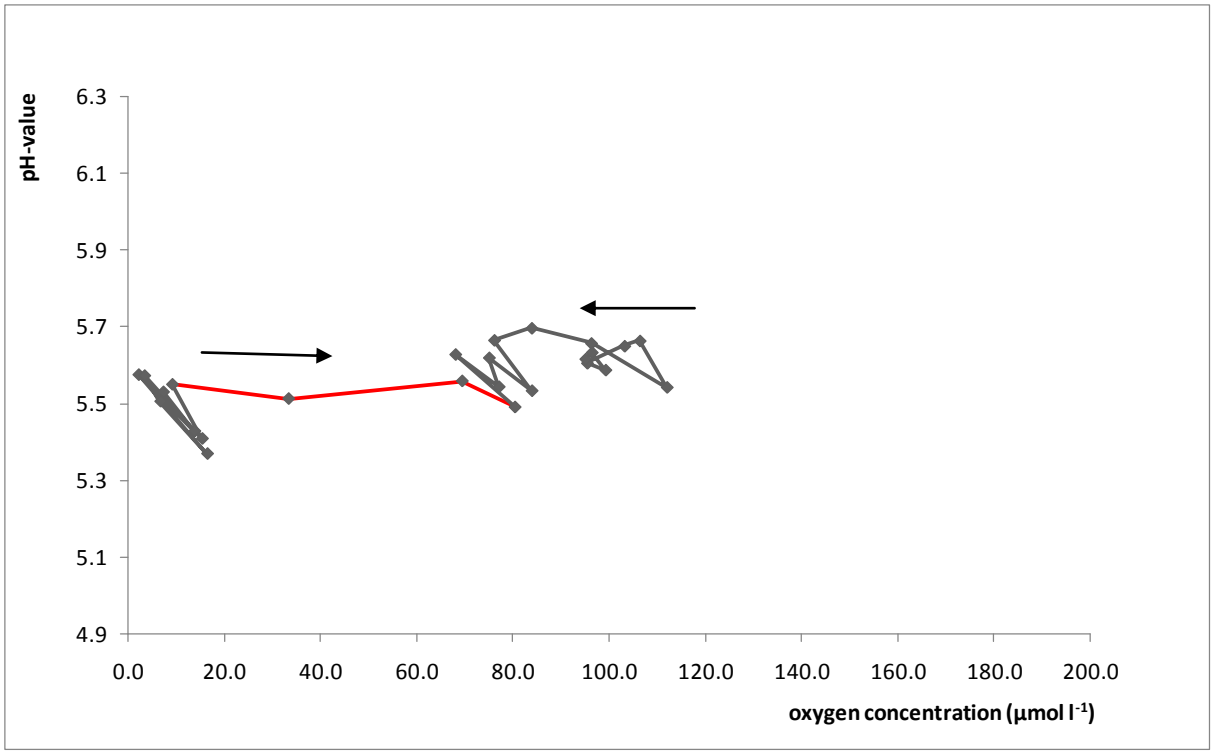

Figure 49. Time course of a single measuring spot of *Juncus articulatus*, rooting in E400-soil (position -12/28 in Fig. 38). Red line represents the approach of the root tip towards this measuring spot and the green line represents the transition of the root tip. Arrows indicate chronology of the measuring spots.

In a last experiment the effect of the soil oxygen concentration on the soil pH was tested, to verify that the effect of oxidative acidification is the primary source of protons in this study. Figure 50 shows that artificial changes in rhizospheric oxygen concentration results in reciprocally proportional changes of rhizospheric pH. The stepwise decrease of the atmospheric oxygen concentration from 100 % to almost 0 % air saturation caused a decrease in ROL from 90 µmol l^{-1} to 7 µmol l^{-1} and an increase of rhizospheric pH from 5.4 to 5.9. Although the standard deviation of the measured pH values increased, the experiment clearly demonstrated that during the subsequent stepwise increase of the atmospheric oxygen concentration, the oxidative acidification started again.

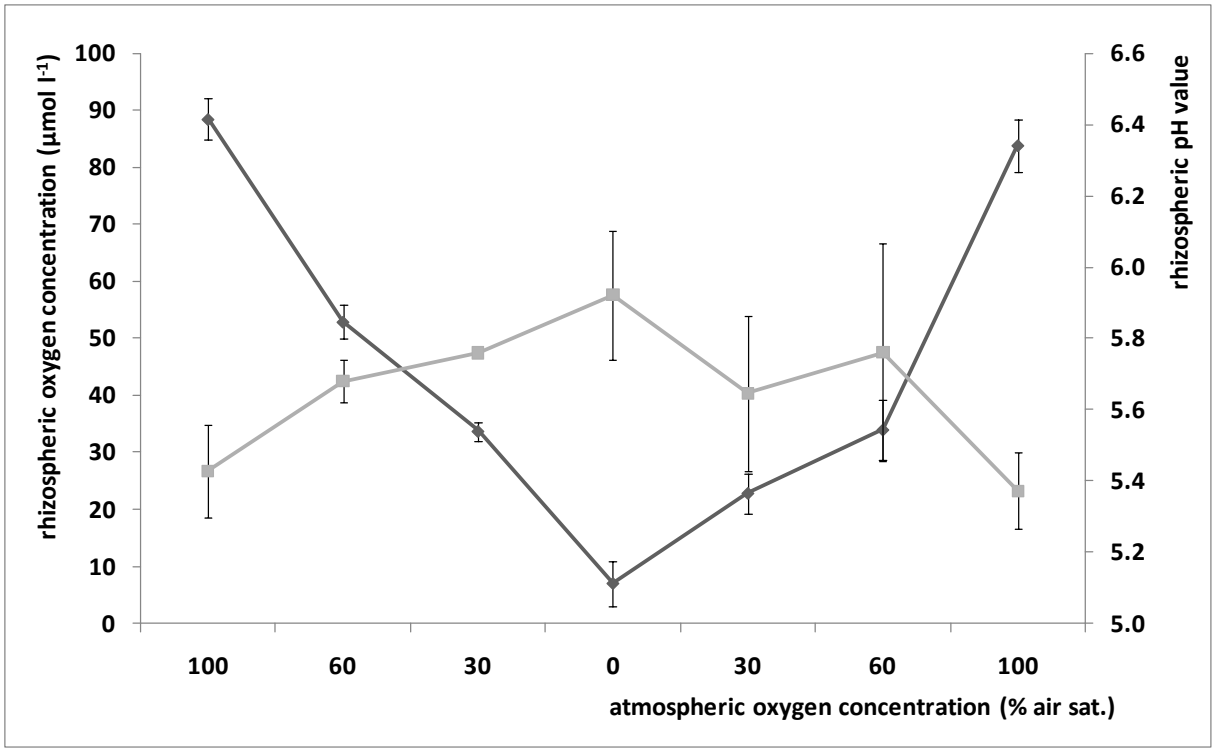

Figure 50. Proof of oxidative acidification as primary source of protons. Dark grey line shows rhizospheric oxygen concentration at the end of phases of stepwise changed atmospheric oxygen concentration. Light grey line shows rhizospheric pH value at the end of phases of stepwise changed atmospheric oxygen concentrations. (n = 8 samples per concentration step).

4. Discussion

4.1. Soil moisture gradient experiment

Use of leaf traits like specific leaf length (SLL) or leaf dry matter content (LDMC) is a common way for estimating and evaluating plant growth strategies, especially with regard to plant stress responses (BOWLER & PRESS 1996; GARNIER *et al.* 1997; WILSON *et al.* 1999). The soil moisture gradient experiments revealed two key results: (I) The soil moisture has a deep impact on the growth performance of the investigated species, with varying consequences on plant growth, depending on the selected monoculture or competition treatments. (II) The interspecific competition itself has also a significant effect on the investigated plant growth parameters. Due to the combination of these two environmental stress factors (soil moisture and interspecific competition), the results prove that the investigated plant species have evolved very different strategies to cope with these stress factors.

For example, due to the competition the SLL of *J. effusus* is strongly reduced especially at dry and low soil moisture conditions whereas the LDMC is strongly increased at all soil moisture levels. This conforms to an efficient nutrient and water conservation strategy (LI *et al.* 2005), resulting in lower growth rates. According to standard categorizations (KEDDY *et al.* 1998; NAVAS & MOREAU-RICHARD 2005) this kind of competitive response would categorize *J. effusus* as a "persister" species, which tolerates the stress situation by conserving the resources and reducing the plant growth rate. In contrast, the strategy of competition-induced rapid biomass production is predominantly performed by *Juncus articulatus*, showing the lowest LDMC in combination with the highest SLL across the entire soil moisture gradient. This species even increases the SLL drastically and concomitantly decreases the LDMC during competition from dry to medium soil moisture levels, whereas at wet and waterlogged soil conditions this reaction is reversed. This combination causes an enormous expansion of the leaf length, at low carbon and nutrient costs (POORTER &

DE JONG 1999; LAVOREL & GARNIER 2002), especially at low and medium soil moisture conditions. This would categorize *J. articulatus* as a "forager" species (KEDDY *et al.* 1998; NAVAS & MOREAU-RICHARD 2005), which acquires the resources faster than other species. But on the other hand this species is allocating nutrients under wet and waterlogged soil conditions, which commonly results in a strong increase of leaf biomass (WILSON *et al.* 1999). The stress reaction of *Juncus inflexus* is intermediate compared to the other two species. *J. inflexus* has a comparable SLL to *J. effusus* and the LDMC is lower for *Juncus inflexus* than for *J. effusus*, but higher than for *J. articulatus*. Especially the LDMC of *J. inflexus* is reduced during the competition at all soil moisture levels along with an increase of the SLL.

It is well known that competition and facilitation are two sides of the same coin of inter-specific interaction in plant communities (CALLAWAY & WALKER 1997). Depending on the environmental conditions and stress factors, the interaction between plant species can either result in competition or facilitation (CALLAWAY & PENNINGS 2000; FREY & LÖSCH 2004). A good estimation for the competitive response of the investigated species under the varying soil moisture conditions is the relative competition index (RCI) for each species (WILSON & KEDDY 1986), calculated by:

$$RCI = (B_{mono} - B_{comp}) / B_{mono} \quad (11)$$

where B_{mono} is the aboveground biomass of the selected species during monoculture and B_{comp} is the aboveground biomass of this species during competition. A result of "1" would correspond to a maximal depression of the investigated species, due to the competition. A result of "0" indicates that this species is not affected by the competition and a negative result indicates that this species is facilitated by the competition. According to the results of the soil moisture gradient experiment, the strongest reaction of all plants to the competition stress can be found at the dry soil moisture levels, where water supply is limited (Tab. 10). In this case, the RCI is

highest for *Juncus effusus* (RCI = 0.7), intermediate for *Juncus articulatus* (RCI = 0.5) and minimal for *Juncus inflexus* (RCI = 0.2). Thus among these three plant species, *J. effusus* is most sensitive to competition stress. And on the other side as mentioned above, all species are able to increase their average leaf length and dry weight at wet and waterlogged soil conditions. Thus, at waterlogged soil conditions the RCI of all three investigated species is negative, indicating a facilitation effect due to interspecific interaction (RCI of *J. effusus* and *J. articulatus* = -0.2; RCI of *J. inflexus* = -0.3). Therefore the competition pressure in this experiment is strongly dependent on soil moisture and shifts towards a collective facilitation for all three plant species at high soil moisture levels. Besides the quasi unlimited water supply, additive effects due to collective aeration of the inundated soil and by this synergetic exploitation of nutrients are common factors that enhance facilitation (CALLAWAY & KING 1996).

Table 10. The relative competition index (RCI) of the investigated species in dependency of the different soil moistures. Positive values indicate competition and negative values indicate facilitation between the three species.

	relative competition index		
Soil moisture	*J. effusus*	*J. inflexus*	*J. articulatus*
dry	0.7	0.2	0.5
low	-0.1	0.2	0.2
medium	-0.1	0.0	-0.2
wet	-0.1	-0.2	-0.4
waterlogged	-0.2	-0.3	-0.2

Examples for the facilitative effect of *Juncus effusus* plants on other species are also provided by ERVIN (2005 and 2007), who reported that tussocks of *J. effusus* facilitate the growth of several species, e.g. *Boehmeria cylindrica*, *Leersia oryzoides*, and *Lonicera japonica*. In these cases, the facilitation effect was driven by the shading of the culms but also depending on the water table, too. Thus, the biodiversity of wetland communities is strongly dependent on the interplay of competition and facilitation

among the different involved plant species, fueled by varying environmental parameters, especially by the soil moisture.

4.2. CO_2 and H_2O Gas exchange and internal aeration

4.2.1. CO_2 and H_2O gas exchange

The results of the gas exchange measurements demonstrate that all three investigated plants show in general similar reactions of the photosynthetic apparatus: The transpiration of all three investigated plant species is mainly driven by leaf-to-air VPD and at its higher values g_s limited, whereas photosynthesis is rather light and temperature dependent. The data of the gas exchange of *J. effusus* are in accordance with findings by other authors (e.g. MANN & WETZEL, 1999). Although these authors did not investigate the diurnal progress of gas exchange rates, they found comparable values for A_{max} and for optimal temperature. Their results likewise as the present data demonstrate that *J. effusus* and also *J. inflexus* and *J. articulatus* are well adapted to low to medium environmental stress conditions reaching under such conditions moderate CO_2 assimilation rates.

However, some differences between the investigated species obviously come up: *J. articulatus* has the highest photosynthetic assimilation rates as well as the highest transpiration rates compared to *J. effusus* and *J. inflexus*. This characterizes *J. articulatus* as species with a tendency towards a quicker biomass production, compared to the other two species, which supports the findings from the soil moisture gradient experiments. Interestingly, even though the maximum photosynthetic assimilation rate is higher for *J. articulatus*, the water use efficiency (WUE; quotient of photosynthetic CO_2 assimilation rate (µmol CO_2 m^{-2} s^{-1}) and H_2O transpiration rate (mmol H_2O m^{-2} s^{-1}); LÖSCH 2002) of all three investigated species is similar due to the higher transpiration rates of *J. articulatus* (*J. effusus* = 1.88; *J. inflexus* = 1.78; *J. articulatus* = 1.93). Thus, the quicker biomass accumulation of *J. articulatus* is

achieved at the cost of an increased loss of water caused by the increased transpiration.

Another effect compensates the seemingly advantage of *J. articulatus* in photosynthetic carbon gain: although the maximum photosynthetic rate of *J. articulatus* is up to 55% higher than the photosynthetic rate of *J. effusus* and *J. inflexus*, the chlorophyll content is much higher in the culms of *J. articulatus* (Tab. 7). One reason for this lies in the lower dry weight per cm culm length of *J. articulatus*. Thus, the efficiency of the maximum photosynthesis per invested mg of chlorophyll is strongly reduced in *J. articulatus* (0.016 µmol CO_2 mg^{-1} chlorophyll s^{-1}), compared to *J. effusus* (0.113 µmol CO_2 mg^{-1} chlorophyll s^{-1}) and *J. inflexus* (0.046 µmol CO_2 mg^{-1} chlorophyll s^{-1}). As a typical pioneer species in wetland habitats, *J. articulatus* is generally not confronted with strong competition pressures for water or nutrients. Hence, the plant growth strategy is obviously to build up biomass quickly, and by this to spread across the habitat and cover potential surfaces until it might become outcompeted and displaced by later succession stages.

However – as it is shown for other wetland plants – it must be emphasized, that the CO_2 assimilation rates can be strongly influenced, if environmental stress conditions change. The most important environmental stress affecting wetland plants is the fluctuation of the water level. It is well known, that – even though wetland plants are adapted to this stress – the photosynthetic CO_2 assimilation of wetland plants is reduced between 18 to even 100% during the beginning of a soil flooding, due to the strong decrease in the soil redox potential (PEZESHKI 2001). However, a substantial recovery of the photosynthetic CO_2 assimilation can occur over time, due to the increase of the soil redox potential, caused by the ROL from the plant roots (COLMER 2003a).

4.2.2. Aerenchyma internal aeration

A comparison of daytime and nighttime levels of the culm internal oxygen concentrations emphasizes that in contrast to *J. inflexus* and *J. articulatus*, culm internal oxygen concentration never raises above nighttime oxygen levels during days of high ambient temperatures in the case of *Juncus effusus*. In all investigated plants, the amount of oxygen decreases with higher temperatures due to an increased respiratory activity of the culm tissue during the course of the day. This effect is compensated by photosynthetic production of oxygen only for *J. inflexus* and *J. articulatus*, but only during the late afternoon, when the temperature regime turns to moderate conditions, i.e. temperatures below 30°C. Therefore, the plant internal oxygen supply towards the roots is reduced, especially in the culms of *J. effusus*. However, the reduced internal oxygen supply during midday will probably not severely affect the growth of the plant roots of the investigated species during phases of higher ambient temperatures for two reasons: (I) It can be expected that this short term culm internal oxygen concentration changes between 80 and 100% air saturation are buffered to a certain extent within the plant internal aerenchyma continuum. These air spaces reduce the impact of phases of decreased internal oxygen supply, as it has been shown for the aquatic macrophyte *Egeria densa* (SORRELL & DROMGOOLE 1986). (II) A shrinking of the oxidative zone around the roots, due to the reduced input of oxygen via radial oxygen loss from the roots is a slower process than the initial rhizospheric oxidation (JENSEN *et al*. 2005). Therefore, the chemical condition of the rhizosphere will not turn into a strongly reducing environment that might disturb the root-rhizosphere network during phases of hampered plant internal oxygen supply (see also chapter 3.8.; e.g. Fig. 42).

The fact, that the internal oxygen concentration in the culms of *J. inflexus* decreased from the base level of 100% air saturation twice a day is on the one hand attributable to high respiratory activities during the high temperatures at midday, whereas the second drop is apparently attributable to a lack of atmospheric oxygen inflow during

the night due to stomatal closure. Equilibrium with the atmosphere is reached during the first hours in the morning, when the stomata open and photosynthesis starts again.

These findings of reduced culm internal oxygen concentrations are contrary to what is known from other studies, where the internal oxygen concentration in the culms of e.g. *Phragmites australis* (BRIX *et al.* 1996) and *Eleocharis sphacelata* (SORELL & TANNER 2000) is raised up to atmospheric conditions during daytime. This contrast is mainly attributable to the fact, that *P. australis* and *E. sphacelata* are species known for pronounced convective internal gas flows (ARMSTRONG & ARMSTRONG 1991; BRIX *et al.* 1992). This convective internal gas flow is common for plants growing in deep water habitats, because the convective oxygen supply of the basal plant organs is superior over long distances to the diffusive oxygen supply particularly in these habitats. Although the diffusive oxygen supply within the plant aerenchyma is slower than convective gas flow, it is independent from the external environmental parameters humidity and wind - the key driving forces of convective gas flow (AFREEN *et al.* 2007) – and thus appropriate for species like *J. effusus*, *J. inflexus* and *J. articulatus* that grow in shallower waters.

Another process that is coupled with the internal aeration and that receives more interest in recent works is, that those plant species that exhibit a strong and efficient internal pressurized ventilating system, will not only transport more oxygen into the soil than others, but also transport elevated amounts of trace gases - especially CO_2 and CH_4 - from the soil into the atmosphere (JOABSSON & CHRISTENSEN 2001; CHANTON *et al.* 2002; CHENG *et al.* 2007). This will depend on the balance between e.g. increased CH_4 oxidation, due to increased oxygen inflow into the soil that supports the growth of methanotrophs living in the rhizosphere (WASSMANN & AULAKH 2000) and even within the plants (RAGHOEBARSING *et al.* 2005), and quicker transport and release of CH_4 by this pressurized ventilation. This might play an essential role, if the

species composition of a wetland changes from species that rely on internal oxygen diffusion only, towards species with strong internal ventilation systems.

4.3. Organic acids in the bulk soil and in the rhizosphere

In contrast to conventional rhizotrones, including those used for split-root investigations, the construction of a partitioned rhizotrone that allows free-choice in-growth of roots into differentially manipulated soil substrates, combined with minimal-invasive multiple factor analysis, provides investigations of soil-rhizosphere-plant interactions with respect to the potential of whole plant responses to below-ground life conditions. In this study, the partitioned rhizotrone was used to investigate the role of the root-soil interface of three aerenchyma plant species (*Juncus effusus*, *Juncus inflexus* and *Juncus articulatus*) on the abundance of organic acids.

Due to the different compartment specific physico-chemical conditions in the bulk soil, a pH-dependent but also a plant species dependent qualitative and quantitative balance of organic acids was obvious. In total there were only four different organic acids that could be detected in all experiments: formate, oxalate, acetate and lactate. Other common organic acids like malate or citrate were not detectable. For example in the parent soil compartment only three out of the four different organic acids could be detected in all experiments, but the composition was different. In the *J. inflexus* experiment oxalate, formate and lactate are detectable, while acetate was below the limit of detection (LOD). On the other hand during the experiments with *J. effusus* and *J. articulatus*, formate was below LOD whereas acetate was detected in considerable amounts. This qualitative shift of the composition of the organic acids in the bulk soil can be related to soil life processes which are influenced across the whole soil volume by the peculiar plant cover, in the experimental case the presence of different *Juncus* spp. rooting in the beginning of the particular study in the uppermost soil layer (parent soil compartment).

It is a well known phenomenon that during phases of anoxia the substrate availability for e.g. methanogenesis or Fe(III) reduction varies over time. For example LUEDERS AND FRIEDRICH (2000) demonstrated that there is an offset of acetate and formate availability as precursors for methanogenesis in rice field soils, due to the varying activity of the microbial communities. Thus, although all experiments of this study were conducted according to the same time schedule, the developmental stages of the individual microbial communities were different. There are a couple of reasons for the qualitatively different patterns of organic acids in the soil solution, but the predominant factor is certainly the individual growth of the roots. As it is shown in chapter 3.8., the roots of the different investigated plant species exhibited different growth rates, oxidation and acidification patterns. Thus, besides direct effects on the rhizospheric soil, the bulk soil biogeochemistry and microbial community is also affected by these species-dependent alterations of the soil (Tab. 8 & 9). Nevertheless, the total amount of organic acids in the parent soil compartment is comparable in all three experiments. According to LUEDERS AND FRIEDRICH (2000), the *J. inflexus* experiment would correspond to an older stage of the soil chemistry dynamics (higher levels of formate concentration), whereas the other two experiments would correspond to an earlier stage of methanogenesis (higher levels of acetate concentration).

However, strong differences arise at the more acidic soil conditions in the test-compartment 'B'. For example acetate was found in considerable amounts during the *J. inflexus* experiment and low amounts of formate were found during the *J. articulatus* experiment, which is contrasting to the findings for e.g. the parent soil compartment. Moreover the total quantities of organic acids increased by up to a factor of three under these strong acidic conditions. The increase in organic acids in the acidic submerged bulk soil indicates reduced microbial degradation of organic substrates due to the lack of inorganic electron acceptors (Fe(III), nitrate, sulphate, etc.) at anaerobic conditions (YAO *et al.* 1999, KÜSEL 2003, LU *et al.* 2006). According to the E_h-pH stability field of iron compounds (SCHEFFER & SCHACHTSCHABEL 2002; KIRK

2004), iron occurs in its reduced form, Fe(II), at strong acidic and anaerobic conditions. The lack of Fe(III) as an electron acceptor appears to be a limiting factor in anaerobic microbial metabolism, that co-determines the catabolism of organic acids as intermediates in the anaerobic degradation of organic matter towards CH_4 and CO_2 (DANNENBERG & CONRAD 1999, HORI *et al.* 2007). Hence, the dissimilatory activity of Fe(III)-reducing bacteria, such as *Geobacter* spp. and *Anaeromyxobacter* spp. (PETRIE *et al.* 2003, LU *et al.* 2006, HORI *et al.* 2007), which are able to oxidize acetate (HORI *et al.* 2007), will be reduced at low pH. Moreover, it could be shown by other authors that low pH inhibits the growth of Fe(III)-reducing bacteria and growth was only observed with glucose as the carbon substrate (PETRIE *et al.* 2003). Interestingly, Fe(III)-reducing bacteria did not use lactate and acetate as electron donors under acidic conditions at pH 3 – 4 (PEINE *et al.* 2000). Therefore, accumulation of organic acids (especially acetate) in strong acidic anoxic soil is not only due to reduced metabolic activity of (i) dissimilatory acetate oxidation, and (ii) methanogenic cleavage of acetate to CO_2 and CH_4, i.e. the acetotrophic reaction (MADIGAN & MARTINKO 2006; HORI *et al.* 2007), but also to reduction of growth of Fe(III)-reducing bacteria and changes in their substrate utilization. Using ^{13}C-labeled acetate in anoxic rice field soil (pH 6) revealed that $^{13}CH_4$ and $^{13}CO_2$ together accounted for about 60% of the supplied acetate ^{13}C, with $^{13}CH_4$ being the predominant product (HORI *et al.* 2007). Even though a very few methanogens are acetotrophic (e.g. *Methanosaeta*), about two-thirds of the methane formed in methanogenic habitats originates from acetate (MADIGAN & MARTINKO 2006). Adaptations of anaerobic bacteria, including methanogens, to low pH in acidic bog sediments also proved that acetate appeared to be the major methane precursor (GOODWIN & ZEIKUS 1987). The authors reported that the rate of methane production from acetate (acetoclastic methanogenesis) was fivefold lower at pH 3.7 than at pH 4.7 to 5.6, with an optimum at pH 5.2. YAVITT and collaborators (2005) also reported a strong decrease of CH_4 production due to acid site conditions (pH < 4). These findings indicate that, besides acetate oxidation, acetoclastic methanogenesis is also strongly restricted at pH < 4, leading to acetate

accumulation, while at pH > 5 unimpeded metabolization of acetate to CH_4 and CO_2 takes place under anoxic conditions. Therefore, as reported in this study, the pH-dependent shift in composition and concentration of organic acids in the anoxic bulk soil pinpoints the significance of pH and redox potential on the microbial process dynamics of anaerobic organic matter degradation with respect to CH_4 and CO_2 emission from submerged soils.

In contrast to the bulk soil, the roots of *J. effusus*, *J. articulatus* and *J. inflexus* revealed a strong impact on the distribution of the organic acids, indicated by a pronounced gradient of decreasing concentration of organic acids from the bulk soil towards the roots. Since the rhizotrone was continuously flooded throughout the experiment, the bulk soil was hypoxic to strictly anoxic in all compartments (see chapter 4.4.), providing the appropriate conditions for anaerobic microbial production of organic acids. On the other hand, the roots of *J. effusus*, *J. articulatus* and *J. inflexus* are able to release large amounts of oxygen into the rhizosphere raising the oxygen level from anoxia to oxic conditions of up to almost 200 μmol O_2 l^{-1} (see chapter 4.4.). Hence, under submerged soil conditions, the roots of wetland plants do not play a role as major sources of carbons and acids in terms of production of organic acids as it is well known for unsaturated soils (JONES 1998; JONES *et al.* 2003). However, the roots of wetland plants can directly manipulate the production and consumption of organic acids by raising the oxygen level in the rhizosphere. The dynamics of oxygen release from roots, driven by oxygen supply from the above-ground photosynthesizing plant parts induces a complete change from anoxic to oxic life conditions on a micro scale. Hence, the population density of anaerobic bacteria which produce organic acids like lactate (e.g. *Lactobacillus*) and acetate (e.g. *Acetobacterium*) by fermenting sugars or reducing CO_2 (MADIGAN & MARTINKO 2006), will strongly decline towards the aerobic root surface, and therefore, the concentration of these organic acids will also decline. But as shown in chapter 4.3., not all roots, and not even the same root release similar amounts of oxygen at the

same time, thus a spatially and temporally heterogeneous pattern of oxygen release is in common for all three investigated plant species. These live roots with negligible oxygen release to the rhizosphere, e.g. those with reduced growth activity, represent attractors for anaerobic biota due to the availability of root exudates as an additional carbon source for anaerobic metabolism. The findings presented in this study put strength on this assumption, because in comparison with the bulk soil, considerably enhanced concentrations of organic acids, especially acetate, were also found at individual roots, whilst neighboring roots showed quite the opposite.

The intrusion of oxygen from the roots into the anaerobic environment will raise the redox potential and thus, favors the oxidation of reduced iron, particularly at low pH. For example, KÜSEL and collaborators (2003) proved that Fe(II) is oxidized to Fe(III) by iron oxidizing bacteria at the root surface of *J. bulbosus*, a wetland plant that released oxygen into the anoxic soil of an acidic coal mining lake. Enhanced iron oxidation even caused a coating of the roots with iron plaques (CHABBI *et al.* 2001, KÜSEL *et al.* 2003). Furthermore, the improved availability of oxidized iron in the proximate environment of the roots of wetland plants will support the metabolic activity and the growth of Fe(III)-reducing bacteria, and therefore, facilitate a rapid microbial-mediated cycling of iron in the rhizosphere (KÜSEL *et al.* 2003, WEISS *et al.* 2003). Hence, the activity of Fe(III)-reducing bacteria, able to oxidize organic acids as mentioned above, will also contribute to the decrease of organic acids like lactate and acetate in an oxygenized rhizosphere. In freshwater sediments rooted by *J. effusus* Fe(III) reduction accounted for 65% of total carbon metabolism in the rhizosphere compared to 22% methanogenesis (RODEN & WETZEL 1996). The authors stated that Fe(III) oxide reduction could mediate a considerable amount of organic carbon oxidation and significantly suppress CH_4 production in freshwater wetlands.

4.4. Non-invasive optical pH and O_2 measurements

The qualification of the single pH-sensitive and the pH-O_2 sensitive hybrid planar optodes – as powerful and convenient tools for non-invasive, and thus genuine, online measurements of the soil pH / O_2 concentration and the influence of plant roots on the spatial and temporal dynamics – is successfully proved. The stability of the sensor dyes, proved to be excellent over a period of more than 8 weeks of measurements in submerged soils. In contrast to pH or O_2-related imaging techniques reported in the literature so far (MARSCHNER 1995; JAILLARD *et al*. 1996; CHABBI *et al.* 2000; KOPITTKE & MENZIES 2004), this is the worldwide first time that the root-mediated heterogeneity of pH and O_2 dynamics were simultaneously quantified under semi-natural and submerged soil conditions without a method-induced disturbance of biological and physicochemical process dynamics in the root–soil system.

A potentially optical disturbance of root growth and pH dynamics by the blue-light excitation of the indicator dye can be neglected. Already in 1978, SCHNEIDER and BOGORAD showed that blue light at a wavelength of 470 nm and with a flux rate of 19.2 pmol photons cm^{-2} s^{-1} nm^{-1}, equivalent to an energy charge of 4 mW cm^{-2} nm^{-1}, during 15 s of illumination had no effect on the spectral absorbance of growing roots of *Zea mays*. Referring to this findings, the application of an extremely low flux rate (0.0035 pmol photons cm^{-2} s^{-1} nm^{-1}) of 99.98% less than the documented rate, and also the low energy charge of 0.9 mW cm^{-2} nm^{-1} (i.e. 75% less) most probably does not induce any artificial effect on root growth or root physiology. This is additionally supported by the fact that no difference in growth rates between roots growing across the sensor foil and roots growing in the bulk soil was observed.

For a correct interpretation of the driving forces of the pH and O_2 dynamics, it is essential to determine the ratio between the diffusion and convection of protons and molecular oxygen (O_2) within the submerged soil. A good guide for interpretation is the so-called Péclet number (KIM *et al.* 1999), which can be calculated as follows:

$$P_{soil} = V * L * D^{-1} \quad (12)$$

Where V is the root growth rate, L is the diameter of the root and D is the diffusion coefficient of the relevant molecules in water (e.g. protons or molecular oxygen). A Péclet number much lower than 1 implies that proton diffusion acts to produce an artificial rhizosphere that is wide relative to the root radius. When P is much larger than 1, the convection of protons by root growth dominates, so that the field of acidified soil around the root tip is narrower.

In this study, the average root growth rate of e.g. *J. effusus* roots was 0.52 mm h^{-1} (0.47 mm h^{-1} for *J. inflexus* and 0.80 mm h^{-1} for *J. articulatus*) and the average root diameter of *J. effusus* roots was 0.95 mm (0.90 mm for *J. inflexus* and 0.80 mm for *J. articulatus*). The diffusion coefficient of protons in a submerged soil can be assumed to be close to water, which is 33.84 mm^2 h^{-1} (KIM *et al*. 1999), whereas the diffusion coefficient of molecular oxygen in a submerged soil is 7.56 mm^2 h^{-1} (ARMSTRONG 1979). Thus, the Péclet number for protons was 0.015 for *J. effusus* (0.013 for *J. inflexus* and 0.019 for *J. articulatus*) and the Péclet number for molecular oxygen was 0.065 for *J. effusus* (0.056 for *J. inflexus* and 0.085 for *J. articulatus*). This indicates that in all investigated cases diffusion will produce a wide acidified and oxygenized rhizosphere around the tips. Convection occurs as a result of growth and causes the acidified and oxidized region to move with the growing tip.

4.4.1. Single pH measurements

The preliminary study for evaluating the two-dimensional quantitative imaging technique, by use of a single pH planar optode in the root–rhizosphere–soil interface of *Juncus effusus* in an alkaline soil, revealed a strong spatial and temporal heterogeneity between (1) individual roots; (2) main and lateral roots; and (3) along

individual roots. The non-invasive measurements of pH proved pronounced short-term fluctuations of pH in the rhizosphere of *J. effusus* within several minutes, and long-term dynamics during more than 8 weeks as well. The results clearly show that growing roots of *J. effusus* have a strong impact on the pH of the surrounding alkaline soil substrate that changes the environmental conditions for the soil-biota-network within a short time. In contrast to findings with maize roots (TAYLOR & BLOOM 1998; WALTER *et al.* 2000; FAN & NEUMANN 2004; PETERS 2004), our measurements show that during daytime, young growing roots were able to acidify the proximate environment by up to one pH unit via their entire surface, comparing to the bulk soil. It is a common phenomenon that the pH of a growing root tip is about one to two units lower than the bulk soil (BEGG *et al*. 1994; HINSINGER *et al*. 2003; KOPITTKE & MENZIES 2004). No specific axial gradient of pH changes during the growth of the root tips of *J. effusus* could be detected. On the contrary, at night-time, the proximal parts of the roots – about 9 mm off the root tip – acidified the soil stronger than the root tips, whereas shortly after the onset of light these differences ceased. Comparable results of this daylight driven acidification and alkalization overnight of similar intensity are reported for *Medicago sativa* (JARVIS & HATCH 1985, flowing solution measurements) and *Vigna unguiculata* (RAO *et al*. 2002, pH indicator agar gel measurements). One possible reason for these diurnal variations could be a photosynthesis-derived increase of ROL. Increased soil oxygen concentration would act as an indirect source of protons, because reduced ions like the highly mobile Fe^{2+} will be oxidized and precipitated on or near the roots. This process also generates protons (see next chapter 4.4.2.). However, this was not the case in this study, as no circadian rhythm of ROL was detected. Hence, the observed daylight-driven acidification must have been caused by another process: It is well known that photosynthesis is a prerequisite for root-induced acidification of the soil resulting from the conversion of NH_4^+ to glutamine (WAGNER 1991; FOYER & NOCTOR 2002). Additionally, as a consequence of submergence, hypoxia and a negative E_h causes NH_4^+ to be the predominant nitrogen source in wet soils (BURESH & PATRICK 1978;

BONIN 1996; BRUNE *et al*. 2000). Thus, NH_4^+ uptake accompanied by equivalent proton release (Fig. 51) is the prevailing way of nitrogen acquisition by wetland plants (MARSCHNER 1995; BLOOM *et al*. 2003). In other cases, NH_4^+ conversion to NO_3^- by nitrification in the aerobic rhizosphere might in fact support the roots with substantial quantities of NO_3^- (Eqn. 15; KIRK & KRONZUCKER 2005). Under these conditions, the effect of an ammonium dependent acidification will be reduced. By the use of the novel 2D pH imaging technique in the current study, this link between photosynthesis and ammonium dependent acidification is clearly visualized and quantified.

4.4.2. pH-O2 hybrid measurements

The specific environmental conditions of the hybrid optode studies demonstrate that the driving forces of rhizospheric pH and O_2 concentration changes are species dependent. First of all, the results clearly show that the roots of all investigated plant species release large amounts of oxygen into the submerged soil, which is a common phenomenon for wetland plants (CHABBI *et al.* 2000; ARMSTRONG *et al.* 2000; WIEßNER *et al.* 2005). As it is mentioned in the chapter above, this considerable input of oxidants is able to cause an acidification of the affected soil area, due to the oxygenation of reduced ions, especially Fe^{2+} (Eqn. 13; Fig. 51; BEGG *et al.* 1994; KIRK & BAJITA 1995).

$$4Fe^{2+} + O_2 + 10H_2O \Leftrightarrow 4Fe(OH)_3 + \mathbf{8H^+} \qquad (13)$$

Assuming, that Fe^{2+} oxidation is the predominant source of protons during the process of oxidative acidification in the soil (Fig. 50) and that the Fe^{2+} concentration is constant – due to the permanent watering with standard Knop nutrient solution (71.9 µmol Fe^{2+} l^{-1}, Tab. 3) – a theoretically maximum proton generation of 143.9 µmol l^{-1} is possible at a computationally oxygen concentration of only 18.0 µmol O_2 l^{-1}. This

includes the assumption that all O_2 molecules are reduced exclusively by Fe^{2+} ions. Without any buffering of the soil or the roots, this huge amount of protons would lead to a very strong acidification of the soil at very low oxygen concentrations, especially within the range of pH 6 to pH 4 which corresponds to a proton concentration of 1.0 to 100.0 μmol l^{-1} (actual range of pH of this study). Hence, according to the average bulk soil oxygen concentrations (Tab. 9), the average bulk soil pH would be expected to be much lower than recorded. The expected pH value at complete Fe oxidation would be pH 3.83 (in A600 soil) or pH 3.84 (in E400 & E910 soil), depending on the initial pH value of the soil.

Furthermore, according to the strong ROL from the roots of all investigated plants, it could be expected that this increase in O_2 concentration would at least lead to an increased acidification of the rhizosphere. However, the strongly oxidized rhizosphere is only acidified in the case of *J. effusus*, whereas the rhizospheric pH along the roots of *J. inflexus* was not affected at all. In contrast, the rhizospheric oxidization was accompanied by a rhizospheric alkalinization in the case of *J. articulatus*. These results point out that the roots of the investigated plant species buffer the oxidative acidification differently during phases of ROL, and that this buffering effect is even stronger than in the bulk soil.

The cause for the discrepancy between potential and effective oxidative acidification lies in the diversity of biotic and abiotic reactions in the soil. For example, the microbiological consumption of oxygen can quickly reduce the availability of oxygen and therefore reduce the amount of protons that can be generated. Some studies report that up to 50% of the released oxygen can be consumed by microorganisms (HOWELER & BOULDIN 1971; KIRK & SOLIVAS 1994). On the other hand, protons can be consumed by several processes in the soil. One possible process is the carbon dioxide (CO_2) uptake of roots (BEGG *et al.* 1994). Under anaerobic conditions the fermentative production of carbon dioxide strongly increases the partial pressure of CO_2 compared to the atmosphere-plant continuum (GREENWAY *et al.* 2006). Thus, this

steep concentration gradient can be a driving force for CO_2 uptake by plant roots and CO_2 transport via the aerenchyma towards the atmosphere (HIGUCHI *et al.* 1984; BRIX 1990; CONSTABLE *et al.* 1992). And the dissolved CO_2 in the rhizosphere solution is in equilibrium with HCO_3^- or CO_3^{2-}, depending on the pH value (Eqn. 14; Fig. 51) and within the relevant pH range of this study (pH 4 to pH 6), dissociation of CO_2 equilibrates between HCO_3^- and CO_2^{aq}. Hence, during a continuous uptake of CO_2 the balance between HCO_3^- and CO_2^{aq} (H_2CO_3, is not stable and indicated in Eqn. 14 as $H_2CO_3^*$) is shifted towards the CO_2 side, consuming one proton per CO_2 taken up.

$$\overset{+\,2OH^-}{CO_2^{aq} + H_2O \Leftrightarrow H_2CO_3^* \Leftrightarrow HCO_3^- + H^+ \Leftrightarrow CO_3^{2-} + 2H_2O} \qquad (14)$$

As stated by other authors (HINSINGER *et al.* 2003; COLMER 2003b, GREENWAY *et al.* 2006), there is unfortunately still no data providing an estimate about the contribution of CO_2 concentration changes to changes in the rhizosphere pH.

Another possible factor that might hamper the effect of oxidative acidification could be excretion of bases by the roots. It is well known that during the uptake of negatively charged molecules – especially nutrients like nitrate (NO_3^-) – other negatively charged ions (e.g. OH^-; HCO_3^-, organic anions) are excreted by plant roots to maintain cation-anion balance (Fig. 51; MARSCHNER *et al.* 1991, MARSCHNER 1995; HINSINGER *et al.* 2003). These excreted anions on the other side can alkalinize the rhizosphere and – by diffusing into the bulk soil – affect the pH of the bulk soil also. However as stated in chapter 4.4.1., during wetland conditions nitrate uptake is only possible, if nitrifying bacteria accompany the aerobic zones of the rhizosphere in the remaining anaerobic wetland soils. But, the nitrification will generate two protons per NH_4^+ molecule (Eqn. 15; Fig. 51; SCHEFFER & SCHACHTSCHABEL 2002), and only one OH^- will be released from the roots during the uptake of one molecule NO_3^- (Fig. 51).

$$NH_4^+ + 2O_2 \Leftrightarrow NO_3^- + H_2O + \mathbf{2H^+} \quad (15)$$

Thus, the net balance will still cause an acidification, if nitrification and nitrate uptake processes would be predominant in the rhizosphere. But in this study nitrate is continuously supplied by the watering with the standard Knop nutrient solution. Therefore NO3- uptake was possible without the presence of nitrifying bacteria. On the contrary, denitrification in the oxygen deficient soils could have also reduced the proton concentration quite efficiently (Eqn. 16). However, only four protons will be consumed during denitrification, whereas five molecules CO_2 are produced that in turn can generate protons again (Eqn. 14).

$$5CH_2O + 4NO_3^- + 4H^+ \rightarrow 2N_2 \uparrow + 5CO_2 + 7\,H_2O \quad (16)$$

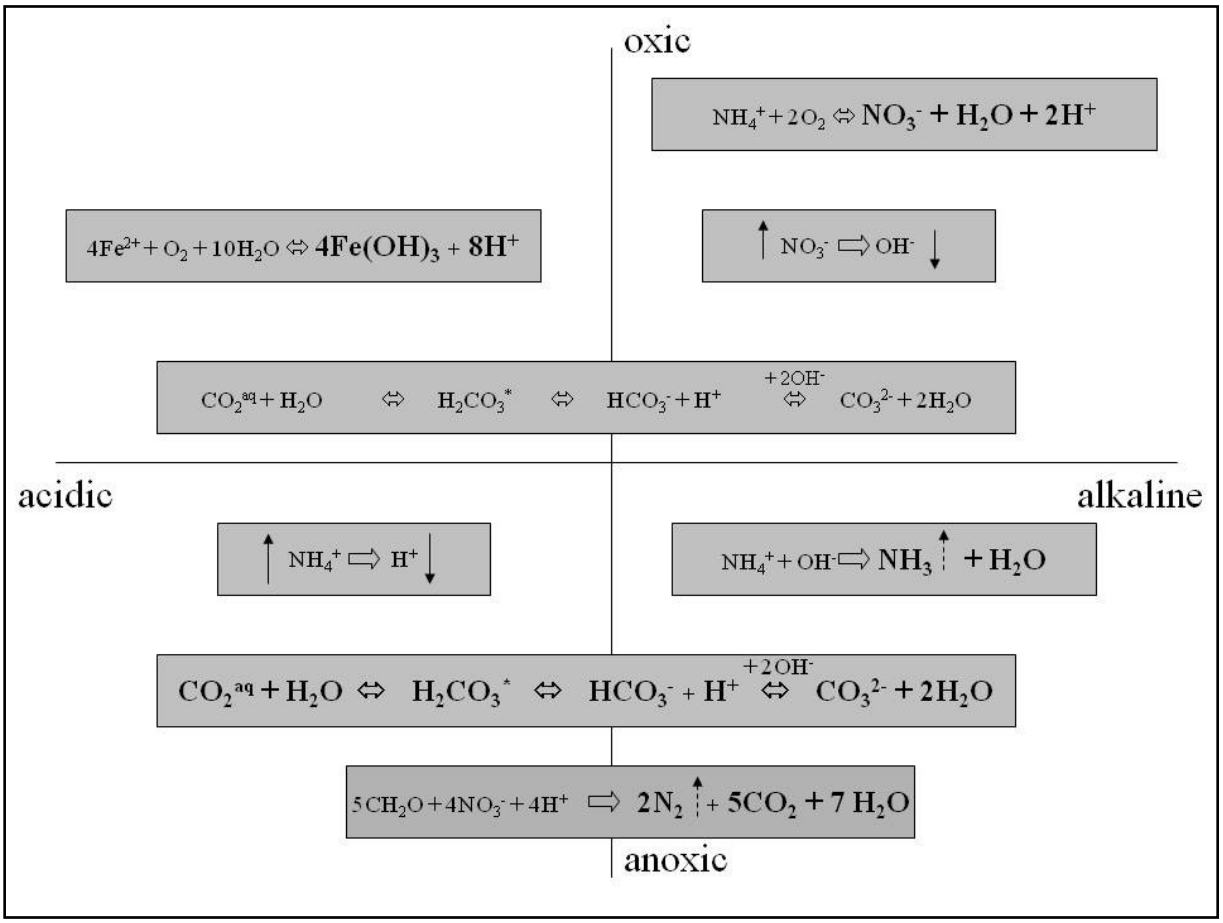

Figure 51. Qualitative overview of the soil processes described in equations 13 - 16 and in the text above. Arrows indicate uptake and release processes by plant roots, dashed arrows indicate volatilization processes.

As it is mentioned above, in the case of *J. effusus* the rhizospheric pH-O_2 relationship fits partly the postulated model of proton generation by oxidation of reduced Fe^{2+}. However, the roots of *J. effusus* do buffer the rhizospheric pH value up to a certain oxygen concentration during the approach of the root tip, but above this threshold the rhizospheric pH value is coupled reciprocally proportional to the rhizospheric oxygen concentration again, as it is characteristic for the bulk soil (chapter 4.4.2.). Nevertheless, the rhizospheric pH never reached the potential saturation level of pH 3.8, according to the maximal proton generation by Fe^{2+} oxidation. Thus, the buffering effect of the roots of *J. effusus* balances the impact of the oxidative acidification up to the threshold of 90 µmol O_2 l^{-1} very efficiently and even beyond this threshold, the maximal acidification is impeded, although it can be expected that a substantial amount of Fe^{2+} is oxidized during peak ROL. Hence it can be concluded, that the roots of *J. effusus* either excrete alkalinizing bases, or take up quantities of CO_2, buffering to a certain threshold the direct vicinity of the root tips. But the impact of this process becomes subsidiary to the oxidative acidification during phases of higher ROL.

This oxidative acidification along the roots of *J. effusus* is not permanent, due to the decline of the ROL as soon as the root tip passed by but starts again as soon as lateral roots are formed. This restriction of ROL to the root tips and the lateral roots is typical for *J. effusus* (VISSER *et al.* 2000; VAN DER WELLE *et al.* 2007) and quite common for wetland plants in general, due to the formation of a barrier to radial oxygen loss in the basal root cortex of the main roots (e.g. *Cladium jamaicense,* CHABBI *et al.* 2000; *Oryza sativa,* COLMER 2003a). This barrier is also responsible for another effect: while the ROL from lateral roots is driven by diurnal rhythms, the ROL from the main roots is constant. This effect is mainly attributable to the fact that due to the cortical barrier along the main roots, aerenchyma internal diurnal fluctuations of O_2 are buffered and therefore the root tips are supplied with a constant O_2 concentration. Moreover, this cortical barrier also restricts the uptake and release of

solutes (SOUKUP *et al.* 2007), which is another reason for the absence of root derived pH changes along the proximal root sections of *J. effusus*.

In contrast to the roots of *J. effusus*, the roots of *J. inflexus* and *J. articulatus* show an even stronger buffering effect. Interestingly, although the pattern of ROL is similar and the range of ROL differs only slightly (maximal ΔO_2 = 13.4 µmol O_2 l^{-1}), the impact of the ROL from the roots of *J. inflexus* on the bulk soil is stronger than the impact of the ROL form the roots of *J. effusus*. This is mainly attributable to the slower root growth rates and therefore longer oxidation times for *J. inflexus* roots (Tab. 9), causing a higher oxygen content in the bulk soil coupled with a stronger acidification. Although the roots of *J. inflexus* release large amounts of oxygen into the soil (Tab. 9), the rhizospheric pH is not acidified as it is the case for *J. effusus*. The rhizospheric pH of *J. articulatus* even increases during ROL. This is remarkably since the ROL from the roots of *J. articulatus* never ceases after the approach of the root tip. This also causes a continuous increase of the bulk soil oxygen content. However, this results in an only weak acidification of the bulk soil. Thus it can be assumed, that the roots of *J. inflexus* and especially the roots of *J. articulatus* excrete higher quantities of bases or take up more CO_2 than *J. effusus*.

As an important result of the non-invasive investigations, the circadian rhythms and the restricted oxygenation/acidification zones around the roots, the critical pH-dependent E_h thresholds for hypoxic to anoxic conditions (Fig. 1, dotted line) and e.g. N_2O/CH_4 production as well (YU & PATRICK 2003), will bring about a narrow transition zone from the rhizosphere (high E_h threshold) to the bulk soil (low E_h threshold). During the illumination of the shoots, this transition zone expands from the roots and shrinks towards the roots during the night. This certainly affects the movements of the microbial community (e.g. methanotrophs, methanogens) within the soil (DAMGAARD *et al.* 1998; SEMENOV *et al.* 1999). Therefore, the zones of production and consumption of methane and dinitrous oxide should be non-philopatric in the root–rhizosphere–soil network, at least during the growing period

of the plant roots. The fact that the oxygen concentration at the root surface is highly variable over time and among different roots supports this assumption. The root tips in fact move a cone-shaped oxic zone through the soil, while the basal parts of the roots and the bulk soil remain under hypoxic to anoxic conditions (VISSER *et al*. 2000). The lateral roots on the other hand form a wide diurnally fluctuating oxic zone again. These different patterns of young, mature and lateral roots over time indicate another species-specific factor that determines pH and oxygen dynamics in the rooted soil. Therefore, the long-term mosaic-like pattern of pH and oxygen, and consequently, the pH-E_h relationship in the soil depends on root-specific differentiation processes.

4.5. Conclusions

The results of this study revealed new insights into the plant-soil interactions in submerged soils, especially with regard to the root derived alteration of the pH and oxygen micro pattern in the rhizosphere. The development of the novel 2D imaging technique successfully integrates a state-of-the-art sensor technology into the field of plant science and the new design of a rhizotrone system for minimal sampling of rhizospheric soil solution under waterlogged conditions is also successfully demonstrated. Summing up the results from the different experiments clearly demonstrates that the three investigated plant species – *Juncus effusus*, *Juncus inflexus* and *Juncus articulatus* – show a variety of different adaptations with respect to the environmental stress conditions that are typical for wetlands.

The soil moisture gradient experiment revealed that – besides a competition effect under dry soil conditions – a strong facilitation effect exists between all three species under wet and waterlogged soil conditions. This, at the first sight surprising result, can be elucidated by taking into account the results from the 2D imaging measurements. By this, it can be assumed that the facilitation is predominantly based on the collective aeration of the soil via the roots of the plants. Because a collective

aeration will occur due to the fact, that all three plant species are able to release large amounts of oxygen into the soil, reaching almost oxygen concentrations close to 200 µmol O_2 l^{-1}, even along single roots and especially along the lateral roots. And thus, it can be concluded that the inundated, collectively rooted soil is strongly aerated, especially in the upper soil layers where the root network is very dense and many lateral roots are formed. This effect was also observed by MANIERO & KAZDA (2005), who measured soil oxygen concentrations of almost 100% air saturation below a dense stand of the well adapted wetland plant species *Carex rostrata*.

This collective aeration of the waterlogged soil functions as a precursor for a set of potentially beneficial processes that arises from oxidative soil conditions in contrast to non-aerated reducing soil conditions. For example the oxygen loss from the plant roots supports the growth of aerobic microorganisms that metabolize soil organic matter more efficiently than anaerobic microorganisms. This enhanced aerobic microbial metabolization can for example result in nitrification of ammonium to nitrate and thus increase the amount of essential plant available nutrients (KIRK & KRONZUCKER 2005). Another beneficial effect of a collective aeration of the submerged soil is the fact that the higher the soil oxygen concentration, the lower the amount of reduced toxic compounds in the soil. This can either happen by abiotic chemical oxidation of the reduced ferrous iron, or by microbial oxidation processes. This is especially relevant for the risk of increased iron toxicity due to large quantities of Fe^{2+} in anoxic soils (KIRK 2004).

Another noteworthy example of a possible conjoint but not necessarily beneficial interaction between plant roots as sources for oxygen and aerobic microbes as metabolizers of soil organic matter is demonstrated in the case of the availability of organic acids in the soil solution. Due to the continuous oxygen support by the plant roots, the soil conditions are favorable for aerobic microbes to metabolize the (anaerobically produced) organic acids along the aerobic root surface (JONES 1998; JONES *et al.* 2003). Hence, a network of wetland plant roots that collectively aerates

the soil will strongly reduce the amount of anaerobically produced organic acids in the soil. This has been demonstrated in chapter 3 where the concentration of organic acids is closely linked to the presence or absence of plant roots, with minimum concentrations at the root surfaces of all three investigated plant species.

Furthermore, any temperature dependent increased respiratory activity which will be accompanied by a proportional reduction of the oxygen concentration, as it is documented by the internal aeration measurements, especially in the case of *J. effusus*, can be bypassed by the rhizospheric oxygen supply from the nearby other species (*J. inflexus* & *J. articulatus*). Thus, even if the oxygen supply of one plant species is comparatively sensitive towards temperature changes, the other plant species can sustain the rhizospheric oxygen supply within the dense inter-specific root-network and by this hold up the growth of the roots and the aerobic microbial communities. An additional positive effect that can enhance the inter-specific facilitation is related to the potentially strong effect of an oxidative acidification, as it was recorded for *J. effusus*. This oxidative acidification will be hampered within the inter-specific root-network, due to the contrarily strong buffering effects of the roots of *J. inflexus* and *J. articulatus* that is documented in chapter 3. Thus although large amounts of oxygen will be transported into the rhizosphere-soil network, the interplay of all three plant species can stabilize the pH value, regardless of the production of protons by oxidative acidification effects. Moreover, the affected plants can still profit from e.g. the oxidation of the phytotoxic Fe^{2+} ions without changing the rhizospheric pH value.

Thus it seems that under waterlogged soil conditions a diverse plant community can be more productive, compared to monocultural stands. However, the facilitation depends on a complex interaction within the root-rhizosphere-soil network that relies on a variety of different environmental parameters (e.g. pH value and soil oxygen concentration) and wetland plants are able to manipulate these parameters very efficiently to optimize the rhizospheric micro-environment and to survive under

these harsh habitat conditions. However, in the long-term the facilitative interplay might not be everlasting, especially if some of these environmental parameters or the abundance of key actors drastically change, then the facilitation eventually declines and some of the species might be outcompeted by the other species.

5. Abstract

It is well known that the formation of a culm and root internal aerenchyma is crucial for plant life in wetland habitats. The plant internal aerenchyma allows a continuous oxygen supply of the roots that grow in oxygen deficient and reducing soils. The supplied oxygen can be even released by the roots into the perirhizal zone (rhizosphere). Furthermore, plant roots are able to release pH relevant molecules (e.g. organic acids), in order to enhance for example the nutrient supply. Both processes strongly affect the biochemistry and microbial network of wetland soils, which in turn is relevant for the production of greenhouse gases like methane (CH_4) and dinitrousoxide (N_2O). These relationships were studied with the three wetland plant species, *Juncus effusus* L., *J. inflexus* L. and *J. articulatus* L., that differ anatomically in the culm internal air spaces.

For analyzing the rhizospheric oxygen and pH dynamics in soils mediated by plant roots, a novel optical method for non-invasive, quantitative imaging of spatial and temporal oxygen and pH changes was developed. This method provides the opportunity for recording long-term dynamics of the micro-pattern of oxygen and pH in the root–soil interface without disturbance of the biological and physico-chemical conditions. In this comparative study the selected species rooted in permanently flooded rhizotrones, which were designed for free-choice root in-growth experiments in differentially manipulated soil compartments. Each compartment was equipped with a raster access port, able to accept up to 1156 microsuction capillaries. This construction provides multilayered (sterile) sampling of soil solution across and along growing roots. The effect of roots on the amount and distribution of organic acids in reductive soils of different pH (pH 3.9 - pH 5.9) was

investigated by use of capillary electrophoresis. For evaluating the response of the above-ground culms to soil flooding, the species specific culm CO_2 and H_2O gas exchange and culm internal oxygen concentration dynamics were measured with conventional gas exchange and O_2 measuring devices in field experiments. The interspecific competition in relation to soil moisture was quantified in standard soil moisture gradient experiments.

The non-invasive optical measurements showed pronounced diurnal variations of oxygen concentration and pH along the roots, particularly along the elongation zone. Long-term records over more than eight weeks revealed considerable spatial and temporal patterns of oxygen (over a range of almost 200 μmol O_2 l^{-1}) and pH dynamics (± 1.4 pH units) in the rhizosphere. A strong effect of oxidative acidification due to oxygen release by the plant roots was clearly visible for *J. effusus*, whereas the roots of *J. articulatus* alkalinized the rhizosphere. In contrast, the roots of *J. inflexus* showed no effects on rhizospheric pH.

Four different organic acids were detectable in all soil solutions (oxalate, acetate, formate and lactate). Maximal concentration of all organic acids occurred at pH 3.9 (acetate: 69.9 μM; lactate: 116.5 μM; formate: 45.2 μM; oxalate: 36.9 μM). The lowest concentration of each organic acid was found at pH 5.9. Hence, the more acid soil provided increased reductive conditions leading to slower anaerobic degradation of organic acids. This indicates unavailability of exogenous electron acceptors (e.g. ferric iron). Concentration of organic acids decreased by up to 98% within 4 mm distance from the proximate bulk soil to the root surface.

Investigation of the CO_2, O_2 and H_2O dynamics of the selected species highlighted that all three species were well adapted to moderate environmental conditions. Transpiration of all three investigated plant species is mainly driven by leaf-to-air vapor pressure deficit, whereas photosynthesis is rather depending on light and temperature conditions.

Soil moisture gradient experiments revealed that the competition pressure between the species is strongly influenced by soil moisture. Plant interactions shift from

strong competition at dry conditions towards a collective facilitation for all three species at high soil moisture levels. Besides the quasi unlimited water supply, additive effects due to collective aeration of the inundated soil and by this synergetic exploitation of nutrients are factors that enhance the facilitation. Thus, under waterlogged soil conditions rush communities of heterogeneous composition can be more productive, compared to monoculture stands.

6. Zusammenfassung

Es ist bekannt, dass die Bildung von spross- und wurzelinternen Aerenchymen essentiell für das pflanzliche Wachstum in Feuchtgebieten ist. Diese pflanzeninternen Hohlraumsysteme gewährleisten eine kontinuierliche Sauerstoffversorgung der im sauerstoffarmen und reduzierenden Boden wachsenden Wurzeln, die diesen zugeführten Sauerstoff in das umliegende perirhizale Milieu (Rhizosphäre) abgeben können. Desweiteren können Pflanzenwurzeln pH relevante Verbindungen und Moleküle (z.B. organische Säuren) zur Optimierung der Nährstoffversorgung ausscheiden. Beide Prozesse beeinflussen entscheidend die Biogeochemie und das mikrobielle Netzwerk der Böden in Feuchtgebieten, welche wiederum relevant für die Produktion von Treibhausgasen, z.B. Methan (CH_4) und Lachgas (N_2O), sind. Diese Beziehungen wurden anhand von drei Sippen, welche anatomische Differenzierungen in den sprossinternen Aerenchymen aufweisen untersucht: *Juncus effusus* L., *J. inflexus* L. und *J. articulatus* L.

Hierzu wurde eine neue optische Methode zur nicht-invasiven, quantitativen Visualisierung von räumlichen und zeitlichen Sauerstoff- und pH-veränderungen entwickelt. Dieses Verfahren ermöglichte die Messung von Langzeitprozessen der mosaikartigen Sauerstoff- und pH-dynamik in der Schnittstelle zwischen Wurzel und Boden, ohne die biologischen und physiko-chemischen Bedingungen zu beeinflussen. Dazu wurden die ausgewählten Arten in dauerhaft gefluteten Rhizotronen kultiviert und analysiert. Die neuartig konzipierten Rhizotrone erlaubten ein freies Wurzelwachstum in unterschiedlich manipulierte

Bodenkompartimente. Jedes Kompartiment war mit einem Rasteranschluss ausgestattet, der mit bis zu 1156 Mikrosaugkapillaren bestückt werden konnte. Diese Konstruktion ermöglichte ein steriles Absaugen der Bodenlösung entlang und quer zu den wachsenden Wurzeln. Der Einfluss der Wurzeln auf den Gehalt und die Verteilung von organischen Säuren in diesen reduktiven Böden unterschiedlichen pH-Wertes (pH 3,9 – pH 5,9) wurde kapillarelektrophoretisch bestimmt. Zur Erfassung der Reaktion der oberirdischen Sprosse auf die Bodenüberflutung wurden die Arten mit speziellen Spross CO_2 und H_2O Gaswechsel- und O_2 Messgeräten in Feldversuchen untersucht. Die interspezifische Konkurrenz in Abhängigkeit der Bodenfeuchte wurde mittels eines Bodenfeuchtegradientenexperiments quantifiziert.

Die nicht-invasiven optischen Messungen zeigten deutliche diurnale Veränderungen der Sauerstoffkonzentration und des pH-Wertes entlang der untersuchten Wurzeln, insbesondere im Bereich der Streckungszone. Langzeituntersuchungen über mehr als acht Wochen zeigten erhebliche räumliche und zeitliche Variationen der Sauerstoffverteilung (über einen Bereich von nahezu 200 μmol l^{-1}) und der pH-Verteilung (± 1,4 pH-Einheiten) in der Rhizosphäre. Die Sauerstoffausscheidung durch die Wurzeln von *J. effusus* bewirkten den Effekt einer oxidativen Ansäuerung, während hingegen die Wurzeln von *J. articulatus* die Rhizosphäre basifizierten. Im Gegensatz dazu zeigten die Wurzeln von *J. inflexus* keinerlei Einfluss auf den Rhizosphären pH.

Vier unterschiedliche organische Säuren konnten in den Bodenlösungen detektiert werden: Oxalat, Acetat, Formiat, Laktat. Die höchste Konzentration aller organischer Säuren war bei pH 3,9 messbar (Acetat: 69,9 μM; Laktat: 116,5 μM; Formiat: 45,2; Oxalat: 36,9), während die niedrigste Konzentration bei pH 5,9 gemessen wurde. Folglich bewirken die stärker reduktiven Bedingungen im saureren Milieu einen verminderten Abbau der organischen Säuren. Dies deutet auf ein Fehlen exogener Elektronenakzeptoren hin (z.B.: Eisen(III)). Desweiteren fiel innerhalb von 4mm zur Wurzeloberfläche hin die Konzentration der organischen Säuren um bis zu 98% ab.

Die Untersuchungen der CO_2, O_2 und H_2O Umsätze der ausgewählten Arten zeigten, dass alle drei Arten an moderate Umweltbedingungen angepasst sind. Die Transpiration aller drei Arten ist primär durch das Blatt-zu-Luft Wasserdampfsättigungsdefizit geprägt, während die Photosyntheseleistung licht- und temperaturabhängig ist. Die Bodenfeuchtegradientenexperimente zeigten, dass der Konkurrenzdruck zwischen den Arten stark von der Bodenfeuchte abhängig ist. Die Interaktionen zwischen den Arten wechseln von starker Konkurrenz unter Trockenstress zu gegenseitiger Wachstumsförderung unter staunassen Bodenbedingungen. Neben der quasi unbegrenzten Wasserversorgung bewirken additive Effekte durch die gemeinsame Belüftung des staunassen Bodens eine synergetische Ausnutzung der Nährstoffe und sind daher Ursachen für die gegenseitige Wachstumsförderung. Es konnte daher nachgewiesen werden, dass heterogene Binsengesellschaften produktiver als Monokulturen sind.

7. Acknowledgements

This PhD thesis could have never been done without the help and support from quite a number of people and companies. They inspired me, pushed me further, technically and financially supported me and finally, they never lost faith in me and my work.

It was my PhD supervisor Professor Dr. Rainer Lösch, who had the foresight that the new techniques, developed and applied during this PhD thesis, will have the potential to open the door for new insights into the complex matter of plant soil interactions, leading to already two exciting projects and cooperation. It was not only his financial support throughout the last years that makes me deeply thankful, but moreover he shared with me his excellent experience and broad knowledge that helped me to learn continuously and to solve uncountable problems. He was always a reliable proof reader of my publications, posters, etc. and a perfect “Advocatus Diaboli” during the steps of technical development.

I am also deeply indebted to PD Dr. Dirk Gansert, who also guided me as a mentor through my thesis. He introduced me into the HYPOP research cooperation, which was one of the technical prerequisites for launching my PhD thesis. He was an absolute indispensible support during the entire time of my PhD thesis and I already miss our daily discussions.

The PreSens GmbH was my key industrial partner throughout the years of my work. With the support and the help from Dr. Christian Krause and his team I developed the 2D imaging system. Their sensors allowed me to gather these fantastic new insights into the rhizosphere of plants.

But having a sensor does not make a method and thus I was reliant on the help of the highly professional experts from our precision mechanic and electronics engineers of the Heinrich-Heine-University, namely Waldemar Seidel, Werner Müller, Michael Laug and Alexander Lanzinger. They always found a perfect solution for every "tiny" technical problem.

Many thanks also to the Phytosphere institute (ICG-3) of the research center Jülich. Professor Dr. Ulrich Schurr and his team, especially Dr. Arnd Kuhn and Dr. Björn Thiele, allowed me to adapt and modify parts of their microsuction technique, so that I was able to develop the new raster access port technology. They also allowed me to use the CE device of their institute.

Working on this thesis would not have made so much fun without the great team of the department of Geobotany. Especially the unshakeable sunny mood of Dr. Guido Dericks lightened every single day. He also ensured that my internal caffeine and nutrient level was kept constant throughout the years.

I would also like to thank the Stender AG, which kindly supported my work by supplying me with the standardized soils used during the experiments.

Finally, I would like to thank my family and friends, for being there all the time!

8. Cited literature

AFREEN, F. ZOBAYED, S. M. A., ARMSTRONG, J. & ARMSTRONG, W. (2007): Pressure gradients along whole culms and leaf sheaths, and other aspects of humidity-induced gas transport in Phragmites australis. Journal of Experimental Botany 58, 1651-1662.

ARMSTRONG, W. (1979): Aeration in higher plants. *Advances in Botanical Research* 7, 223-332.

ARMSTRONG, J. & ARMSTRONG, W. (1991): A convective through-flow of gases in Phragmites australis (Cav.) Trin. ex Steud. *Aquatic Botany* 39, 75-88.

ARMSTRONG, W., COUSINS, D., ARMSTRONG, J., TURNER, D. W. & BECKETT, P. M. (2000): Oxygen distribution in wetland plant roots and permeability barriers to gas-exchange with the rhizosphere: a microelectrode and modeling study with *Phragmites australis*. *Annals of Botany* 86, 687-703.

BAZZANELLA, A., LOCHMANN, H., MAINKA, A. & BÄCHMANN, K. (1997): Determination of inorganic anions, carboxylic acids and amino acids in plant matrices by capillary zone electrophoresis. *Chromatographia* 45, 59-62.

BEGG, C.B.M., KIRK, G.J.D., MACKENZIE, A.F. & NEUE, H.-U. (1994): Root-induced iron oxidation and pH changes in the lowland rice rhizosphere. *New Phytologist* 128, 469-477.

BEZBARUAH, A.N. & ZHANG, T.C. (2004): pH, redox, and oxygen microprofiles in rhizosphere of bulrush (*Scirpus validus*) in a constructed wetland treating municipal wastewater. *Biotechnology and Bioengineering* 88, 60-70.

BLOSSFELD, S. (2005): Interne Sauerstoffversorgung in *Juncus effusus* L. *Geobotanische Kolloquien Frankfurt* 19, 69-76.

BLOSSFELD, S. & GANSERT, D. (2007): A novel non-invasive optical method for quantitative visualization of pH dynamics in the rhizosphere of plants. *Plant, Cell and Environment* 30, 176-186.

BLOOM, A.J., MEYERHOFF, P.A., TAYLOR, A.R. & ROST, T.L. (2003): Root development and absorption of ammonium and nitrate from the rhizosphere. *Journal of Plant Growth Regulation* 21, 416-431.

BONIN, P. (1996): Anaerobic nitrate reduction to ammonium in two strains isolated from coastal marine sediment: A dissimilatory pathway. *FEMS Microbiology Ecology* 19, 27-38.

BORISOV, S. M., NEURAUTER, G., SCHROEDER, C., KLIMANT, I., WOLFBEIS, O.S. (2006): A modified dual lifetime referencing method for simultaneous optical determination and sensing of two analytes. Applied Spectroscopy 60, 1167–1173

BOWLER, J. M. & PRESS, M. C. (1996): Effects of elevated CO_2, nitrogen form and concentration on growth and photosynthesis of a fast- and slow-growing grass. *New Phytologist* 132, 391-401.

BRIX, H. (1990): Uptake and photosynthetic utilization of sediment-derived carbon by *Phragmites australis* (Cav.) Trin. ex Steudel. *Aquatic Botany* 38, 377-389.

BRIX, H., SORRELL, B. K., ORR, P. T. (1992): Internal pressurization and convective gas flow in some emergent freshwater macrophytes. *Limnology and Oceanography* 37, 1420 – 1433.

BRIX, H., SORRELL, B. K., SCHIERUP, H.-H. (1996): Gas fluxes achieved by in situ convective flow in *Phragmites australis*. *Aquatic botany* 54, 151 – 163.

BRUNE, A., FRENZEL, P. & CYPIONKA H. (2000): Life at the oxic-anoxic interface: microbial activities and adaptions. *FEMS Microbiology Reviews* 24, 691-710.

BURESH, R. J. & PATRICK, W. H. JR. (1978): Nitrate reduction to ammonium in anaerobic soil. *Soil Science Society of America Journal* 42, 913 - 918.

CALLAWAY, R. M. & KING, L. (1996): Temperature-driven variation in substrate oxygenation and the balance of competition and facilitation. *Ecology* 77, 1189 - 1195.

CALLAWAY, R. M. & PENNINGS S. C. (2000): Facilitation may buffer competitive effects: indirect and diffuse interactions among salt marsh plants. *American Naturalist* 156, 416 - 424.

CALLAWAY, R. M. & WALKER, L. R. (1997): Competition and facilitation: A synthetic approach to interactions in plant communities. *Ecology* 78, 1958 - 1965.

CASARIN, V., PLASSARD, C., SOUCHE, G. & ARVIEU, J-C (2003): Quantification of oxalate ions and protons released by ectomycorrhizal fungi in rhizosphere soil. *Agronomie* 23, 461-469.

CHABBI, A., MCKEE, K.L. & MENDELSSOHN, I.A. (2000): Fate of oxygen losses from *Typha domingensis* (Typhaceae) and *Cladium jamaicense* (Cyperaceae) and consequences for root metabolism. *American Journal of Botany* 87, 1081-1090.

CHABBI, A., HINES, M.E. & RUMPEL, C. (2001): The role of organic carbon excretion by bulbous rush roots and its turnover and utilization by bacteria under iron plaques in extremely acid sediments. *Environmental and Experimental Botany* 87, 237-246.

CHANTON, J. P., ARKEBAUER, T. J., HARDEN, H. S. & VERMA, S. B. (2002): Diel variation in lacunal CH_4 and CO_2 concentration and $\delta^{13}C$ in *Phragmites australis*. *Biogeochemistry* 59, 287 – 301.

CHENG, X., PENG, R., CHEN, J., LUO, Y., ZHANG, Q., AN, S., CHEN, J. & LI, B. (2007): CH_4 and N_2O emissions from *Spartina alterniflora* and *Phragmites australis* in experimental mesocosms. *Chemosphere* 68, 420 - 427.

CHRISTEN, H.R. (1988): *Grundlagen der allgemeinen und anorganischen Chemie*. 9th edition, Salle, Frankfurt.

COLMER, T.D. (2003a): Aerenchyma and an inducible barrier to radial oxygen loss facilitate root aeration in upland, paddy and deep-water rice (*Oryza sativa* L.). *Annals of Botany* 91, 301-309.

COLMER, T.D. (2003b): Long-distance transport of gases in plants: a perspective on internal aeration and radial oxygen loss from roots. *Plant, Cell and Environment* 26, 17-36.

CONSTABLE, J. V. H., GRACE, J. B. & LONGSTRETH, D. J. (1992): High carbon dioxide concentrations in aerenchyma of *Typha latifolia*. *American Journal of Botany* 79, 415 - 418.

DAMGAARD, L.R., REVSBECH, N.P. & REICHARDT, W. (1998): Use of an oxygen-insensitive microscale biosensor for methane to measure methane concentration profiles in a rice paddy. *Applied Environmental Microbiology* 64, 864-870.

DANNENBERG, S. & CONRAD, R. (1999): Effect of rice plants on methane production and rhizospheric metabolism in paddy soil. *Biogeochemistry* 45, 53-71.

DASSONVILLE, F. & RENAULT, P. (2002): Interactions between microbial processes and geochemical transformations under anaerobic conditions: a review. *Agronomie* 22, 51-68.

DESSUREAULT-ROMPRÉ, J., NOWACK, B., SCHULIN, R. & LUSTER, J. (2006): Modified micro suction cup/rhizobox approach for the in-situ detection of organic acids in rhizosphere soil solution. *Plant and Soil* 286, 99-107.

ELLENBERG, H. (1953): Physiologisches und ökologisches Verhalten derselben Pflanzenarten. *Mitteilungen der deutschen botanischen Gesellschaft* 65, 350 - 361.

ERVIN, G. N. (2005): Spatio-temporally variable effects of a dominant macrophyte on vascular plant neighbors. *Wetlands* 25, 317 - 325.

ERVIN, G. N. (2007): An experimental study on the facilitative effects of tussock structure among wetland plants. *Wetlands* 27, 620 – 630.

FAN, L. & NEUMANN, P.M. (2004): The spatially variable inhibition by water deficit of maize root growth correlates with altered profiles of proton flux and cell wall pH. *Plant Physiology* 135, 2291-2300.

FISCHER, W.R., FLESSA, H. & SCHALLER, G. (1989): pH values and redox potentials in microsites of the rhizosphere. *Journal of Plant Nutrition and Soil Science* 152, 191-195.

FRENZEL, P. & KAROFELD, E. (2000): CH_4 emission from a hollow-ridge complex in a raised bog: The role of CH_4 production and oxidation. *Biogeochemistry* 51, 91-112.

FREY, W. & LÖSCH, R. (2004): *Lehrbuch der Geobotanik*. Second edition, Spektrum Akademischer Verlag, Heidelberg.

FOYER, C.H. & NOCTOR, G. (2002): Photosynthetic nitrogen assimilation: inter-pathway control and signalling. In *Photosynthetic nitrogen assimilation and associated carbon and respiratory metabolism* (eds. C.H. Foyer & G. Noctor), pp. 1-22. Kluwer Academic Publishers, Dordrecht.

GAMBRELL, R.P. & PATRICK, W.H. JR. (1978): Chemical and microbiological properties of anaerobic soils and sediments. In *Plant life in anaerobic environments* (eds. D.D. Hook & R.M.M. Crawford), pp. 375-425. Ann Arbor Science, Ann Arbor.

GANSERT, D. & BLOSSFELD, S. (2008): *The application of novel optical sensors (optodes) in experimental plant ecology*. In: Lüttge, U., Beyschlag, W., Murata, J. (eds) Progress in Botany Vol. 69, part 4. pp. 333-358. Springer, Berlin.

GANSERT, D. & BURGDORF, M. (2005): Effects of xylem sap flow on carbon dioxide efflux from stems of birch (*Betula pendula* Roth) *Flora* 200, 444 – 455.

GANSERT, D., STANGELMAYER, A., KRAUSE,C., BORISOV, S., WOLFBEIS, O., ARNOLD, M. & MÜLLER, A. (2006): Hybrid optodes (HYBOP) In: *Biophotonics: Visions for a better health care* (eds. J. Popp & M. Strehle), pp. 477-518. Wiley VCH, Weinheim.

GARNIER, E., CORDONNIER, P., GUILLERM, J.-L. & SONIÉ, L. (1997): Specific leaf area and leaf nitrogen concentration in annual and perennial grass species growing in Mediterranean old-fields. Oecologia 111, 490 – 498.

GOODWIN, S. & ZEIKUS, J.G. (1987): Ecophysiological adaptations of anaerobic bacteria to low pH: analysis of anaerobic digestion in acidic bog sediments. *Applied and Environmental Microbiology* 53, 57-64.

GÖTTLEIN, A., HELL, U. & BLASEK, R. (1996): A system for microscale tensiometry and lysimetry. *Geoderma* 69, 147-156.

GÖTTLEIN, A., HEIM, A., KUHN, A.J. & SCHRÖDER, W.H. (2005): In-situ application of stable isotope tracers in the rhizosphere of an oak seedling. *European Journal of Forest Research* 124, 83-86.

GREENWAY, H., ARMSTRONG, W. & COLMER, T. D. (2006): Conditions leading to high CO_2 (>5 kPa) in waterlogged-flooded soils and possible effects on root growth and metabolism. *Annals of Botany* 98, 9 - 32.

GREGORY, P.J. & HINSINGER, P. (1999): New approaches to studying chemical and physical changes in the rhizosphere: an overview. *Plant and Soil* 211, 1-9.

HIGUCHI, T., YODA, K. & TENSHO, K. (1984): Further evidence for gaseous CO_2 transport in relation to root uptake of CO_2 in rice plant. *Soil Science and Plant Nutrition* 30, 125 – 136.

HINSINGER, P., PLASSARD, C., TANG, C. & JAILLARD, B. (2003): Origins of root-mediated pH changes in the rhizosphere and their responses to environmental constraints: A review. *Plant and Soil* 248, 43-59.

HINSINGER, P., GOBRAN, G.R., GREGORY, P.J. & WENZEL, W.W. (2005): Rhizosphere geometry and heterogeneity arising from root-mediated physical and chemical processes. *New Phytologist* 168, 293-303.

HORI, T., NOLL, M., IGARASHI, Y., FRIEDRICH, M.W. & CONRAD, R. (2007): Identification of acetate-assimilating microorganisms under methanogenic conditions in anoxic rice field soil by comparative stable isotope probing of RNA. *Applied and Environmental Microbiology* 73, 101-109.

HOU, A.X., CHEN, G.X., WANG, Z.P., VAN CLEEMPUT, O. & PATRICK, W.H. JR. (2000): Methane and nitrous oxide emissions from a rice field in relation to soil redox and microbial progresses. *Soil Science Society of America Journal* 64, 2180-2186.

HOWELER, R. H. & BOULDIN, D. R. (1971): The diffusion and consumption of oxygen in submerged soils. Soil Science Society of America Journal 35, 202 – 208.

HUBER, C., KLIMANT, I., KRAUSE, C. & WOLFBEIS, O.S. (2001): Dual lifetime referencing as applied to a chloride optical sensor. *Analytical Chemistry* 73, 2097-2103.

JAILLARD, B., RUIZ, L. & ARVIEU, J.C. (1996): pH mapping in transparent gel using color indicator videodensitometry. *Plant and Soil* 183, 1-11.

JAILLARD, B., PLASSARD, C. & HINSINGER, P. (2003): Measurements of H^+ fluxes and concentrations in the rhizosphere. In: *Handbook of soil acidity* (ed. Z. Rengel), pp. 231-266. M. Dekker, New York.

JARVIS, S.C. & HATCH, D.J. (1985): Rates of hydrogen ion efflux by nodulated legumes grown in flowing solution culture with continuous pH monitoring and adjustment. *Annals of Botany* 55, 41-51.

JENSEN, S. I., KÜHL, M., GLUD, R. N., JØRGENSEN, L. B. & PRIEMÉ, A. (2005): Oxic microzones and radial oxygen loss from roots of *Zostera marina*. *Marine Ecology Progress Series* 293, 49 – 58.

JOABSON, A. & CHRISTENSEN, T., R. (2001): Methane emissions from wetlands and their relationship with vascular plants: an Arctic example. *Global Change Biology* 7, 919 – 932.

JONES, D.L. (1998): Organic acids in the rhizosphere – a critical review. *Plant and Soil* 205, 25-44.

JONES, D.L., DENNIS, P.G., OWEN, A.G. & VAN HEES, P.A.W. (2003): Organic acids behavior in soils – misconceptions and knowledge gaps. *Plant and Soil* 248, 31-41.

KEDDY, P., FRASER, L. H. & WISHEU I. C. (1998): A comparative approach to examine competitive response of 48 wetland plant species. *Journal of Vegetation Science* 9, 777 – 786.

KIM, T.K., SILK, W.K. & CHEER, A.Y (1999): A mathematical model for pH patterns in the rhizospheres of growth zones. *Plant, Cell and Environment* 22, 1527-1538.

KIRK, G.J.D. (2004): *The biogeochemistry of submerged soils*. John Wiley & Sons, Chichester.

KIRK, G.J.D. & BAJITA, J. B. (1995): Root-induced iron oxidation, pH changes and zinc solubilization in the rhizosphere of lowland rice. *New Phytologist* 131, 129 - 137.

KIRK, G.J.D. & KRONZUCKER, H.J. (2005): The potential for nitrification and nitrate uptake in the rhizosphere of wetland plants: A modelling study. *Annals of Botany* 96, 639–646.

KIRK, G.J.D. & SOLIVAS, J. L. (1994): Coupled diffusion and oxidation of ferrous iron in soils. III: Further development of the model and experimental testing. *European journal of soil science* 45, 369 – 378.

KLIMANT, I., MEYER, V. & KÜHL, M. (1995): Fiber-optic oxygen microsensors, a new tool in aquatic biology. *Limnology and Oceanography* 40, 1159 – 1165.

KLIMANT, I., HUBER, C., LIEBSCH, G., NEURAUTER, G., STANGELMAYER, A. & WOLFBEIS, O.S. (2001): Dual lifetime referencing (DLR) – a new scheme for converting fluorescence intensity into a frequency-domain or time-domain information. In: *New trends in fluorescence spectroscopy: application to chemical and life sciences* (eds. B. Valeur & J.C. Brochon), pp. 257-275. Springer, Berlin.

KOPITTKE, P.M. & MENZIES, N.W. (2004): Effect of Mn deficiency and legume inoculation on rhizosphere pH in highly alkaline soils. *Plant and Soil* 262, 13-21.

KÜSEL, K., CHABBI, A. & TRINKWALTER, T. (2003): Microbial processes associated with roots of bulbous rush coated with iron plaques. *Microbial Ecology* 46, 302-311.

LAVOREL, S. & GARNIER, E. (2002): Predicting changes in community composition and ecosystem functioning from plant traits: revisiting the Holy Grail. *Functional Ecology* 16, 545 - 556.

LE MER, J. & ROGER, P. (2001): Production, oxidation, emission and consumption of methane by soils: a review. *European Journal of Soil Biology* 37, 25-50.

LI, Y., JOHNSON, D. A., SU, Y., CUI, J. & ZHANG, T. (2005): Specific leaf area and leaf dry matter content of plants growing in sand dunes. *Botanical Bulletin of Academia Sinica* 46, 127-134.

LÖSCH, R. (2002): Wasserhaushalt der Pflanzen. Second edition, Quelle & Meyer, Wiebelsheim.

LU, Y., ABRAHAM, W.-R. & CONRAD, R. (2007): Spatial variation of active microbiota in the rice rhizosphere revealed by *in situ* stable isotope probing of phospholipid fatty acids. *Environmental Microbiology* 9, 474-481.

LU, Y., ROSENCRANTZ, D., LIESACK, W. & CONRAD, R. (2006): Structure and activity of bacterial community inhabiting rice roots and the rhizosphere. *Environmental Microbiology* 8, 1351-1360.

LUEDERS, T. & FRIEDRICH, M. (2000): Archaeal population dynamics during sequential reduction processes in rice field soil. *Applied and Environmental Microbiology* 66, 2732 – 2742.

MADIGAN, M.T. & MARTINKO, J.M. (2006): *Brock Biology of Microorganisms*. 11th Edition, Pearson Prentice Hall, Upper Saddle River, NJ, pp. 1088.

MAINIERO, R. & KAZDA, M. (2005): Effects of *Carex rostrata* on soil oxygen in relation to soil moisture. *Plant and Soil* 270, 311 - 320.

MANN, C. J. & WETZEL, R. G. (1999): Photosynthesis and stomatal conductance of *Juncus effusus* in a temperate wetland ecosystem. - *Aquatic Botany* 63, 127-144

MARSCHNER, H. (1995): *Mineral nutrition of higher plants*. Second Edition, Academic Press, London.

MARSCHNER, H. & RÖMHELD, V. (1983): *In vivo* measurement of root-induced pH changes at the soil-root interface: Effect of plant species and nitrogen source. *Zeitschrift für Pflanzenphysiologie* 111, 241-251.

MARSCHNER, H., HÄUSSLING, M. & GEORGE, E. (1991): Ammonium and nitrate uptake rates and rhizosphere pH in non-mycorrhizal roots of Norway spruce [*Picea abies* (L.) Karst.]. *Trees* 5, 14 – 21.

MISHRA, S., RATH, A.K., ADHYA, T.K. & RAO, V.R. (1997): Effects of continuous and alternate water regimes on methane efflux from rice under greenhouse conditions. *Biology and Fertility of Soils* 24, 399-405.

NAVAS, M.-L. & MOREAU-RICHARD, J. (2005): Can traits predict the competitive response of herbaceous Mediterranean species? *Acta Oecologica* 27, 107 – 114.

NYE, P.H. (1981): Changes of pH across the rhizosphere induced by roots. *Plant and Soil* 61, 7-26.

PEINE, A., TRITSCHLER, A., KÜSEL, K. & PFEIFFER, S. (2000): Electron flow in an iron-rich acidic sediment - evidence for an acidity driven iron cycle. *Limnology and Oceanography* 45, 1077-1087.

PELDSZUS, S. (2007): Organic acids. In: Nollet, L. (Ed.), *Handbook of Water Analysis.* CRC Press, Boca Raton, pp. 393 – 408.

PETERS, W.S. (2004): Growth rate gradients and extracellular pH in roots: how to control an explosion. *New Phytologist* 162, 571-574.

PETRIE, L., NORTH, N.N., DOLLHOPF, S.L., BALKWILL, D.L. & KOSTKA, J.E. (2003): Enumeration and characterization of iron(III)-reducing microbial communities from acidic subsurface sediments contaminated with uranium(VI). *Applied and Environmental Microbiology* 69, 7467-7479.

PEZESHKI, S. R. (2001): Wetland plant responses to soil flooding. *Environmental and Experimental Botany* 46, 299 – 312.

PIJNENBORG, J.W.M., LIE, T.A. & ZEHNDER, A.J.B. (1990): Simplified measurement of soil pH using an agar-contact technique. *Plant and Soil* 126, 155-160.

PORRA, R. J. (2002): The chequered history of the development and use of simultaneous equations for the accurate determination of chlorophylls a and b. *Photosynthesis Research* 73, 149 – 156.

PORTER, H. & DE JONG, R. (1999): A comparison of specific leaf area, chemical composition and leaf construction costs of field plants from 15 habitats differing in productivity. *New Phytologist* 143, 163 - 176.

RAGHOEBARSING, A. A., SMOLDERS A. J. P., SCHMID, M. C., RIJPSTRA, W. I. C., WOLTERS-ARTS, M., DERKSEN, ,J., JETTEN, M. S. M., SCHOUTEN, S., SINNINGHE DAMSTE, J. S., LAMERS, L. P. M., ROELOFS, J. G. M., OP DEN CAMP, H. J. M. & STROUS, M. (2005): Methanotrophic symbionts provide carbon for photosynthesis in peat bogs. *Nature* 436, 1153 – 1156.

RAO, T.R., YANO, K., IIJIMA, M., YAMAUCHI, A. & TATSUMI, J. (2002): Regulation of rhizosphere acidification by photosynthetic activity in cowpea (Vigna unguiculata L. Walp.) seedlings. *Annals of Botany* 89, 213-220.

REVSBECH, N.P., PEDERSEN, O., REICHARDT, W. & BRIONES, A. (1999): Microsensor analysis of oxygen and pH in the rice rhizosphere under field and laboratory conditions. *Biology and Fertility of Soils* 29, 379-385.

RODEN, E.E. & WETZEL, R.G. (1996): Organic carbon oxidation and suppression of methane production by microbial Fe(III) oxide reduction in vegetated and unvegetated freshwater wetland sediments. *Limnology and Oceanography* 41, 1733 – 1748.

ROTHFUSS, F. & CONRAD, R. (1993): Vertical profiles of CH_4 concentrations, dissolved substrates and processes involved in CH_4 production in a flooded Italian rice field. *Biogeochemistry* 18, 137-152.

SCHEFFER, F. & SCHACHTSCHABEL, P. (2002): *Lehrbuch der Bodenkunde*. 15th edition, Spektrum, Heidelberg.

SCHNEIDER, H.A.W. & BOGORAD, L. (1978): Light-induced, dark-reversible absorbance changes in roots, other organs, and cell-free preperations. *Plant Physiology* 62, 577-581.

SCHOPFER, P. & BRENNICKE, A. (2006): *Pflanzenphysiologie*. 6th edition, Elsevier, München.

SEMENOV, A.M., VAN BRUGGEN, A.H.C. & ZELENEV, V.V. (1999): Moving waves of bacterial populations and total organic carbon along roots of wheat. *Microbial Ecology* 37, 116-128.

SORRELL, B.K. (1999): Effect of external oxygen demand on radial oxygen loss by *Juncus* roots in titanium citrate solutions. *Plant, Cell and Environment* 22, 1587-1593.

SORRELL, B. K. & DROMGOOLE, F. I. (1986): Errors in measurements of aquatic macrophyte gas exchange due to oxygen storage in internal airspaces. *Aquatic Botany* 24, 103 – 114.

SORRELL, B. K. & TANNER, C. C. (2000): Convective gas flow and internal aeration in *Eleocharis sphacelata* in relation to water depth. *The Journal of Ecology* 88, 778 - 789.

SOUKUP, A., ARMSTRONG, W., SCHREIBER, L., FRANKE, R. & VOTRUBOVÁ, O. (2007): Apoplastic barriers to radial oxygen loss and solute penetration: a chemical and functional comparison of the exodermis of two wetland species, *Phragmites australis* and *Glyceria maxima*. *New Phytologist* 173, 264 – 278.

STERN, O. & VOLMER, M. (1919): Über die Abklingzeit der Fluoreszenz. *Physikalische Zeitschrift* 20, 183 – 188.

TAYLOR, A.R. & BLOOM, A.J. (1998): Ammonium, nitrate, and proton fluxes along the maize root. *Plant, Cell and Environment* 21, 1255-1263.

THIELE, B., WESSEL-BOTHE, S., MEIJBOOM, F., KLAUTH, P., LINDENMAIR, J., RIST, R., SCHOELGENS, E. & KUHN, A.J. (2005): Determination of organic acids in soil solution with high spatial-temporal resolution using the rhizotrone methodology. In: Li, J., (Ed.), *Plant nutrition for food security, human health and environmental protection*. Tsinghua Univ. Pr., Peking, pp. 454-455.

VALENTINE, D.L. (2002): Biogeochemistry and microbial ecology of methane oxidation in anoxic environments: a review. *Antonie van Leeuwenhoek* 81, 271-282.

VISSER, E.J.W., COLMER, T.D., BLOM, C.W.P.M. & VOESENEK, L.A.C.J. (2000): Changes in growth, porosity, and radial oxygen loss from adventitious roots of selected mono- and dicotyledonous wetland species with contrasting types of aerenchyma. *Plant, Cell and Environment* 23, 1237-1245.

VAN DER WELLE, M. E. W., NIGGERBRUGGE, K., LAMERS, L. P. M. & ROELOFS, J. G. M. (2007): Differential responses of the freshwater wetland species *Juncus effusus* L. and *Caltha palustris* L. to iron supply in sulfidic environments. *Environmental Pollution* 147, 222 – 230.

WAGNER, A. (1991): *Ökophysiologische Untersuchungen zur Stickstoffernährung dikotyler Arten mit unterschiedlichen Reaktions- und Stickstoffzahlen.* Göttinger Dissertationen, Hartung-Gorre, Konstanz.

WALTER, A., SILK, W.K. & SCHURR, U. (2000): Effect of soil pH on growth and cation deposition in the root tip of *Zea mays* L. *Journal of Plant Growth Regulation* 19, 65-76.

WANG, Z.Y.J., KELLY, M. & KOVAR, J.L. (2004): In Situ Dynamics of Phosphorus in the Rhizosphere Solution of Five Species. *Journal of Environmental Quality* 33, 1387–1392.

WASSMANN, R. & AULAKH, M.S. (2000): The role of rice plants in regulating mechanisms of methane missions. *Biology and Fertility of Soils* 31, 20-29.

WEISENSEEL, M.H., DORN, A. & JAFFE, L.F. (1979): Natural H^+ currents traverse growing roots and root hairs of barley (*Hordeum vulgare* L.). *Plant Physiology* 64, 512-518.

WEISS, J.V., EMERSON, D., BACKER, S.M. & MEGONIGAL, J.P. (2003): Enumeration of Fe(II)-oxidizing and Fe(III)-reducing bacteria in the root zone of wetland plants: Implications for a rhizospheric iron cycle. *Biogeochemistry* 64, 77-96.

WIEßNER, A., KAPPELMEYER, U., KUSHK, P. & KÄSTNER, M. (2005): Influence of the redox condition dynamics on the removal efficiency of laboratory-scale constructed wetland. *Water Research* 39, 248-256.

WILSON, S. D. & KEDDY, P. A. (1986): Species competitive ability and position along a natural stress/disturbance gradient. *Ecology* 67, 1236 – 1242.

WILSON, P. J., THOMPSON, K. & HODGSON, J. G. (1999): Specific leaf area and leaf dry matter content as alternative predictors of plant strategies. *New Phytologist* 143, 155 – 162.

WITHINGTON, J.M., ELKIN, A.D., BULAI, B., OLESINSKI, J., TRACY, K.N., BOUMA, T.J., OLEKSYN, J., ANDERSON, L.J., MODRZYNSKI, J., REICH, P.B. & EISSENSTAT, D.M. (2003): The impact of material used for minirhizotron tubes for root research. *New Phytologist* 160, 533-544.

YAO, H., CONRAD, R., WASSMANN, R. & NEUE, H.U. (1999): Effect of soil characteristics on sequential reduction and methane production in sixteen rice paddy soils from China, the Philippines, and Italy. *Biogeochemistry* 47, 269-295.

YAVITT, J.B., WILLIAMS, C.J. & WIEDER, R.K. (2005): Soil chemistry versus environmental controls on production of CH4 and CO2 in northern peatlands. *European Journal of Soil Science* 56, 169-178.

YU, K.W. & PATRICK, W.H. JR. (2003): Redox range with minimum nitrous oxide and methane production in a rice soil under different pH. *Soil Science Society of America Journal* 67, 1952-1958.

YU, K.W., WANG, Z., VERMOESEN, A., PATRICK, W.H. JR. & VAN CLEEMPUT, O. (2001): Nitrous oxide and methane emissions from different soil suspensions: effect of soil redox status. *Biology and Fertility of Soils* 34, 25-30.

ZHANG, T.C. & PANG, H. (1999): Applications of microelectrode techniques to measure pH and oxidation-reduction potential in rhizosphere soil. *Environmental Science and Technology* 33, 1293-1299.

9. List of References

Publications

2007: "The application of novel optical sensors (optodes) in experimental and biogeochemical interaction.
D. Gansert & **S. Bloßfeld**
In: *Progress in Botany* 69 (4), 333-358 (Lüttge, U.E.; Beyschlag, W. & Murata, J. Eds.) Springer, Berlin, Germany

2007: "Welchen Einfluss haben Pflanzen auf die Emission von klimarelevanten Treibhausgasen?"
S. Bloßfeld
In: *Biodiversität und Klima - Vernetzung der Akteure in Deutschland III* - (Korn, H.; Schliep, R. & Staedler, J. Eds.) (*in press*)

2007: "A novel non-invasive optical method for quantitative visualization of pH dynamics in the rhizosphere of plants"
S. Bloßfeld & D. Gansert
Plant, Cell and Environment 30 (2), 176-186.

2005: "Internal aeration of *Juncus effusus* L."
S. Bloßfeld
Geobotanische Kolloquien 19, 69-76

2005: "Sauerstoff-Freisetzung an den Wurzeln nordamerikanischer und europäischer Helophyten". *Diploma-thesis, Heinrich-Heine-University Duesseldorf*
S. Bloßfeld

Research projects/ cooperation

PROCOPE 2008
"Physico-chemical factors affecting the availability of trace elements in the rhizosphere"
R. Lösch, T. Sterckeman (INRA, Laboratoire Sols et Environnement, Nancy, France) &
S. Bloßfeld
German-french academic exchange project funded by the German Academic Exchange Service (DAAD) & Ministère de l'Education Nationale, de l'Enseignement Supérieur et de la Recherche

The N-sight project
Multinational cooperation for the integration of the optical pH-measurement technology into agricultural fertilizer research/application and development of new optical sensors for detection of urea and its decomposition products.
B. Wade (Agrotain International, St. Louis, Missouri USA), I. Klimant (Institute of Analytical Chemistry and Radiochemistry, Graz, Austria), **S. Bloßfeld**, C. Krause (PreSens GmbH, Regensburg, Germany), & C. Watson (Agri-Food and Bioscience Institute, Belfast, Northern Ireland).

Invited talks

"Welchen Einfluss haben Pflanzen auf die Emission von klimarelevanten Treibhausgasen?"
Federal Nature Conservation Agency, International Nature Conservation Academy (INA), Isle of Vilm, Germany (September 2006)

"Die Sauerstoffmessung mit Optoden"
Leibniz-Institute of Freshwater Ecology and Inland Fisheries (IGB) Central Chemical lab, Working group „Biogeochemistry". Berlin, Germany (January 2005)

Contributed talks

"Hybrid optodes – state-of-the-art sensors for non-invasive and simultaneous 2D imaging of rhizospheric pH and O_2 dynamics"
S. Bloßfeld & D. Gansert
Plant life in extreme and changing environment. Meeting of the specialist groups "Experimental Ecology" and "Desert Ecology" in cooperation with the German Society of Limnology. Tharandt, Germany (March 2008)

"Non-invasive and simultaneous 2D imaging of pH and O2 dynamics in the rhizosphere by use of a novel rhizobox for optical measurement, minimal-invasive sampling and experimental treatment"
S. Bloßfeld, D. Gansert, B. Thiele, A. J. Kuhn & R. Lösch
RHIZOSPHERE 2, International Conference. Montpellier, France (August 2007)

"Non-invasive quantitative 2D imaging of root induced pH dynamics in the rhizosphere"
S. Bloßfeld, D. Gansert
11th annual meeting of the workgroup "Experimental Ecology" of the Ecological Society of Germany, Austria and Switzerland. Castle Reisensburg, Germany (April 2006)

Posters

"Räumliche und zeitliche Dynamik der Sauerstoffkonzentration und des pH-Wertes im Wurzelraum von Sumpfpflanzen"
S. Bloßfeld
1st Day of the scientific Newcomers of the Heinrich-Heine-University. Duesseldorf, Germany (July 2005)

"Spatial and Temporal Dynamics of Radial Oxygen Loss from Single Attached Roots of some North American and Central European Wetland Plants"
S. Bloßfeld, J. Busch, R. Lösch, I. A. Mendelssohn
9th International Symposium on Biogeochemistry of Wetlands. Baton Rouge, LA, USA (March 2005)

"In vivo Measurement of Oxygen Concentrations in the Rhizosphere of single attached Helophyte Roots using Micro-Optodes"
J. Busch, **S. Bloßfeld,** R. Lösch, I. A. Mendelssohn
8th Conference of the International Society for Plant Anaerobiosis. Perth, Western Australia (September 2004)

Other scientific activities

Mentor of an US-American undergraduate student, sponsored by the DAAD (German Academic Exchange Service) RISE - *Research Internships in Science and Engineering* program.
May 2007 - August 2007

Participant of the international Summer School
Sustainable Use of Natural Resources (SUN) Water: its essential role in soil, vegetation and atmosphere. Research Centre Juelich, Juelich, Germany (August 2006)

Measurements for the diploma-thesis at the Wetland Biogeochemistry Institute, Louisiana State University, Baton Rouge, USA
April 2004 - July 2004

10. Erklärung

Hiermit erkläre ich, dass ich die vorliegende Dissertation eigenständig und ohne unerlaubte Hilfe angefertigt habe. Ich habe diese Dissertation in der vorgelegten oder in ähnlicher Form noch bei keiner anderen Institution eingereicht. Dies ist mein erster Promotionsversuch.

Düsseldorf, den 08. September 2008

Dipl.-Biol. Stephan Bloßfeld